The role of autophagy in aging-related Osteoarthritis

Paloma López de Figueroa

UDC Doctoral Thesis 2017

Director: Beatriz Caramés Pérez and Francisco Javier Blanco García

Tutor: Francisco Javier Blanco Garcia

Doctorado en Ciencias de la Salud

UNIVERSIDADE DA CORUÑA

La Dra. Beatriz Caramés Pérez y el Dr. Francisco Blanco García, del Grupo de Investigación en Reumatología del Instituto de Investigación Biomédica de A Coruña (INIBIC).

CERTIFICAN:

Que la presente memoria de tesis titulada: "The Role of Autophagy in Aging-related Osteoarthritis" presentada por Dña. Paloma López de Figueroa para optar al grado de Doctor, fue realizada bajo nuestra dirección y cumple con todos los requisitos de originalidad y rigor científico necesarios para su defensa.

Fdo. Beatriz Caramés Pérez

Fdo. Francisco Blanco García

En A Coruña, de de 2017

RESUMEN

Una característica común en las patologías relacionadas con el envejecimiento es la progresiva acumulación de macromoléculas dañadas que provocan daño celular y finalmente la muerte. La autofagia es un mecanismo fundamental en la homeostasis celular que regula la eliminación de moléculas dañadas y realiza una función protectora y de supervivencia celular. Estudios recientes indicaron una disminución de autofagia en el cartílago y condrocitos envejecidos y artrósicos. Por otro lado, existen claras evidencias de que la disfunción mitocondrial juega un papel fundamental en la aceleración del proceso de envejecimiento. En este sentido, diferentes líneas de evidencia han demostrado una desregulación mitocondrial en el cartílago artrósico. Basándonos en estas premisas, los objetivos propuestos en esta Tesis Doctoral han sido: (1) Estudiar los efectos de un defecto de autofagia sobre la función mitocondrial mediante aproximaciones farmacológicas y genéticas y (2) Identificar dianas terapéuticas asociadas a una disminución de autofagia en la patología del sistema musculoesquelético. Para llevar a cabo estos estudios empleamos aproximaciones farmacológicas y genéticas para inhibir la autofagia y estudiar su efecto sobre la función mitocondrial en condrocitos humanos. Además, hemos analizado el proteoma de los condrocitos humanos asociados a una disminución de autofagia para la identificación de potenciales dianas terapéuticas. Finalmente, validamos la diana identificada empleando la tecnología de edición genética CRIPSPR/Cas9 en condrocitos humanos y un modelo de delección genética en ratón. En conclusión, nuestros datos destacan el papel de la autofagia como un mecanismo de protección crítico frente al daño articular, por lo tanto, intervenciones farmacológicas encaminadas a activar la autofagia podrían tener actividad condroprotectora frente a los procesos degenerativos del sistema muscoloesquelético.

RESUMO

Unha característica común nas enfermidades relacionadas co envellecemento é a progresiva acumulación de macromoléculas danadas que provoca danos celulares e finalmente a morte. A autofaxía é un mecanismo fundamental na homeostase celular que regula a eliminación das moléculas danadas e realiza unha función protectora e supervivencia celular. Estudios recentes indicaron unha diminución da autofaxía no cartílaxe e condrocitos envellecidos e artrose. Por outro lado, existen claras evidencias de que a disfunción mitocondrial xoga un papel fundamental na aceleración do proceso de envellecemento. Neste sentido, diferentes liñas de evidencia demostraron unha disregulación mitocondrial no cartílaxe artrósico. Tendo en conta isto, os obxectivos propostos nesta Tese doutoral foron: (1) Estudar os efectos dun defecto de autofaxía sobre a función mitocondrial mediante aproximacións farmacolóxicas e xenéticas e (2) Identificar as dianas terapéuticas asociadas cunha disminución da autofaxía na patoloxía do sistema musculoesquelético. Para levar a cabo estes estudos empregamos aproximacións farmacolóxicas e xenéticas para inhibir a autofaxía e estudiar o seu efecto sobre a función mitocondrial nos condrocitos humanos. Ademais, analizamos o proteoma dos condrocitos humanos asociados cunha diminución de autofaxía para a identificación de dianas terapéuticas potenciais. Finalmente, validamos a diana identificada empregando a tecnoloxía de edición xenética CRIPSPR / Cas9 en condrocitos humanos e un modelo de delección xenética en rato. En conclusión, os nosos datos destacan o papel da autofaxía como un mecanismo de protección crítico fronte ao dano articular, polo tanto, as intervencións farmacolóxicas encamiñadas a activar a autofaxía poderán ter actividade condroprotectora fronte ós procesos dexenerativos do sistema musculoesquelético.

ABSTRACT

A common feature in pathologies related to aging is the progressive accumulation of damaged macromolecules that cause cellular injury and finally death. Autophagy is a fundamental mechanism in cellular homeostasis that regulates the elimination of damaged molecules and performs a protective function and cell survival. Recent studies have indicated a decrease in autophagy in the cartilage and aged and osteoarthritic chondrocytes. On the other hand, there is clear evidence that mitochondrial dysfunction plays a key role in the acceleration of the aging process. In this sense, different lines of evidence have shown mitochondrial dysfunction in osteoarthritis cartilage. Based on these premises, the objectives proposed in this Doctoral Thesis have been: (1) To study the effects of a defect of autophagy on mitochondrial function through pharmacological and genetic approaches and (2) Identify therapeutic targets associated with a decrease in autophagy in the pathology of the musculoskeletal system. To carry out these studies we use pharmacological and genetic approaches to inhibit autophagy and study this effect on mitochondrial function in human chondrocytes. In addition, we analysed the proteome of human chondrocytes associated with a decrease in autophagy for the identification of potential therapeutic targets. Finally, we validate the target identified using the genetic editing technology CRIPSPR/Cas9 in human chondrocytes and a model of genetic deletion in mouse. In conclusion, our data highlights the role of autophagy as a critical protective mechanism against joint damage; therefore, pharmacological interventions aimed at activating autophagy may have condroprotective activity against the degenerative processes of the musculoskeletal system.

Table of contents

Figure and table Index

Abbreviations

OA	Osteoarthritis
LCL	Lateral collateral ligament
LCP	Posterior cruciate ligament
LCM	Medial collateral ligament
LCA	Anterior cruciate ligament
LBP	Low back pain
IVD	Intervertebral disc
DD	Degenerative disc
NP	Nucleus pulposus
AF	Annulus fibrosus
VBs	Vertebral bodies
CEPs	Cartilaginous end plates
ECM	Extracellular matrix
PG	Proteoglycan
GAG	Glycosaminoglycan
HA	Hyaluronic acid
COMP	Cartilage oligomeric matrix protein
mRNA	Messenger RNA
SV40	Virus T antigen 49
Col2A1	II Collagen
OARSI	Osteoarthritis Research Society International
KL	Kellgren and Lawrence
JSN	Joint space narrowing
MMP	Matrix Metalloproteinase
ADAMTS	Disintegrin and Metalloproteinase with Thrombospondin motifs
Il-1β	Interleukin 1 beta

TNF-α	Tumor necrosis factor alpha
PGE2	Prostaglandin E2
COX-2	Cyclooxygenase 2
ATP	Adenosine triphosphate
ROS	Reactive oxygen species
CMA	Chaperone-mediated autophagy
ULK-1	Serine/threonine-protein kinase ULK1
LC3/Map1LC3b	Microtubule-associated proteins 1A/1B light chain 3B
mTOR	Mammalian Target of Rapamycin
mTORC1	Mammalian Target of Rapamycin complex 1
mTORC2	Mammalian Target of Rapamycin complex 2
Akt	RAC-alpha serine/threonine-protein kinase
PI3K	Protein I3 kinase
SGK1	Serum and glucocorticoid-regulated kinase 1
PKC	Protein kinase C
AMPK	AMP-activated protein kinase
PARP	Poli ADP ribosa polimerasa
AGE	Advanced glycation end products
SSP	Senescence secretory phenotype
CAAX	C-cysteine, A-aliphatic, X-any residue
ZMPSTE24	Zinc Metallopeptidase STE24
FTI	Farnesyltransferase inhibitors
SIRT1	Sirtuin 1
FOXO3	Forkhead box O3
HGPS	Hutchinson-Gilford Progeria syndrome
LD	Neonatal restrictive lethal dermopathy
MRC	Mitochondrial Respiratory chain

Il-6	Interleukine 6
Il-8	Interleukine 8
NSAID	Nonsteroidal anti-inflammatory drug
ΔΨm	Mitochondrial membrane potential
CRISPR	Clustered regularly interspaced short palindromic repeats
FCS	Fetal calf serum
EDTA	Ethylenediaminetetraacetic acid
JC-1	5',6,6'-Tetrachloro-1,1',3,3'-tetraethyl-imidacarbocyanine iodide
PBS	phosphate buffered saline
DCFH-DA	2,7-dichlorodihydrofluorescein diacetate
PS	phosphatidylserine
PI	Propidium iodure
NGS	Normal goat serum
MALDI	Matrix Assisted laser desorption/ionization
TOF	Time of Flight
iTRAQ	Isobaric tag for relative and absolute quantification
SDS	Sodium Dodecyl Sulfate
RP-LC	Reversed phase liquid chromatography
WB	Western-Blot
HRP	Horserradisch peroxidase
CFU	Colony Forming Unit
RT-PCR	Reverse transcriptase Polimerase chain reaction
qPCR	Quantitative real time Polimerase chain reaction
DMEM	Dulbecco's modified Eagle's medium
cDNA	Complementary DNA
LMNA	Lamin A/C
ACTB	Actin B

CHUAC	University Hospital of A Coruña
HT	Heterocygous
KO	Knock Out
ANOVA	ANalysis Of VAriance

CHAPTER 1: INTRODUCTION

1.1 Joint

1.1.1 Definition

The human skeleton consists of a large number of bones to make the movement possible. They are assembled together by the joints. Therefore, The joint is a specialized structure, a point of union of two or more bones, which allows stability and movement (1). Depending on the degree of mobility that allows the articulation, and the way of contact between the bones, the joints are classified as diarthrosis, sinarthrosis or amphiarthrosis.

1.1.2 Types of body joints

Synarthrosis joints or Fibrosis (fixed) permit little or no are the ones that do not allow practically movement, because they are united by more or less dense tissue. There are different types depending on the morphology, and even the type of elements that come into contact, which may be two cartilages (sinchondrosis) or have a fibrous nature (sinfibrosis) as occurs with the bones of the skull or the joint between the tooth and Dental alveoli, or even synostosis as occurs in the bone welds that appear after the disappearance of growth cartilage.

The **amphiarthrosis** or semi-mobile joints may be slightly articulated the joints in which the bones are joined by cartilaginous tissue or a fibrocartilaginous mass, while peripherally the articular ligaments are differentiated. Such is the case of the joints of the vertebral bodies, which only allow small movements. In spite of this, when the movements of the set of articulations of the spine are added, it can describe extensive movements of flexion, extension or rotation.

Diarthrosis joints or synovial (mobile) joints are the most frequent that provide a greater range of movement. A synovial joint consists of smooth articular surfaces of cartilaginous nature, which cover the ends of the bones, and are the articular cartilage. The joint is surrounded by the articular capsule, of a fibrous nature. The internal capsule is covered by a delicate synovial membrane, which secretes small amounts of lubricating liquid or synovium. In some joints, a pad of cartilaginous tissue constituting

a meniscus or articular joint is arranged to regularize the contact surfaces between the bones.

Finally, the joint capsule may be reinforced by a series of articular ligaments (2, 3). Within them, the greater to less mobility are distinguished: the enanthroses that allow movement in three planes (humeral-scapular articulation); The condyle (temporomandibular joint) and reciprocating or saddle (trapezium-metacarpal joint) both with two axes of movement: the trochlear joints (interphalangeal joints) and the trochloid (atloidoaxoid joints) that only allow mobility on single axis. To conclude, the artery (intercarpal joints), in which, due to its flat shape, it only allows small sliding movements. (4, 5)

1.1.3 The diarthrosis or Synovial Joints

The joint is a specialized point of union of two or more bones, which allows stability and movement. There are different types of joints, synovial joints being the most frequent in the body. Synovial joints make pain-free movement possible and are composed of multiple structures: an articular capsule, continuous with periosteum that surrounds joint cavity; a synovial membrane – thin membrane that covers the joint cavity, responsible for the secretion of synovial fluid to maintain joint lubrication and provide nutrition to the articular cartilage; and hyaline articular cartilage which covers the end of bones in a joint. Other tissues such ligaments, muscles and tendons may be also present and provide additional support to synovial joints (2, 3).

The knee is one of the largest and most complex synovial joints in the body. The knee consists of 2 joints: the femorotibial joint and the patellofemoral joint. The bony architecture of the femur, tibia, and patella contribute to the stability of the knee joint, along with static and dynamic restraints of the ligaments, capsule, and musculature crossing the joint.

Tendons connect the knee bones to the leg muscles to provide stability to the knee in the knee movement. The anterior cruciate ligament prevents the femur from sliding retrograde on the tibia (or the tibia sliding forward on the femur). The posterior cruciate ligament prevents the femur from sliding forward on the tibia (or the tibia from sliding backward on the femur). The medial and lateral collateral ligaments prevent the

femur from sliding side to side. The structure of synobial joints are presented in Figure 1.1

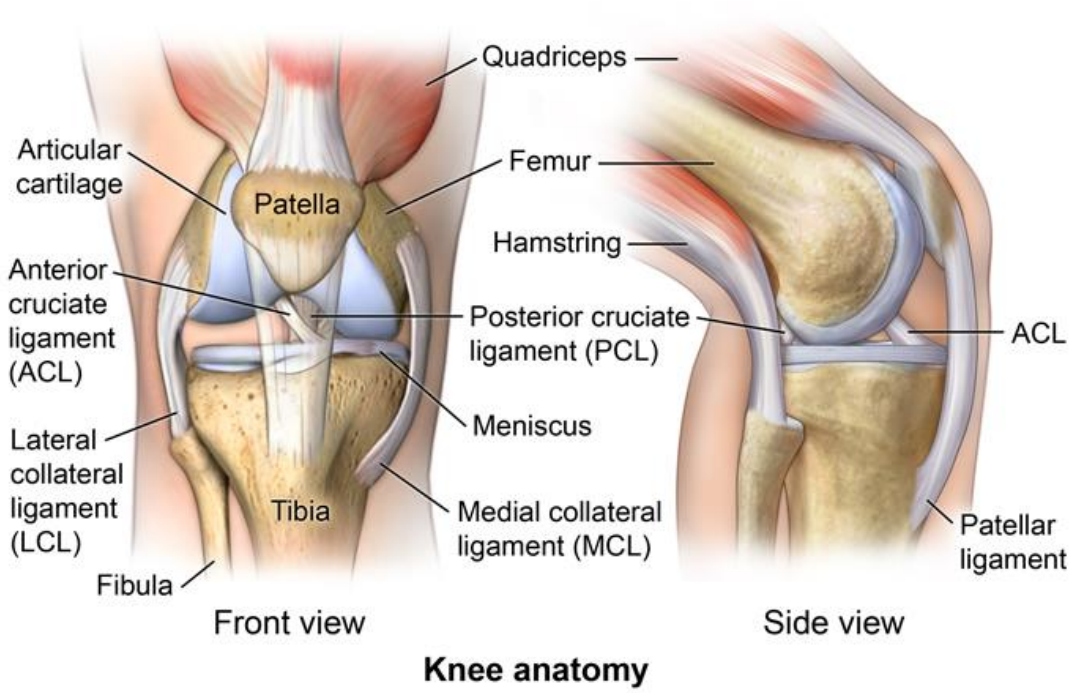

Figure 1.1: Knee anatomy. Schematic representation of the major structure of normal synobial joint (available online in http://comportho.com/2016/07/page/2/)

1.1.4 The amphioarthrosis or semi-mobile joints: The spine

Low back pain (LBP) is an important cause of disability worldwide and the second most common cause of physician visits. There are many causes of back pain, including disc herniation and intervertebral disc (IVD) degeneration are the most common diagnoses and targets for intervention.

Intervertebral discs (IVDs) are pads of fibrocartilage which lie between the vertebrae of the spine (**Figure 1.2**). They allow the vertebral column to turn and, and distribute compressive loading on the adjacent vertebral bodies. The mechanical properties of discs are important because human lumbar IVDs are often physically disrupted, which may give rise to degenerative changes and to chronic back pain (6).

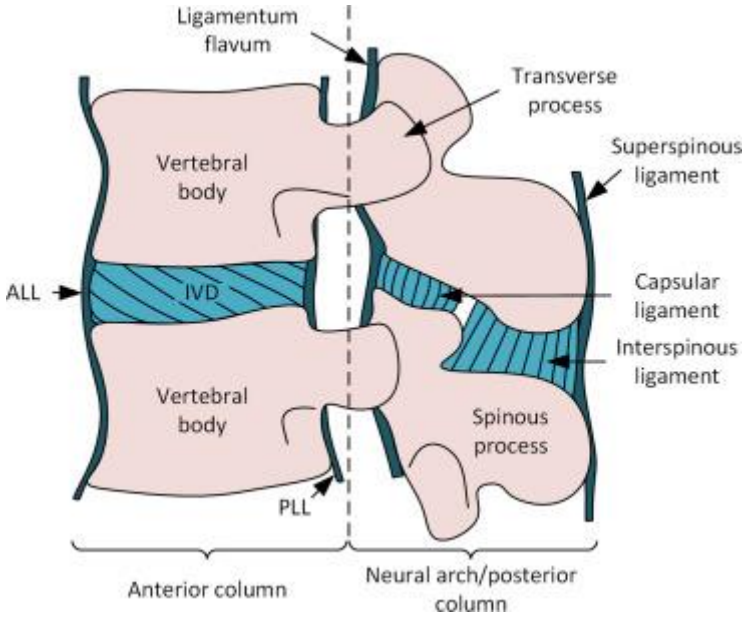

Figure 1.2: Graphical representation of a motion segment of spine, sagittal view. ALL and PLL refer to the anterior and posterior longitudinal ligaments, respectively (6).

The IVD has three main components, a soft, deformable, nucleus pulposus (NP), which is surrounded by the fibrous concentric layers of the anulus fibrosus (AF), and bonded above and below to adjacent vertebral bodies (VBs) by the thin layers of the cartilaginous end plates (CEPs).

The nucleus pulposus (NP) is gelatinous that accounts for 40–50% of the volume of the adult disc and 25–50% of the transverse cross-sectional area, composed predominantly of type II collagen and proteoglycans, with high water content that contributes to its hydrostatic pressurization and resistance to compressive forces, and this pressure generates tension in the surrounding AF. Proteoglycan accounts for 35–65% of the dry weight of the NP, and is important for binding water into the tissue. The collagen type II fibrils, which account for 5–20% of dry weight, provide a loose, 3-dimensional fiber network, which holds the nucleus. The rest of the dry weight of the NP is non-collagenous proteins and elastin. The NP water content decreases with age, from approximately 90–70% from the ages of 1– 80 years old, imitating a similar reduction in proteoglycans. In the degenerative process, loss of proteoglycans and water content are observed, which results in redistribution of load onto the fibrochondrocyte-like cells in the annulus fibrosus (AF).

The AF consists of concentric of 15–25 concentric layers, the lamellae, rich in collagen and elastin, which are approximately 0.05–0.5 mm thick, of increasing thickness from outer to inner. (7) Approximately 48% of the lamellar layers are circumferentially incomplete and the percentage of incomplete layers increases with age. Each layer consists of coarse and strong collagen type I fiber bundles, as in tendon, with their orientation alternating between ± 25–45° in relation to the transverse plane **(Figure. 1.3)**. The complex organization of collagen fibers in the AF permits it to develop tensile, like a "hoop", stress due to the pressure in the nucleus.

In the healthy IVD, the AF contains 65–70% water. Dry weight is approximately 20% proteoglycan, 50–70% collagen, and 2% elastin.

The CEPs are thin layers of hyaline cartilage that bind the disc inferiorly and superiorly to the adjacent bony endplates (BEPs). They are approximately 0.6 mm thick, while they are generally thinner towards the center where they are in contact with the NP. Thickness decreases with age. Dimensions in the transverse plane reflect those of the adjacent vertebral bodies, and so increase from an anteriorposterior length of 16–19 mm and lateral width of 17–29 mm in the cervical spine, rising to an anterior-posterior length of 30–36 mm and lateral width of 43– 54 mm in the lumbar spine. (6)

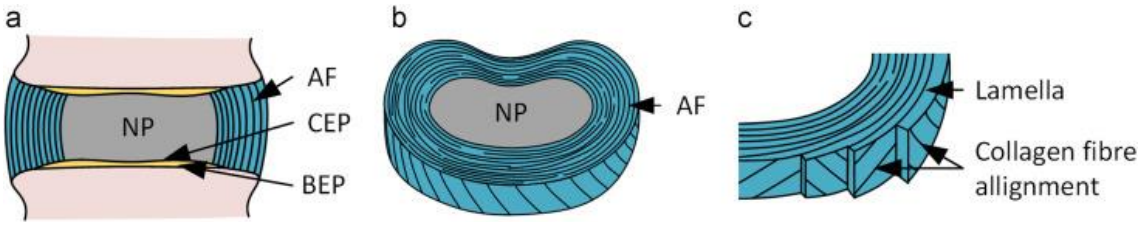

Figure 1.3: Gross anatomy of a disc. (a) Cross section of a disc in the coronal plane, (b) diagram of a transversely sliced IVD and (c) diagram showing the alternating fiber alignment in successive lamellae.(6).

Spine degeneration is a natural part of the aging process that is most common in the neck (cervical) and lower back (lumbar). Disc degeneration (DD) is a multifactorial process characterized by cellular and biochemical changes in disc tissue that result in structural failure. While DD is a part of normal aging, a significant number of people with indications of DD on MRI are actually asymptomatic, with no history of pain or disability. Numerous alterations are observed in DD, each of which provides understandings into the disease process.

1.2 Articular cartilage.

1.2.1 Composition

Hyaline cartilage is a specialized connective tissue, avascular, aneural and alymphatic, consisting of two elements, one cellular and the other extracellular (8). The extracellular matrix (ECM) is nourished through the diffusion of the fluid from the joint cavity, where nutrients cross the synovial barrier from the synovial fluid and diffuse through the matrix of articular cartilage to reach the cells. The ECM consists mainly of water, collagen (mainly collagen type II) and proteoglycans that correspond to 97-98% of the total weight, while chondrocytes represent only 1-2% of the total.(9)

1.2.1.1 The extracellular matrix

Extracellular Matrix (ECM) represents 95% of the dry weight of articular cartilage. As already mentioned, the ECM is constituted by a liquid fraction and by a series of macromolecules that provide the cartilage its special biomechanical characteristics. The water content of the matrix is not evenly distributed along the cartilage layers, its concentration is higher in the surface area gradually decreasing to the deep zone, it is around 80% near the cartilage surface, decreasing to around 65% in the Deep zone (8). The major component of ECM is the collagen (60 to 70% of the dry weight) and the major type is II collagen (95%) that interacts with other types of collagen such as type IX and XI (also VI, XII and XIV).

Type IX and XI collagens stabilize the collagen fibrils assembled from type II collagen, while type VI collagen, mainly present in territorial matrix, anchor chondrocytes to the matrix (10). Further collagen types, including types III, XII and XIV, are also found but in smaller amounts(11). Type X collagen only appears in the calcified cartilage zone of articular cartilage or in the hypertrophic zone of the growth plate (12). Collagens are composed of a triple helix of three identical polypeptide chains (α- chains) which provide the shear and tensile strength to maintain the integrity of articular cartilage. Overall, the collagen forms a highly organized fibrillary network that immobilizes proteoglycan aggregates and serves as a tensile element (8).

The ECM is also rich in proteoglycans (PGs), which are macromolecules synthetized by chondrocytes and constitute the second largest group of the ECM components, accounting to 10- 15% of the tissue wet weight (13).

They consist of glycosaminoglycans (GAG), long unbranched polysaccharide made of repeating disaccharide units, covalently attached to a central core protein. The glycosaminoglycan chains are composed of negatively charged carboxyl or sulfated groups, which attract positively charged ions and have the ability to retain large amounts of water in the matrix. This leads to different ion concentrations between articular cartilage and surrounding tissues. As a consequence of this osmotic imbalance, water is drawn into the tissue causing swelling and expansion of the matrix network, crucial for the biomechanical properties of cartilage (10). Among the most outstanding GAGs in the ECM, there are chondroitin sulfate 4 and 6, keratan sulfate and dermatan sulfate and hyaluronic acid (HA).

The aggrecan being the largest and most abundant PG (90% of the total cartilage matrix proteoglycan mass). Aggrecan, that occupies most of the interfibrillar space of the matrix cartilage, has more than one hundred chondroitin sulfate and keratan sulfate chains that are associated with HA to constitute multimeric aggregates via link protein, which stabilizes this interaction. Aggrecan make available a really high fixed charged density, creating an elevated osmotic environment necessary to retain the water needed for nutrient and solute transport (14, 15). The matrix also contains non-collagenous proteins, such as fibronectin and Cartilage Oligomeric Matrix Protein (COMP), whose function is to form part of the maintenance of cartilage structure and repair mechanisms. (9, 16, 17).

Although these proteins are less studied, they have a role in tissue assembly and in maintaining the properties and functions of the tissue (10, 15). Structure and composition of ECM of articular cartilage are presented in **figure 1.4.**

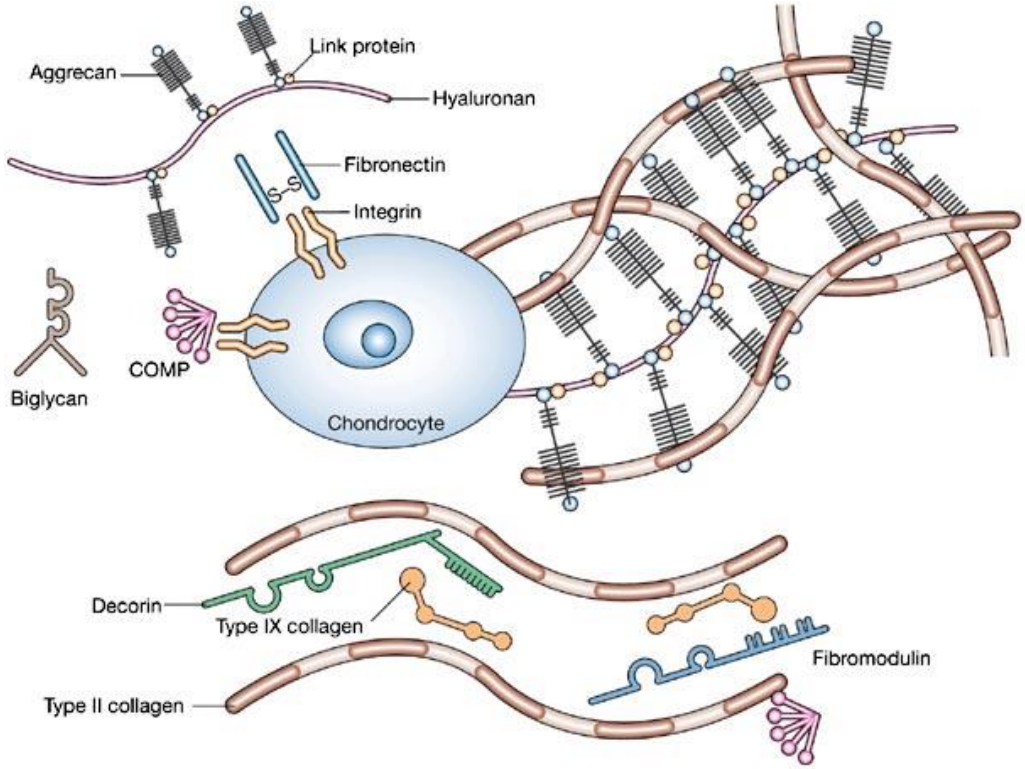

Figure 1.4: Structure and composition of ECM of articular cartilage. Three classes of proteins exist in the articular cartilage: collagen, proteoglycans and other non-collagenous proteins. The interaction between highly negatively charged cartilage proteoglycans and type II collagen fibrils is responsible for the compressive and tensile strength of the tissue. (18)

1.2.1.2 Chondrocytes

Chondrocytes are the only cellular elements present in adult hyaline cartilage. Chondrocytes represent only 2-5% of the total tissue volume (19) and are considered as highly specialized cells an play a key role in the biosynthesis and maintenance of ECM components, ensuring periodic replacement of the constituent elements of the matrix to conserve the normal conditions in adult cartilage, the balance between anabolic and catabolic processes (20, 21). Chondrocytes can vary in size, shape and number per unit of tissue from the surface to the deep layers in the cartilage. They are able to respond to biochemical, structural or physical stimuli by synthesizing different enzymes, growth factors, cytokines and components of the ECM. Chondrocytes live in an avascular environment, with low levels of nutrients and oxygen. As a consequence, chondrocyte metabolism operates at low oxygen tension, ranging from 10% at the surface to 1% in deep zone, mainly supplied by the synovial fluid due to a lack of blood vessels (19). Low oxygen tension, the more physiological environment for chondrocytes, is the best

environment, where they can synthetize higher amounts of PGs and collagen, and reduce the mRNA expression and protein release of catabolic enzymes(22). In order to adapt to these low oxygen concentrations, healthy chondrocytes obtain energy from glucose, mainly through the glycolytic pathway(23). With ageing, chondrocytes tend to decrease, as well as their anabolic activity, because their ability to replace the collagen is altered and only the synthesis of proteoglycans appear to be maintained, albeit to a very limited way (21).

The lack of chondrocytes of human origin suitable for in vitro experiments has limited the progress of studies related with pathologies related to cartilage. Developing cell lines that express the phenotype and characteristics of human chondrocytes has been a key are of attention (24).The TC28-a2 line was obtained by retrovirus-mediated transfection. Primary costal chondrocytes from a healthy donor were transfected with virus T antigen 49 (SV40). It is a virus that codes for a multifunctional regulatory protein that is used for the immortalization of cells. Infection of cells with SV40 causes continuous growth, preventing them for entering into apoptosis, which results in a proliferation state (25). The expression of type II collagen (Col2A1) is a widely marker of differentiated chondrocytes and a major component of ECM. T/C28-a2.chondrocytes express transcripts for matrix proteins, collagens and aggrecanes which are all deposited in the extracellular matrix (ECM). In addition, this cell line conserves the chondrocyte morphology and to maintain the continuous proliferation in monolayer, making it very useful for the study of chondrocyte biology (25, 26).

1.2.2 Structure and function of articular cartilage

Cartilage is a heterogeneous tissue, made up of a single layer of cells that varies from the surface to the deepest layer in terms of composition, organization and metabolic activity. Thus, four structural and functional zones can be distinguished: superficial zone, intermediate or transition zone, deep zone and an area of calcified cartilage. These zones are not perfectly delimited, but instead there are gradual changes in its composition and structure of both collagen, a major component of ECM, and chondrocytes. (27)

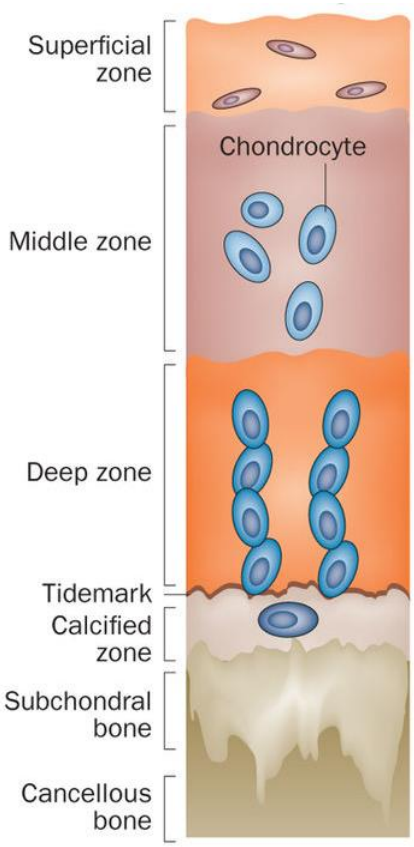

Figure 1.5: Structure of the articular cartilage. In the articular cartilage four zones can be distinguished: superficial zone, intermediate zone, deep zone and a zone of calcified cartilage. Between the deep layer and the layer of calcified cartilage is a calcification front, tidemark. The picture represents of healthy and OA cartilage illustrating the zonal architecture and distribution of chondrocytes (28) .

There are differences in the structure and composition of collagen and chondrocytes according to the depth within the hyaline cartilage. In the case of collagen, we can observe that the structure varies from fine fibres in parallel to the surface to being perpendicular to the surface in the deep zone and to its disappearance in the zone of calcified cartilage. On the other hand, the chondrocytes are arranged parallel to the surface and are smaller in surface areas. The deeper is the zone the more disorganized the chondrocytes, often arranged in clusters perpendicular to the surface or in a scattered way. Viability and morphological properties also vary with deep. A summary of the main structural and composition differences of articular cartilage layers is shown in **Table 1.1**

Table 1.1: Structure and composition of articular cartilage layers.

	Superficial zone	Transition zone	Deep zone	Calcified cartilage
Collagen	Fine & parallel fibers to the surface	Oblique course through the matrix	Same orientation as columns of chondrocytes	
Chondrocyte	Small and flattened parallel to the joint surface	Large and spherical.	Elliptical & forming columns of 2-6 cells which are perpendicular to the surface	Scattered, fewer and viable

1.3 Osteoarthritis

Osteoarthritis (OA) is the most common joint disease, being ageing one of the determining factors in the development of this pathology. Almost 80% of those over 75 years old have radiological or clinical abnormalities of OA. It is a degenerative pathology of the joints characterized by the alteration of the cartilage. Its pathogenesis is complex, since many genetic, metabolic and local factors play a role in decreasing cartilage and increasing in subchondral bone and synovial inflammation (9, 29).

In 1987 OA was defined as "heterogenous group of conditions leading to joint symptoms and signs associated with defective integrity of articular cartilage in addition to associated changes in the underlying bone and at the joint margins" (30). Since, a variety of definitions emerged but there is a consensus that OA is a heterogeneous disease considered as a whole joint disease.

Nowadays, the Osteoarthritis Research Society International (OARSI) defines OA as a "*disorder involving movable joints characterized by cell stress and extracellular matrix degradation initiated by micro and macro-injury that activates maladaptive repair responses including pro-inflammatory pathways of innate immunity. The disease manifests first as a molecular derangement (abnormal joint tissue metabolism) followed by anatomic, and/or physiologic derangements (characterized by cartilage degradation, bone remodeling, osteophyte formation, joint inflammation and loss of normal joint function), that can culminate in illness*" (31, 32).

1.3.1 Clinical features

The clinical manifestations are very variable depending on the affected joint and the moment of the evolution. The fundamental symptom is chronic pain presented by the patient due to inflammation of periarticular structures, increased intraosseous pressure, periosteal disturbance, synovitis or muscle contracture. In fact, the first events observed in OA occur in cartilage, at the joint surfaces areas, but structures around articular cartilage are also affected, including synovium, ligaments, muscles, meniscus, intra-articular fat, and subchondral bone (33, 34). Thus, phenotypic changes in cells of superficial layer, fibrillation with progressive loss of articular cartilage, cartilage

calcification, subchondral bone remodeling, sclerosis, osteophyte formation, and mild to moderate inflammation in synovial lining are some characteristic features in OA (35, 36). Some of the more relevant features are presented in **Figure 1.6.**

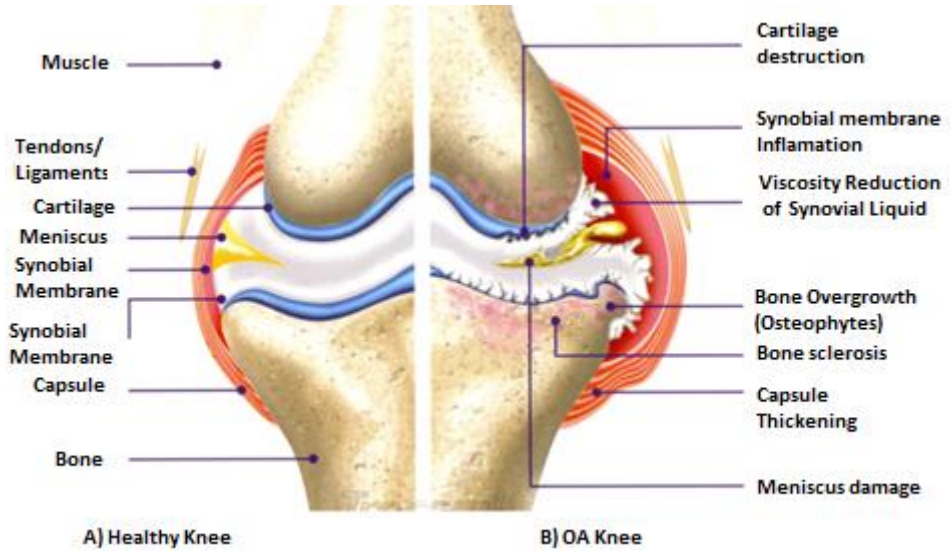

Figure 1.6: Clinical characteristics of a healthy knee vs. OA knee. We can observe the state of the Normal knee in comparison with the OA knee is shown. Degradation of articular cartilage, presence of osteophytes, synovial inflammation and abnormal exposure of bone are among the main pathological characteristics (37).

The appearance and improvement of advantage medical imaging of the musculoskeletal system using X-ray techniques have significantly enhanced both the diagnosis and the study of arthroscopic pathology. Thus, through the images obtained by this technology, Kellgren and Lawrence, established the scale of radiological OA clinical graduation according to the condition of the joint that bears his name whose values range from 0 to 4 according to the observed radiological signs. (38) A patient is usually considered as an arthritic when his KL degree is equal to or greater than 2.

More recently the *Osteoarthritis Research Society International (OARSI)* considered as criteria related to osteoarthritis the following critical aspects:

- Presence of marginal osteophytes in the femoral and tibia condyles of the medial and lateral compartments.
- Reduction of joint space in the medial and lateral area.

  Depending on the degree of involvement, the scale ranges from 0 to 3.

In addition to the radiological manifestations, during OA, other symptoms occur such as joint pain and stiffness, resulting in a symptomatic definition of osteoarthritis. When both signs are taken into account, it must be bear in mind that there is not always a correlation between them, since there may be radiological signs but not pain. Depending on the degree of joint space narrowing (JSN) and osteophyte classification, the scores of the scale range from 0 to 3 (**Table 1.2**)

Table 1.2: OARSI classification score to OA.

Radiologic Scale OARSI in OA knee

Score	***JSN classification* (% reduction)**	**Osteophytes classification**
0	Normal	normal
1	Medium (1-33%)	Grade I
2	Moderate (34-66%)	Grade II
3	Severe (67-100%)	Grade III

1.3.2 Articular Cartilage in OA

Adult healthy cartilage is characterized by maintaining a homeostatic balance between anabolic (ECM synthesis) and catabolic (ECM degradation) processes. However, in the development of OA it is characterized by increased catabolic processes of articular cartilage due to the degradation of ECM, the appearance of clusters of chondrocytes, increased cartilage calcification increased area of the tidemark and onset of the subchondral bone (16). As the process continues, the increased catabolic activity, mediated by an up-regulation of cartilage-degrading proteinases and inflammatory mediators, occurs in conjunction with a decrease in matrix metalloproteinase enzyme inhibitors and ECM synthesis.

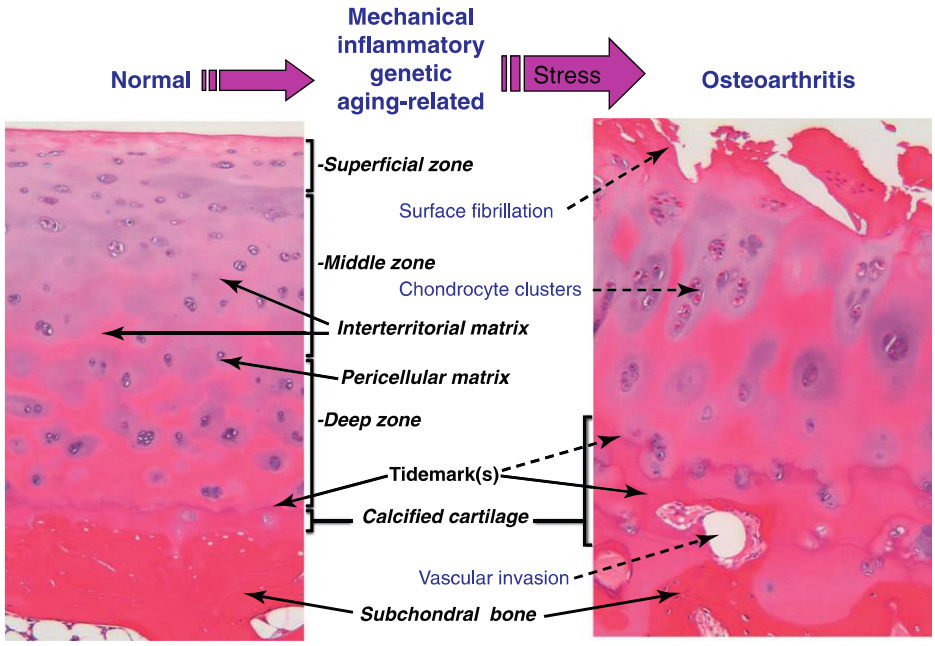

Figure 1.7: Scheme of pathway to catabolic and anabolic process (39).

In OA cartilage, proteases are considered the most important elements involved the degradation of cartilage and ECM. The products of the proteolytic activity by this enzymes can trigger a catabolic response leading to a process of cell death with apoptosis characteristics (40). Matrix metalloproteinases (MMPs) and 'aggrecanase' a disintegrin and metalloproteinase with thrombospondin motifs (ADAMTSs) are well established to play key roles in OA. MMPs are responsible for degrading ECM, eliminating molecules such as collagen (MMP-1 and MMP13), proteoglycans, gelatin or fibronectin (MMP-3 and MMP-10).

On the other hand, proinflammatory cytokines such as IL-1β interleukin and tumor necrosis factor alpha (TNF-α) also influence cartilage degradation, which induce the formation of other interleukins such as IL-6 and IL-8, which stimulates the formation of MMPs and increment the level of nitric oxide. In addition, they are able to stimulate other molecules such as prostaglandin E2 (PGE2) and the enzyme cyclooxygenase 2 (COX-2) (41, 42).

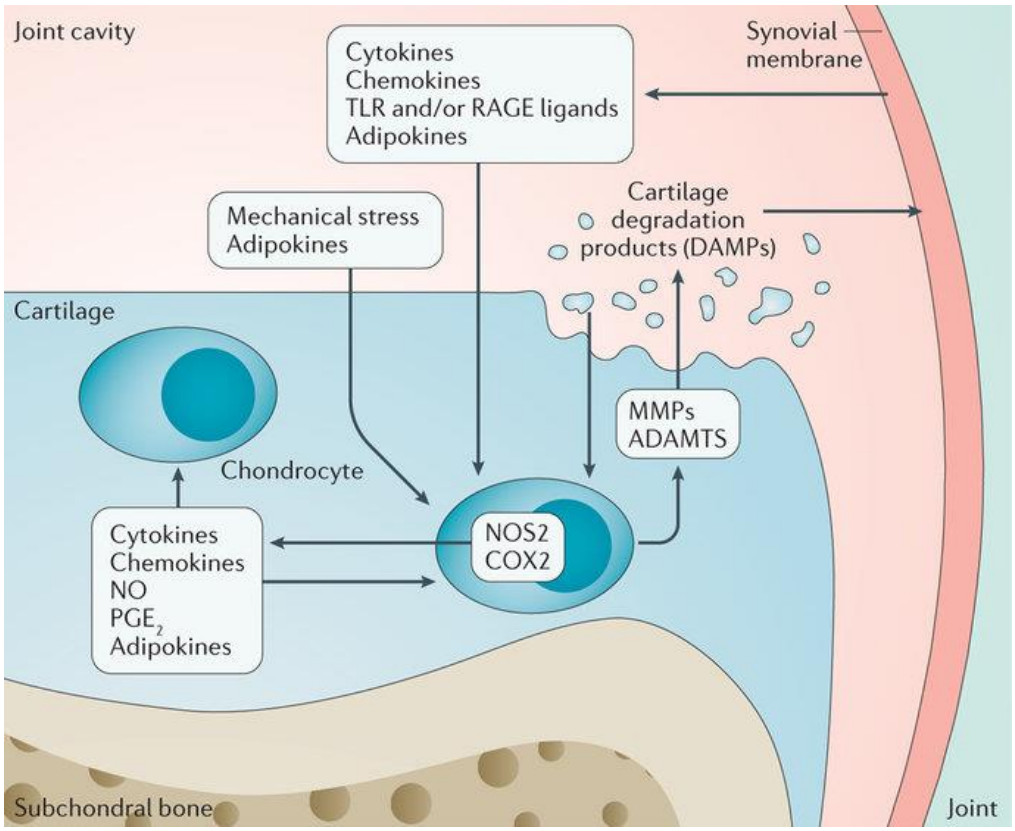

Figure 1.8: Scheme of pathway to catabolic and anabolic process. This pathway is mediated by Matrix metalloproteinases (MMPs) and 'aggrecanase' a disintegrin and metalloproteinase with thrombospondin motifs (ADAMTSs). (43)

Furthermore, it is important to mention that once the collagen network is degraded, it cannot be restored to its initial state (44). Therefore the therapeutic challenge is and will be to avoid damage or promote the repair of the physiological and functional properties of the initial hyaline cartilage at early stages (45). It is important to note that the articular cartilage chondrocytes have traditionally been classified as highly glycolytic cells. However, until relatively recently it was believed that mitochondria did not mediate the pathogenesis of the disease. Recent studies in this regard have shown a mitochondrial dysfunction in OA, associated with excessive production of reactive oxygen species (ROS), accompanied by alterations in ATP production, calcium levels and redox status, which may explain in part some of the processes that lead to cartilage degradation during OA(20, 46).

1.4 OA Risk Factors

OA has been considered as a disease associated to ageing and to the mechanical stress of joints, without taking into account other risk factors. This concept changed and OA is now considered a disease where many interconnected with mediators such as metabolic, hormonal and humoral, and recycling pathways have been shown to contribute to the initiation and progression of the disease (47). Nowadays, OA is considered a multifactorial disease, whose causes are not yet completely understood. The development and progression of the disease can be a result of the interaction between various systemic and local factors that include age, sex, ethnicity, genetics, nutrition, osteoporosis, smoking, obesity and metabolic disease, sarcopenia, and local mechanical risk factors (48).

Aging is a main risk factor for OA, and the phenotype of aging-associated changes in both cartilage cells and extracellular matrix (ECM) has been characterized in detail. Cell density in cartilage decreases with aging, remaining cells express certain features of cellular senescence, produce reduced amounts of ECM and increased levels of matrix degrading enzymes and inflammatory mediators, Recent progress in understanding mechanisms related to cartilage cell aging includes the demonstration that chondrocytes are less responsive to anabolic stimuli and deficient in defenses against oxidative stress.

Osteoarthritis is not a consequence of aging, but it does increase its prevalence is dramatically increased due to the mechanical changes suffered over time by the periarticular musculature joint, as well as the decreased stability to withstand increased load to withstand increased load.

Aging modifies the structure and function of articular cartilage and other joint tissues such as subchondral bone, muscle, soft tissues, synovial membrane, and synovial fluid. (49, 50)

Consequently, based on differential risk factors, OA can now be classified according to a variety of OA phenotypes including, age-related metabolic, inflammatory, hormonal, pain-related, genetic and injury-related phenotypes (51, 52). At this moment, there are no efficient treatments to stop OA progression. This failure might be a consequence of evaluate OA as a unique disease without consider the

different OA phenotypes (49, 50). It is likely that these different phenotypes may need different therapeutic approaches.

In fact, understanding the underlying mechanisms of disease progression can help to differentiate OA phenotypes, and thus provide the right treatment to the right patient. This knowledge could enable the development of more effective and tailored therapies (34, 49, 53)

1.5 Prevalence and treatments

About one tenth of the world's population over 60 years old is estimated to have symptomatic problems that can be attributed to OA. As other musculoskeletal disorders, it causes significant pain, disability and decreased quality of life. The prevalence of the OA increases with age (**Figure 1.9**) and is highly related to obesity. Therefore, due to the adoption of new, more sedentary lifestyles, it is expected that by 2030 the affected population over 60 will be 30%.

Population studies, usually based on radiographs, have demonstrated a transition from normality to the development of pathology in the joint. Generally, most patients with chronic knee pain between the ages of 35 and 50 are likely to develop OA in the next decade. The most commonly recognized risk factors for knee OA (obesity, mechanical injury, occupational or excessive leisure physical activity, and osteoarthritis of the hand) have a greater effect on incidence and progression (54, 55).

Although the prevalence and incidence of osteoarthritis varies among the different studies, if there is an agreement about the proportion of adults affected, as documented in epidemiologic studies on the prevalence of knee, hip and hand as shown in the **figure 1.9** (56).

Osteoarthritis also involves an economic cost related to diagnosis, follow-up and treatment. It is the second pathology that generates more expenses, below the cardiomyopathies. According to a study carried out by ArtRoCad study, the treatment of hip and knee, supposes a direct and indirect cost of almost 5000 million a year.

The burden of OA is expected to the increase with ageing of the population, the absence of therapeutics and the increase of the lifespan in the population (57).

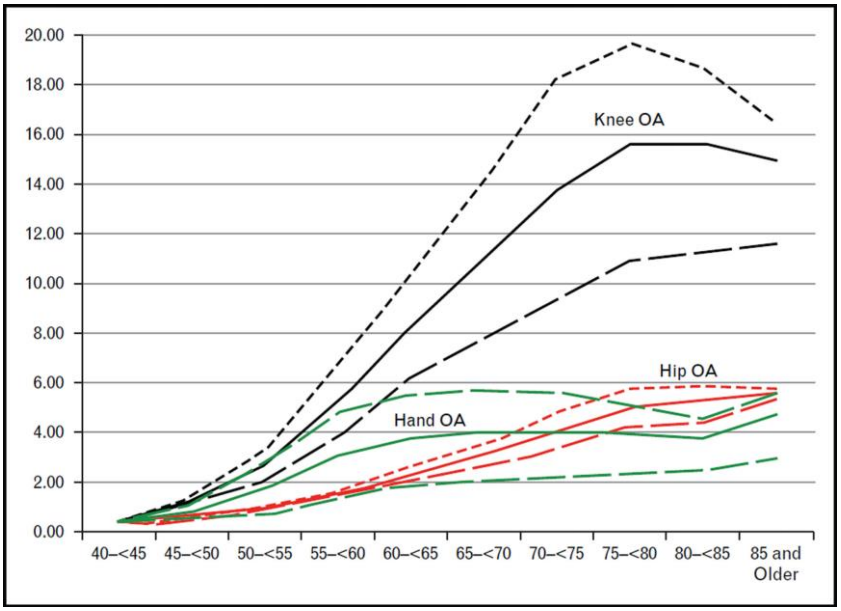

Figure 1.9: incidence of disease with age. Note that the impact of knee OA in the elderly is Higher compared to the other joints (56).

1.6 Molecular mechanisms of aging related disease of musculoskeletal system: The autophagy

To maintain homeostasis, cells need to constantly adapt to environmental cues, by balancing between biosynthetic and degradative processes. In eukaryotic cells, two main degradative processes can occur: proteasomal degradation, responsible for the breakdown of short-lived proteins; and autophagy, responsible for the degradation of long-live proteins, protein aggregates, and entire organelles (58).

1.6.1 Autophagy

In recent years, we have witnessed an explosion of research on a cell biology pathway called autophagy, or from the Greek roots "self-eating" process. It is an evolutionarily conserved intracellular process that occurs in all eukaryotic cells, with a number of similar basic components shared between yeast and mammals (59).

Autophagy occurs constitutively and exerts two main functions: quality control, through the removal and degradation of damaged intracellular components, and maintenance of the cellular energetic balance, or cellular homeostasis, through the release of nutrients from macromolecules. However, additional functions have been suggested, including cellular remodeling and tissue differentiation, cellular survival and response to stress, cell death, senescence, and anti-aging functions. Indeed, autophagy is now considered essential in many physiological and pathological conditions (60, 61).

Three forms of autophagy have been identified: macroautophagy, microautophagy and chaperone-mediated autophagy (CMA). All of them promote proteolytic degradation of cytosolic components at the lysosome. However, they display different mechanisms for the delivery of the cytoplasmic material to the lysosomes. Moreover, micro and macroautophagy have the capacity to engulf large structures, such as entire organelles, through selective and nonselective mechanisms. On the other hand, CMA can only degrade soluble proteins in a selective manner (59, 60). Macroautophagy is the most intensively characterized type of autophagy and, due to increased interest in macroautophagy in articular cartilage; this thesis will focus solely on macroautophagy, hereafter referred to as "autophagy".

Autophagy is a degradation lysosomal process essential for survival, differentiation, development and cellular homeostasis. It is a degradation mechanism

that plays a fundamental role in the regulation of energy and nutrients, as well as in the elimination of organelles and/or macromolecules that are toxic to the cell (62). It can be activated by different factors that induce stress in the cell, such as nutrient deprivation, hypoxia or an increase in ROS production (63). However, in certain pathological conditions, autophagy may act as a type of cell death mediated by the formation of lysosomal vacuoles in the cytoplasm. This type of cell death is known as type II cell death, to differentiate it from type I cell death or apoptosis, which is characterized by chromatin condensation and DNA fragmentation and subsequent disintegration independently of vacuole formation (64).

The most important characteristic of autophagy is the formation of autophagosomes with double membrane by the sequestration of vesicles or organelles in the cytoplasm after the activation of the autogenic machinery or Atg genes.

1.6.2 The Autophagy pathway

The Atg genes are involved in the regulation of autophagy by control of the process of induction and nucleation of autophagy vesicles or autophagosomes, in addition to its expansion and fusion with lysosomes, permitting the degradation by lysosomal enzymes and the degraded material can be recycled and used by the own cell.

The process starts with a double membrane structure, called the phagophore or isolation membrane. The phagophore elongates and engulfs intracellular cargo, resulting in the formation of a double membrane structure named the autophagosome. Consequently, the outer membrane of the autophagosome fuses with the lysosome to form the autolysosome. In here, the degradation of the autophagosomal contents and of the inner membrane of the autophagosome happens, by lysosomal acid proteases (65). Proton pumps, such as ATPases, present in the lysosomal membranes, are responsible for the acidification of the autophagolysosome content. This acidification is required for the activation of lysosomal enzymes responsible for content degradation (66). Then, amino acids and other products generated from the degradation are transported back to the cytoplasm through membrane permeases, where they can be re-used for biosynthesis or energy production (67).

The Atg genes were discovered in yeasts and are highly conserved in the eukaryotes (68). More than 30 Atg proteins have been identified in the last decade, and it was discovered that autophagy is highly regulated at multiple steps (69), Atg1, Atg6, Atg8 (ULK, Beclin 1, LC3 in humans, respectively) and Atg5 are considered the four most important regulators in the autophagy process. ULK1 acts as an intermediary in autophagosome formation; Beclin 1 is part of a complex consisting of PI3K type III and Vps34 that allows the sequestering and nucleation of the vesicles (70). Finally, the formation and expansion of the autophagosome depends on two systems: LC3 and Atg 12-Atg 5. During autophagy, LC3-I is converted into LC3-II through a lipidation process, so it is associated with LC3 -II with vesicles of autophagy with double membrane or autophagosomes (71). A general scheme of the pathway is shown in **Figure 1.10.**

In the elongation/enclosure step, the final step of autophagosome formation, two ubiquitin-like conjugation systems are required, Atg12 and microtubule-associated protein 1 (MAP1) light chain 3 (LC3):

- In the first one requires the conjugation of Atg12-Atg5, which is produced by two ligases, Atg7 and Atg10. Conjugated Atg12-Atg5 then associates with Atg16L dimers to form a multimeric Atg12- Atg5-Atg16L complex, which associates with the phagophore membrane (71, 72). This complex is present on the outer side of the isolation membrane and is essential for its proper elongation and dissociates from the membrane immediately before or after autophagosome formation (68).
- The second time requires the cleavage of the C-terminus of the unprocessed form of LC3 (pro-LC3) by Atg4 to produce the soluble form LC3-I, or cytosolic LC3. LC3-I subsequently conjugates with phosphatidylethanolamine (PE), with the participation of Atg7 and Atg3. The resulting lipidated form of LC3, LC3-II, associates with newly forming autophagosome membranes and is present in both the inner and outer membranes of the autophagosome. This conversion of LC3-I to LC3-II is a key regulatory step in autophagosome formation (71). LC3-II allows the expansion and closure of the autophagy vacuole which means

it is required for autophagosome formation and is commonly used as a marker for autophagosomes (73).

- LC3-II in the outer membrane of the autophagosome is removed by Atg4 that cleaves the PE, returning it to the cytosol for reuse. LC3-II in the inner membrane is digested with the cargo. (74). These two conjugation systems seem to be interconnected. The Atg12-Atg5-Atg16L complex plays an essential role in Atg8/LC3-PE conjugation, and has an E3(ubiquitin ligase)-like activity for LC3 lipidation, contributing to the expansion of the autophagosomal membrane and to the correct localization of LC3 lipidation (75-77) .

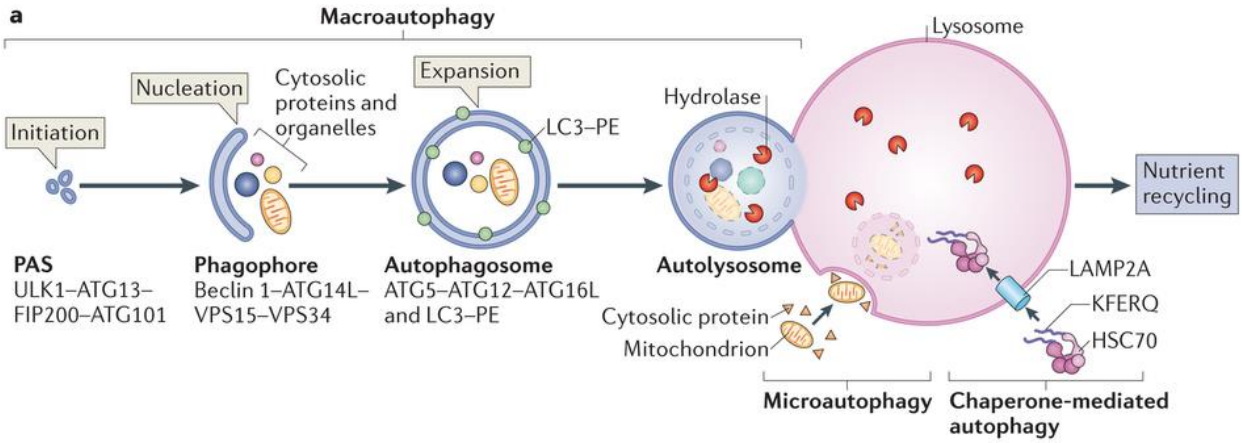

Figure 1.10: scheme of autophagy pathway. The most important steps of the cascade are shown: initiation, nucleation, expansion and fusion of the autolysosome with the lysosome (78)

The amount of LC3-II is related to the formation of autophagosomes and consequently to the activation of the autophagy process (37, 79).

In addition, it is important to highlight the role of the rapamycin target in mammalian cells or mTOR, as the most important regulator of the autophagy process (80). The mTOR complex is a protein kinase that regulates important functions in the cell, such as transcription control, cell cytoskeleton organization, regulation of growth, proliferation and cell survival. The complex mTOR is composed of two components: mTOR complex 1 (mTORC1) and mTOR complex 2 (mTORC2) (40, 61). In fact,

mTORC1, it is responsible for the stimulation of anabolic processes such as protein and lipid synthesis, promotes growth, ribosome biogenesis, gene transcription, and metabolism, and also the control of regulation of autophagy (81, 82).

Effectively, mTORC1 is highly sensitive to cellular nutrient content. In high nutrient and energy conditions, mTORC1 is activated downstream of growth factor receptor signaling, involving activation of Akt and PI3Kinases, and promotes cell growth through induction of ribosomal protein expression and increased protein translation. In starvation and energy conditions mTORC1 is inactivated, resulting in diminished cell growth and allowing the restauration of energy and nutrient levels by autophagy activation.(83)

On the other hand, mTORC2 is involved in the regulation of the cytoskeleton (84). mTORC2 signaling controls members of the AGC kinase family including Akt, serum/glucocorticoid-induced protein kinase1 (SGK1) and protein kinase C (PKC), thus playing an important role in actin cytoskeletal organization, and cell survival and metabolism. Although it seems that mTORC2 is insensitive to nutrients, it responds to growth factors, although the exact mechanism is still unknown. (83)

Both, the deficiency of nutrients by starvation or the use of pharmacological compounds such by Rapamycin or Torin 1 inhibits mTOR, activating the formation of autophagosomes and consequently the activation of the autophagy process.

Rapamycin is a macrolide antibiotic with immunosuppression activity that induces autophagy by blocking mTORC1. In this way, it regulates the participation of PI3-kinase/AKT and the activation of the protein Kinase AMP (AMPK) (62, 83). On the other hand, Torin 1 is a molecule considered highly specific of mTOR, since it inhibits both complexes (85).

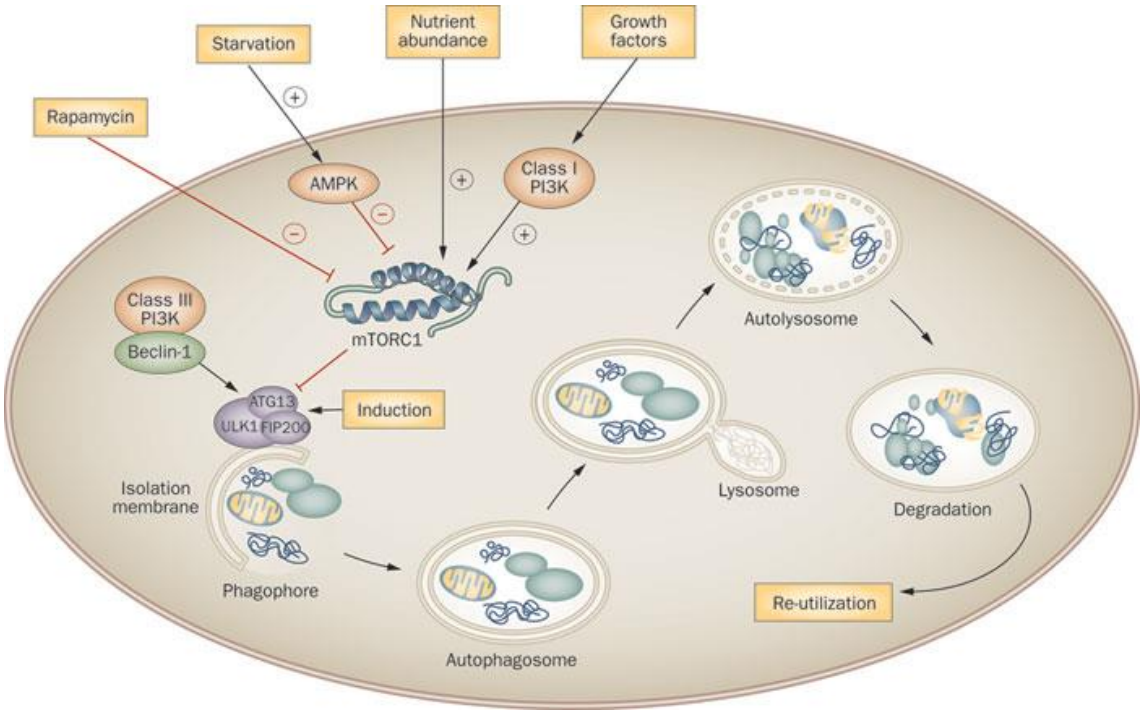

Figura 1.11: Autophagy regulation by mTOR. MTOR is the major regulatory complex of autophagy composed of two components mTORC1 and mTORC2. Blocking this complex with mTOR inhibitors such as rapamycin permits the autophagosome formation and consequently the activation of the autophagy process, to degrade the dysfunctional organelles or mutant protein and to reuse as energy (62).

1.6.3 Autophagy as a key mechanism in aging-related Disease

Autophagy is a mechanism of lysosomal degradation essential for survival, differentiation, development and cellular homeostasis. Autophagy fulfills an adaptive neurodegeneration, heart disease and aging (21). Basal autophagy is key to maintaining function of protection against various pathologies, such as infections, cancer, cellular homeostasis and is rapidly activated when increased demand for intracellular nutrients or energy. In addition, it is also activated to protect the cell against oxidative stress, infections or accumulation of protein aggregates or dysfunctional organelles, such as mitochondria (80). Autophagy defects are directly related to abnormalities in musculoskeletal development, neurodegeneration, cardiomyopathies, and even death (86, 87) . A better understanding of autophagy mechanisms may lead in the discovery of new therapeutic approaches to prevent joint damage.

1.6.4 Autophagy and OA.

The articular cartilage is an avascular, aneural, alymphatic, and viscoelastic connective tissue that obtains its nutrition and oxygen supply by diffusion from synovial fluid and subchondral bone. (88)

The articular cartilage is characterized by a low rate of cell renewal, so an activation of autophagy could be essential to maintain cell integrity, function and cell survival.(89) Although the mechanism implicated in the development of OA remains undetermined, it is known that there is an interruption of the homeostatic state and an increase in chondrocytes.

Autophagy is an essential component of chondroptosis and, in excess; it can also lead to autophagic cell death in chondrocytes. Nevertheless, autophagy can play a dual role in chondrocyte fate, as compelling studies have congregated on the cytoprotective role of autophagy in OA development. More exactly, it seems that the chondrocyte death process evolves during OA progression and depending on the cartilage layer considered. Induction of autophagy by Rapamycin reduced IL-1β-induced intracellular ROS production, possibly by removing damaged mitochondria, thereby protecting chondrocytes from IL-1β-induced OA-like changes (90).

In this sense, it has been demonstrated that the expression of autophagy mediators (ULK1, Beclin1 and LC3) is increased in human normal cartilage, promoting the maintenance of cartilage homeostasis. This increase was observed predominantly in the superficial zone. However, the expression of these mediators decreased in human aging and OA cartilage and this decrease was correlated with an increase in cell death by apoptosis.

This increase was observed predominantly in the superficial zone. However, the expression of these mediators decreased in human aging and OA cartilage and this decrease was correlated with an increase in cell death by apoptosis (37, 91). During the initial degenerative phase, autophagy is increased in OA chondrocytes and cartilage, with increased expression of LC3 and Beclin1 messenger RNA in OA chondrocytes, might be as a compensatory response to cellular stress, with damage occurring when prolonged stress exceeds the capacity of this mechanism (92). In cartilage with mild OA, ULK1, Beclin1, and LC3 protein expression are decreased in the cartilage

superficial zone, though these three proteins are strongly expressed in the OA cell clusters as well as in the middle and deep zones (37, 93). In mouse OA knee joints, expression of ULK1, Beclin1, and LC3 are decreased together with glycosaminoglycan loss, whereas poly (ADP-ribose) polymerase (PARP) p85 expression is increased with gradual cartilage degradation. This reduction in autophagy regulators is accompanied by increased apoptosis (92).

In this sense, spontaneous aging model in mice indicated that basal autophagy levels are diminished with age, which might contributes to the accumulation of damaged macromolecules or dysfunctional organelles (94). These pathological features are key in the development of many diseases aging-related diseases, such as OA (95, 96). By contrast, other studies showed an increase in LC3-II and Beclin1 expression in OA chondrocytes, suggesting an up-regulation of autophagy in OA chondrocytes compared to normal chondrocytes (90). Another study described that OA tissues display numerous autophagic LC3 puncta while no elevation in punctate LC3 was observed in healthy cartilage (97). The authors justified these opposite observations with the different location of harvested OA cartilage that potentially corresponds to different OA stages. The authors proposed that during OA progression, autophagy can act as an adaptive response to protect cells. However, once severe OA is established, a decrease in autophagy was detected, indicating that failure of autophagy could contribute to OA progression (90). Genetic studies support the importance of autophagy in physiological and pathological events. In most experimental models, suppression of this mechanism leads to cell death, indicating that autophagy promotes cell survival and protection (86). Additionally, the cartilage-specific deletion of mTOR upregulates autophagy and protects mice from developing OA (37, 91). In this sense, many studies identified correlations between the mTOR signaling pathway and autophagy. Upregulated mTOR expression in OA is correlated with increased chondrocyte apoptosis and reduced expression of key autophagy genes, including ATG3, ATG5, ATG12, ULK1, MAP1LC3B and Beclin-1. Interestingly, Rapamycin treatment, which promotes autophagy by mTOR inhibition, increased levels of autophagy markers and autophagosome formation in healthy chondrocytes, in response to mechanical damage and in an experimental OA model in mice. (37, 91)

1.6.5 Role of Autophagy in Mitochondrial Function

The mitochondria is present in the most eukaryotic cells like the fundamental organelles, for the generation of cellular energy in the form of ATP by the process of oxidative phosphorylation (98). In addition, it plays an important role in many cellular events, ionic homeostasis and various anabolic and catabolic processes.

The mitochondria contains the mitochondrial respiratory chain (MRC)or the electron transport chain (ETC), consisting of 5 multimeric protein complexes: CoQ1 NADH dehydrogenase (complex I), succinate dehydrogenase (Complex II), ubiquinone cytochrome C reductase (Complex III), cytochrome C oxidase (IV complex), and ATP synthase (V complex) (99). ETC also requires two small electron carriers, ubiquinone (coenzyme Q10) and cytochrome c (100). The movement of electrons between the four first complexes of the chain produces a proton gradient through the inner mitochondrial membrane that is used by the V complex to generate ATP. While this process is efficient, a reduced number of electrons can partially reduce oxygen giving rise to the formation of superoxide free radical, which can cause oxidative damage in the mitochondria and contribute to decline in its function (101). In this regard, over the past decade, numerous studies have shown that alterations in mitochondrial proteins are implicated in the development of some human diseases, such as Alzheimer's, Parkinson's, Type 2 diabetes, cardiovascular diseases and aging-related pathologies (102), such as the topic of my thesis, OA.

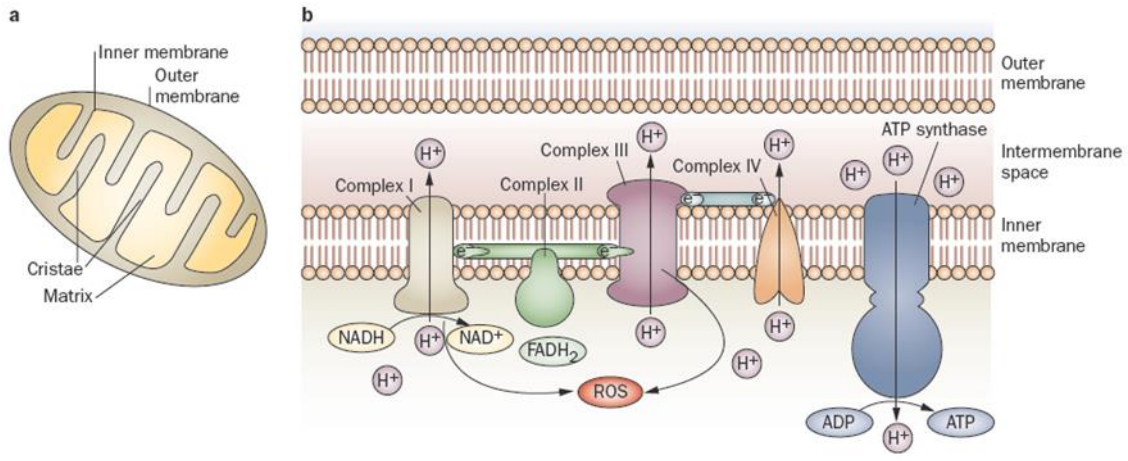

Figure 1.12: Structure and function of mitochondria. A, image of the morphology of a mitochondria, where the mitochondrial crests formed by the invagination of the double membrane are represented. **B**, Mitochondrial respiratory chain located on the double membrane of the mitochondria, where mitochondrial respiratory chain complexes are represented. We can see the flow of e^- and H^+, for obtaining energy from the mitochondria. Image obtained from Blanco et al, 2011 (20).

The role of mitochondria is being studied in detail, and recent studies have emphasized its important potential in understanding many aging-related pathologies, including OA. In this sense, several studies have described the occurrence of a failure in mitochondrial function in OA pathology associated with excessive production of reactive oxygen species (ROS) (20, 103). In addition, OA chondrocytes have been shown to decrease the activity of complexes I, II and III compared to normal chondrocytes, consequently causing a reduction in mitochondrial membrane potential, a decrease in ATP synthesis, and finally Cell death (99, 104). A defect in the transmembrane potential of mitochondria leads to a cascade of signals linked to programmed cell death or apoptosis. On the other hand, increased citrate synthase activity in OA chondrocytes suggests that mitochondrial mass is increased as a possible compensatory mechanism for electron deficiency, as well as low ATP levels and altered membrane potential. The ETC is one of the most important sites for the regulation of ROS production. The Inhibition of activity in complex III with Antimicin A has been shown to increase ROS production (16, 105).

In addition, *in vitro* studies that use human articular chondrocytes have indicated that the use of specific ETC inhibitors suppress the synthesis of both proteoglycans and collagen, fundamental components of the cartilage structure (106) and increase the production of inflammatory mediators (99). In this sense, inhibition of complex I using Rotenone reduces the content of proteoglycans in the superficial and intermediate zone of the cartilage and an increase in the liberty of glycosaminoglycans from the cartilage to the supernatant. On the other hand, the inhibition of complexes III or V in chondrocytes induced the production of proinflammatory mediators, such as IL-1, IL-6 and IL-18 cytokines or prostaglandin E2 (PGE2). All of these findings suggest that mitochondria may be an interesting organelle to study in our model of defective autophagy related to cartilage degradation (107).

Previous studies have shown that mitochondria represent one of the most important pathways of chondrocyte degradation. Patients with different genetic polymorphisms in mitochondrial DNA (mtDNA) have higher probability of suffering from osteoarthritis, as well as their regulation of metalloproteases and OA biomarkers (108).

The T haplogroup a slower progression OA, unlike as compared to the carriers of haplogroup H. When the thickness of the cartilage was analyzed, there was also a smaller decrease in the haplogroup T than in H, similarly as occurred in other non-H haplogroups, whose cartilage degradation was slower (109).

The relationship between mitochondria and autophagy is dual. First, mitochondria may be the selective target of autophagy or Mitophagy (110)., an important process for the removal of damaged mitochondria that are potentially hazardous to ROS production. Second, mitochondria actively contribute to autophagy in response to multiple mechanisms, since mitochondrial membranes are the first organelle to mediate autophagy vesicles formation (111, 112). In addition, defects in autophagy are associated with different human diseases such as cancer and neurodegenerative diseases, which are also related to mitochondrial dysfunction.

At the cellular level, a failure in autophagy leads to an increase in the reactive oxygen species (ROS) and abnormal gene expression that can trigger cell death (38). Increased levels of ROS can cause oxidative damage in mitochondrial DNA (mtDNA), lipid peroxidation and activation of pathways that can accelerate cartilage degradation. In addition, high levels of ROS can lead to the elimination of collagen and hyaluronic acid (113). ROS are intimately associated with accelerated aging and with the development of degenerative pathologies. In addition, ROS increase is stimulated by the deposition of proteins that stimulate the production of ROS and the accumulation of defective mitochondria

Therefore, understanding the relationship between mitochondria and autophagy is critical to understanding the cellular and molecular mechanisms of aging-related diseases (114).

1.6.6 Autophagy and Aging

Aging is a natural and inevitable process by which living organisms approach the twilight of their existence. Human aging is a complex physiological process, characterized by the declining ability of the different organs and tissues to respond to stress, increasing homeostatic imbalance and risk of disease,(115) which is accompanied by the gradual decline and adaptation of different body systems to the un avoid able passage of time. It is characterized by a progressive loss of structure, function, co-ordination and physiological integrity, leading to impaired homeostasis in all systems.

One of the hallmarks of aging is cellular senescence. Normal cells possess a finite lifespan. Cells are continually exposed to a variety of harmful exogenous and endogenous factors that may induce stress and cause reversible or irreversible damage leading to complete recovery or cell death, respectively.(116)

Clearly, age is one of the most important risk factors for OA, followed by other factors such as metabolic diseases, joint trauma, joint instability or genetic factors. As we age, our tissues undergo age-related changes. OA is a multifactorial disease in which cartilage degradation is a central feature. The ageing includes changes in metabolic activity, mitotic activity, sensitivity of chondrocytes to growth factors, responsiveness to anabolic stimuli. Age-related changes in articular cartilage contribute to the development and progression of OA.

In aging, articular cartilage chondrocytes show not only failure in proliferative and synthetic capacity but also have increased secretion of pro-inflammatory mediators, matrix degrading enzymes and oxidative stress, all of which can contribute to the development and progression of OA (117).

Osteoarthritis (OA) is closely associated with aging, but its mechanism is not well understood. Many factors, including senescence, low chondrocyte metabolic rate, mitochondrial dysfunction, oxidative stress, and abnormal accumulation of advanced glycation end products (AGEs) may all play a key role in the pathogenesis of age-related OA (103, 118).

As mentioned earlier, "chondrosenescence", is an age-dependent deterioration of chondrocyte function, characterized by expression of senescence-associated markers, erosion of chondrocyte telomere length and mitochondrial dysfunction due to oxidative damage causing the age related loss of chondrocyte function (119). In this new framework chondrosenescence is intimately linked with inflammation and the disturbed interplay between autophagy and inflammasomes. This refined definition contextualizes the pro-inflammatory phenotype of chondrosenescent cells during the aging process and in age-related joint diseases, implicating mitochondrial dysfunction, oxidative stress and activation of inflammasomes.

Extracellular matrix changes with aging also contribute to the propensity to develop OA and include the accumulation of proteins modified by non-enzymatic glycation. Thus, the survival of the chondrocytes is important for maintaining a suitable cartilage matrix. Damage to chondrocyte function and survival would lead to the breakdown of the articular cartilage. The release of soluble and insoluble factors secreted by senescent chondrocytes further contributes to the inflammatory microenvironment that is believed to drive the catabolic degradation of extracellular matrix (ECM) macromolecules in articular cartilage (119).

The OA chondrocytes show a senescence secretory phenotype (SSP) consisting on the overproduction of cytokines (interleukins 1 and 6), growth factors and matrix metalloproteinases (MMP) (115). MMPs are important regulators of the degradation of ECM during OA development. Among the MMPs, MMP-3 and MMP-13 are important for degrading components of ECM, including collagens, proteoglycans, and other extracellular matrix macromolecules in cartilage. The serum level of MMP-3 was found to be elevated with aging in patients with OA, and this protease is capable of cleaving proteoglycans. In addition, MMP- 3 can indirectly activate pro-MMP-9, a gelatinase. Recent studies elucidated that elevated MMP-13 was noted at the deep zones of arthritic cartilage, and this protease appears to be the major MMP responsible for matrix degradation.(120) Reactive Oxygen Species (ROS) play a major role in the induction of the SSP. In chondrocytes, an increase in ROS production leads to hyper-peroxidation, protein carbonylation and DNA damage which alter chondrocyte function. ROS overproduction also induces changes in metabolic pathways such as PI3K-Akt and ERK (115).

Alterations in protective mechanisms such as decreased antioxidant defense and reduced autophagy, also occur with aging, disturbing the anabolic-catabolic equilibrium and reducing the remodeling and repair ability of cartilage (121, 122).

Autophagy plays a crucial role in the homeostatic regulation of energy and nutrients, by removing macromolecules and damaged organelles, allowing cell survival under limited nutrient conditions. A failure in homeostasis can lead to neurodegenerative diseases, cardiomyopathy, abnormal musculoskeletal development and premature death (62, 80).

Autophagy is closely associated with the retardation of aging and therapy for age-related diseases due to its cellular housekeeping role by removing dysfunctional cellular organelles and proteins. However, autophagy declines with aging and during OA. Furthermore, the reduction of autophagy is often accompanied with increases in apoptosis and cartilage degeneration. It has been proposed that autophagy maintains its declination tendency after its peak at the early stage of OA and further causes the aggravation of OA.

As discussed earlier, articular cartilage is characterized by a low rate of renewal, , which fails to regenerate and remodel the cartilage adequately (123), autophagy seems to play an essential role in cell survival, since a reduction in the expression of autophagy in cartilage of mice and elderly humans is observed is accompanied by an increase in apoptosis of chondrocytes (62, 124).

In cartilage, aging-related loss of autophagy leads to chondrocyte death and OA, while stimulation of autophagy exerts protective effects on cartilage deterioration. Aging also interferes with epigenetic mechanisms such as activity of histone acetylases that control the pattern of DNA methylation, and induces up- or down-regulation of microRNAs expression. A deeper knowledge of the mechanisms involved in chondrocyte aging could identify potential targets for the treatment of OA, a prevalent and therapeutic-orphan disease (115).

More recently, autophagy has been studied as a mechanism that can regulate age-related changes in articular cartilage. Aging human chondrocytes and old mice exhibit a reduction in constitutive autophagy some mechanisms occurring during the aging process can explain the impaired autophagy observed, including defects in autophagy induction and inefficient lysosomal clearance. For instance, the altered

hormonal regulation of autophagy observed in aged tissues can be a possible explanation. In fact, in old organisms the ability of glucagon to upregulate autophagy appears compromised (89). Moreover, the interactions of the signaling network involving longevity factors, determinate pathways involving pro-longevity factors such as Sirtuin 1 (SIRT1) and transcription factor forkhead-box O3 (FOXO3), and pro-senescence factors like mTOR, NF-kB and p53 are also autophagy regulators and thus can be involved in aging (125).

On the other hand and as we said before, the activation of autophagy by inhibition of mTORC1 presumably maintains cellular function during ageing by allowing enhanced degradation of aged cellular components, thus protecting from toxicity, and consequently slowing aging. Additionally, other processes regulated by mTORC1 can also contribute to the pro-longevity effects of mTOR inhibition, including reduction of protein synthesis, regulation of mitochondrial function, reduction in inflammation, increased stress resistance and preserved stem-cell function (126).

A large body of evidence suggests that the activation of autophagy by rapamycin, extend the lifespan of mice and protects them against degenerative pathologies. However, increased autophagy does not always have a beneficial effect, in fact may also contribute to the opposite effect, as seen in progeroid premature aging mice. Interestingly, rapamycin reduces the senescence in cells derived from patients with Hutchinson-Gilford, which is characterized by the accumulation of progerin, a defective variant of lamina A, which is detected in low amounts during normal aging. Activation of autophagy by rapamycin promotes the removal of diseased cells, and therefore limits normal progerin accumulation with age (127). Proper regulation of autophagy is likely to be a determinant of healthy aging, and further studies are needed to determine the exact role of autophagy in OA and how it is regulated (128).

1.6.6.1 The role of autophagy in age related targets: Lamin A/C

The nuclear lamins are proteins of the intermediate filaments that form part of the network of proteins that underlies the nuclear envelope. They participate in the regulation of the structure and form of the nucleus, and they provide the organization of heterochromatin, transcription factors and nuclear complexes. There are two types of

sheets, type A (isoforms A and C) and type B (sheet B1 and B2). All sheets other than sheet C are subjected to a post-translational maturation process at their C-terminal CAAX (C-cysteine, A-aliphatic, X-any residue). The CAAX modification involves a series of events including CAAX cysteine farnesylation, endoproteolytic elimination of terminal residues (aax) and finally carboxymethylation of farnesylated cysteine (129).

Subsequent to modification of the C-terminal end of prelamin A, the 15 amino acids of the "glue" of prelamin A are cleaved endoproteolysis giving rise to mature A-lamina. The enzyme mediating this cleavage step is the Zn^{2+} membrane metalloprotease (Zmpste24). The Zmpste24 plays a double role in the maturation process of prelamin A, on the one hand it participates in the elimination of the endoproteolytic of the terminal end -AAX, but on the other hand, it is the only one to participating in the carboxymethylation of farnesylated cysteine.

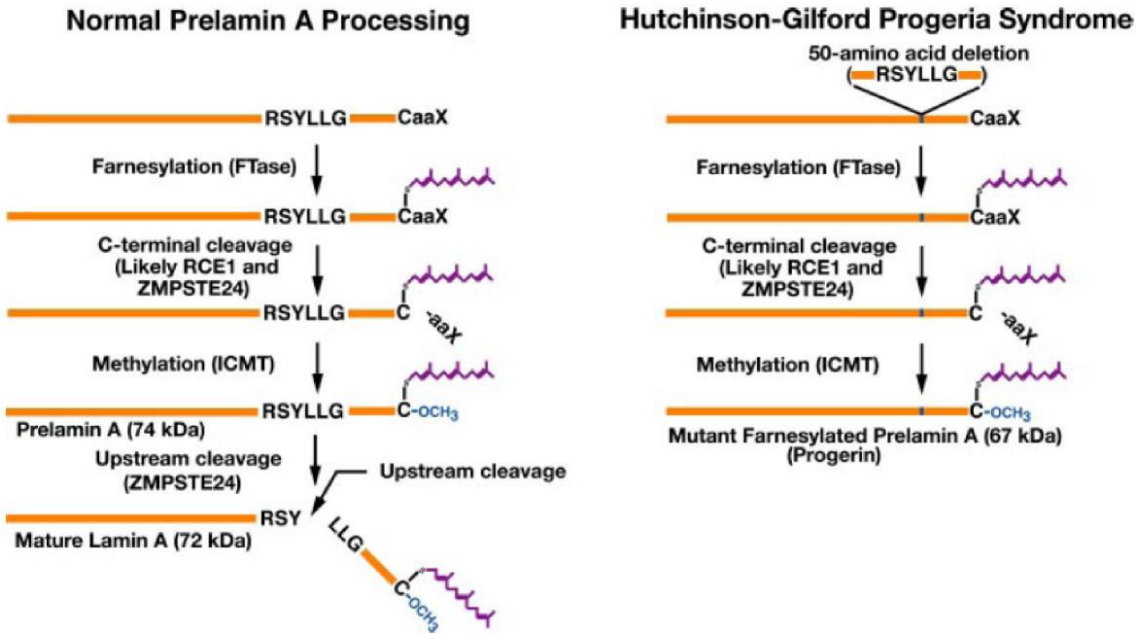

Figure 1.13: Maturation pathway of prelamin A. In the absence of Zmpste 24, the excision of -AAX does not occur which produces an accumulation of farnesylated prelamin in the nuclear membrane of the cell. It is not performed in the endoproteolytic cleavage process, resulting in anomalous maturation of lamin A, resulting in progerin accumulating in cells (130).

However, this whole process can be blocked by farnesyltransferase inhibitors (FTI). The absence of farnesylation, prevents the endoproteolytic prelamin processing so there is no accumulation of farnesylated prelamin.

The reason for the removal of the tail of prelamin A is not entirely clear, but its non-cleavage is associated with disorders ranging in severity from mild to deadly neonatal progeroid syndrome. These diseases, in order of increasing severity, include metabolic disorder, mandibuloacral type B dysplasia, Hutchinson-Gilford Progeria syndrome (HGPS) and neonatal restrictive lethal dermopathy (LD). These diseases are either caused by mutations in the genes encoding any lamin A isoforms, or in the enzyme Zmpste 24.

The HGSP is the most known and studied disease, related to premature aging resulting from an active mutation at the cryptic splicing site in the lamina A gene. This error eliminates the coding zone for Zmpste24, so it does not occur the cleavage in the prelamin A, resulting in a mutant form of lamin A, called progerin. Progerin produces toxic effects in the cell, which leads to damage in chromatic and cellular senescence, causing acceleration in aging. HGSP, as well as other progeroid disorders or laminophaties, highlight spot the importance of correct maturation of prelamin A by Zmpste24 (129, 131).

Lamin A/C was previously found dysregulated in OA cartilage, but the mechanism that regulates this alteration is still unknown (132).

Aging is the most important risk factor correlated with OA (133) and is intimately associated to decreased basal autophagy activity (134). The role of lamin A/C in the context of defective autophagy might shed light in the molecular mechanism of cartilage aging and joint disease.

CHAPTER 2: SIGNIFICANCE, HYPOTHESIS AND OBJETIVES

Significance to the musculoskeletal system

OA is a major musculoskeletal cause of disability in the elderly, but current therapeutic approaches, including moderate exercise, lifestyle modification and pain medications, do not prevent initiation and progression of the disease. OA affects nearly to 27 million people in the United States, accounting for 25% of visits to primary care physicians, and half of all NSAID prescriptions. It is estimated that 80% of the population have radiographic evidence of OA by 65 years of age. Given the epidemiological evidence, the identification and validation of novel and effective targets for OA is expected to have a dramatic impact on OA prevention and treatment.

Recent progress has led to the characterization of some pathogenic pathways, but little is known about mechanisms of aging and OA. The results showed in this doctoral thesis will contribute to a better understanding of the role of autophagy in aging and how defective autophagy contributes to OA.

Key Points

1. Aging-related pathologies, including osteoarthritis (OA), are the major causes of disability and contribute substantially to the global burden of disease.
2. OA, the most common disease related to aging, is characterized by the destruction of articular cartilage, the degradation of the extracellular matrix and a reduction of cellularity.
3. Autophagy is a key mechanism of cell homeostasis and exerts a protective and promoting function.
4. Mitochondrial function is central in aging and is associated to the development of OA.
5. Autophagy defects are found in aging and OA. As a result, damaged macromolecules accumulate and lead to cell death accelerating the breakdown of tissue. The molecular mechanisms of action regulating this degenerative process are still unknown.

Hypothesis

"A reduction in autophagy related to the aging process contributes to the accumulation of damages organelles and proteins, which would lead to a failure in the mechanisms of cartilage homeostasis, contributing to the development of OA".

Objectives

The general goal of this thesis is to elucidate the role of autophagy in the mitochondrial function, and to identify molecular regulators of autophagy. Our study leads to the discovery of new therapeutic strategies for aging-related musculoskeletal disorders such as OA. To address this problem, we propose the following specific objetives:

Objective 1: To study the effects of defective autophagy to mitochondria function using pharmacological and genetic approaches:

1.1. Modeling mitochondrial dysfunction in human chondrocytes.
1.2. To study the effect of mitochondrial dysfunction on autophagy pathway in human chondrocytes.
1.3. To evaluate the effect of pharmacological activation of autophagy in human chondrocytes with mitochondrial dysfunction.

Objetive 2: To identify potential targets of defective autophagy associated with the pathology of muskuloletal system

1.1. Differential proteomic screening of defective autophagy in human chondrocytes.Identification and validation of regulators of defective autophagy related to aging and OA in human chondrocytes.
1.3. To analyse the consequences of laming A/C accumulation in the musculoskeletal system by using an *in vitro* and *in vivo* model of accelerated aging.

CHAPTER 3: MATERIAL AND METHODS

3 Cell culture

3.1 Primary chondrocyte isolation and culture.

Normal human articular cartilage was harvested at the time of autopsy from the femoral condyles and the tibial plateaus of donors who had no history of joint disease and had macroscopically normal cartilage surfaces. OA human cartilage was obtained from patients undergoing knee replacement. Briefly, cartilage slices were incubated for 15 minutes at 37°C with trypsin (0.5 mg/ml; Sigma-Aldrich, St. Louis, MO, USA). After the trypsin was removed, the cartilage slices were incubated overnight at 37°C with 2 mg/ml of clostridial collagenase (Sigma-Aldrich) in DMEM with 5% Fetal Calf Serum (FCS), with shaking.

The isolated chondrocytes were recovered and plated in DMEM supplemented with 10% FCS, L-glutamine, and 1% antibiotics (Penicillin-Streptomycin, Sigma-Aldrich) and were allowed to attach to the culture flasks. The cells were incubated at 37°C in a humidified gas mixture containing 5% CO2 balanced with air. The chondrocytes were used in the experiments in the first passage at confluence.

The Ethics Committee of Galicia, Spain, approved this study.

3.1.1 Culture of cell lines in monolayer

The immortal juvenile human chondrocytes, T/C28a2, used in this study were developed and donated by Mary Goldring as we described in the Introduction section (24). Cells were cultured in Dulbecco's modified Eagle's medium (DMEM; Life Technologies) supplemented with 10% (FCS; Life Technologies) 10% FCS, L-glutamine, and 1% antibiotics (Penicillin-Streptomycin, Sigma-Aldrich) and maintained at 37°C in the presence of 5% CO2. Cells were cultured in monolayer and grown to confluence.

3.2 General conditions of the cell culture experiments

To perform the experiments, T/C-28a2 cells or primary human chondrocytes were plated in different formats depending on the study to be performed: 6-well plates ($1.5x10^5$ or $5x10^5$ cells /well) for transfection studies or protein isolation, respectively; 12-well plates ($2.5\ x10^5$ cells/well) for determination of mitochondrial membrane potential ($\Delta\psi m$), Reactive Oxygen Species (ROS) production, or quantification of cell death by apoptosis; 8-well chamber slides ($1x10^5$ cells/well) for microscopy experiments (Hoescht and LC3 quantification) and 96 well plates for clone isolation in CRISPR / Cas9 genetic editing technique.

Experiments were performed when the cells have acquired proper confluence. The chondrocytes were plated in 10% FCS and then media was changed to DMEM 2% FCS, under basal conditions or in the presence of different stimuli. For transfection experiments, human chondrocytes were plated in 6-well dishes in DMEM containing 10% FCS without antibiotics prior to transfection.

3.2.1 Stimuli used in the experiments

All the stimuli used in the development of this project were prepared as solutions according to the manufacturer's recommendations. The solvent used for resuspension, the recommended storage concentration and the final concentration are summarized in Table 3.1.

Oligomycin (Oligo, 10µg/ml, Sigma-Aldrich), a mitochondrial respiratory chain complex V inhibitor was employed to induced mitochondrial dysfunction in human chondrocytes at the indicated times. Rapamycin (Rapa, 10µM, Calbiochem), a mTORC1 inhibitor, or Torin1 (50nM, Tocris Biosciences), a mTORC1 and mTORC2 inhibitor, were employed to induced autophagy in human chondrocytes at the indicated times. Antimycin A (40µg/ml), Valinomycin (µM), H_2O_2 (100µM), or Tumor Necrosis Factor α (TNFα; 10ng/ml) and Actinomycin D (1µg/ml), all from Sigma-Aldrich, were used as positive controls for mitochondrial dysfunction, mitochondrial membrane depolarization, ROS production, and cell death by apoptosis, respectively.

Table 3.1: Stimuli used in the experiments

Name	Solvent	Concentration	Function
Oligomycin	DMSO	10µg/ml	MRC Complex V Inhibitor
Antimycin A	DMSO	40µg/ml	MRC Complex III Inhibitor
Rapamycin	DMSO	10µM	mTORC1 Inhibitor
Torin1	DMSO	50µg/ml	mTORC1/C2 Inhibitor
Valinomycin	DMSO	1µM	Mitochondrial Dysfunction
TNFα	Water	10ng/ml	Proinflammatory cytokine
Actinomycin D	DMSO	1µg/ml	Transcription Inhibitor
Hydrogen Peroxide	Water	100µM	ROS production

3.3 Mitochondrial function studies

3.3.1 Determination of mitochondrial membrane potential (MMP)

To determinate the mitochondrial membrane potential, the fluorophore JC-1 (5',6,6'-Tetrachloro-1,1',3,3'-tetraethyl-imidacarbocyanine iodide) and cationic cyanine dye DiIC1 (1, 1 ', 3,3,3', 3'-hexamethylindodicarbo-cyanine iodide) were employed.

Briefly, the chondrocytes were cultured in 12-well plates at 2.5 × 10 5 cells/well and treated with experimental conditions. After the incubation time, the cells were washed with PBS, trypsinized and centrifuged at 1800 rpm for 10 min at 4 ° C. Then, the cellular precipitates were resuspended in 0.5 ml of PBS and centrifuged again. Subsequently, after decanting the supernatant, the precipitate was resuspended in 300 µl of a mixture of fluorophore (10 µg/ml) and DMEM medium with 2% FCS. The samples were then incubated in 1.5 ml open tubes for 20 min at 37 ° C in a humidified oven with 5% CO_2, covered with silver paper to protect them from light. After the incubation time, the cells were washed with PBS to finally be resuspended in 350 µl of PBS and analyzed on a flow cytometry (FACScan, Cell-Quest program, BD).

JC-1 is a cationic carbocyanine which has the property of emitting two types of fluorescence depending on membrane potential changes. If the membrane potential is not altered, the fluorophore will emit red fluorescence, as it has the ability to aggregate it and reach the mitochondrial intermembrane space. In contrast, if the membrane potential is decreased, the fluorophore cannot access the mitochondrial intermembrane space and therefore will remain in monomeric form by emitting green fluorescence.

As a positive control, Valinomycin (1µM, Sigma), which is characterized as a potent membrane depolarizer, was used. Analysis of data was performed using a flow cytometer (FACScan, Cell-Quest program, BD). The cytometer was calibrated to detect the fluorescence of the monomeric form through the detector FL1 (green fluorescence at 390nm) and the fluorescence signal of the aggregated form through the detector FL2 (red fluorescence at 340nm). In each experiment, 10,000 events were analysed. The values obtained were plotted as a function of the relationship between red fluorescence (unchanged potential) and green fluorescence (potential decreased) for JC-1 experiments.

DilC_1 accumulates primarily in mitochondria with active membrane potential. However, DilC_1 staining intensity decreases when the mitochondrial membrane

potential is disrupted. Photomultiplier settings were adjusted to detect $DilC_1$ fluorescence signal on the FL4 detector. Mean fluorescence intensity values for FL4 were obtained in all experiments. In each experiment, 10,000 events were analyzed. Results are expressed as the ratio of $DilC_1$ fluorescence intensity values. $DilC_1$, which accumulates in the mitochondria when the membrane potential is active, so the fluorescence intensity decreases when the membrane potential is low, when cells are treated with reagents that disrupt mitochondrial membrane potential.

The cytometer was calibrated to detect the $DilC_1$ signal in FL4. In each experiment 10,000 events were analysed, the results were expressed as a function of the fluorescence intensity of $DilC_1$.

3.3.2 Quantification of reactive Oxygen Species Production

The dye 2,7-dichlorodihydrofluorescein diacetate (DCFH-DA; Sigma-Aldrich) was used to evaluate the intracellular production of Reactive Oxygen Species Production (ROS). Briefly, chondrocytes were treated as indicated, and the cells were washed and incubated for 30 minutes with DCFH-DA (10 μM) in 1 ml of DMEM. DCFDA is deacetylated by cellular esterases to a non-fluorescent compound, which is later oxidized by ROS into 2',7'–dichlorofluorescein (DCF). DCF is a highly fluorescent compound which can be detected by fluorescence spectroscopy with maximum excitation and emission spectra of 495 nm and 529 nm, respectively. After washing, the cells were resuspended in phosphate buffered saline (PBS), and visualized by flow cytometry (FACScan, Cell-Quest program, BD Biosciences) in the FL1 channel, with fluorescence levels indicating the percentage of positive cells for intracellular ROS production.

For MitoSOX Red–based flow cytometric detection of mitochondrial superoxide, cells were treated as indicated and then incubated for 30 minutes with MitoSOX Red superoxide indicator in Hanks' balanced salt solution with Ca^{+2}/Mg^{+2} (HBSS, all from Life Technologies). After washing, the cells were resuspended in PBS and visualized by flow cytometry in the FL2 channel, with fluorescence levels indicating the percentage of positive cells for mitochondrial superoxide. In each experiment, 10,000 events were analysed.

Cell Death Studies

3.3.3 Determination of Cell Death by Apoptosis

To determine early and late apoptosis, chondrocytes were labeled with Annexin V and Propidium Iodide, respectively (ImmunoStep). Human chondrocytes were cultured as described above. Before reaching confluence, the cells were plated in 12-well plates at $2.5x10^5$ cells per well and cultured in DMEM with 10% FCS for 24 hours. Then, medium was replaced with DMEM with 2% FCS, and the chondrocytes were preincubated for 4 hour with Rapamycin (10μM) or Torin1 (50nM) and then stimulated Olygomycin (10μM) for 18 hours. After the incubation time, cells were trypsinized, washed with PBS and centrifuged at 1500 rpm. After decanting the supernatant, the precipitate was resuspended in PBS and centrifuged again at 3000 rpm/5 min and then incubated with Annexin-V and PI.

Annexin-V, is a fluorophore active in normal live cells, while phosphatidylserine (PS), a fluorophore that attaches to the cytoplasmic surface of the cell membrane. However, in apoptotic cells, PS is translocated from the inner to the outer leaflet of the plasma membrane, thus exposing PS to the external cellular environment. The human anticoagulant, Annexin V, is a 35–36 kDa Ca2+-dependent phospholipid- binding protein that has a high affinity for PS. Annexin V can identify apoptotic cells by binding to PS exposed on the outer leaflet (135).

On the other hand, PI is impermeant to live cells and apoptotic cells, but stains only dead cells with red fluorescence, binding tightly to the nucleic acids in the cell.

Then, the cells were analyzed on a FACSCalibur instrument (Becton Dickinson). For each condition, 10,000 events were collected. Results are expressed as the percentage of Annexin V–positive cells or the percentage of PI–positive cells.

3.4 Autophagy function studies

3.4.1 Immunofluorescence

Human chondrocytes were cultured on 8-well slides (Corning Costar) and treated with different stimuli as indicated. Then, the cells were fixed with 4% paraformaldehyde–PBS for 10 minutes at room temperature, and permeabilized with 0.3% Triton X-100 in PBS at room temperature for 15 minutes. Then, the cells were blocked in 5% normal goat serum (NGS) in PBS for 30 minutes and incubated for 1 hour at room temperature with rabbit polyclonal light chain 3 (LC3) antibody (1:500 dilution, catalog no. PM036; MBL International) in 1% NGS/PBS. A fluorescent dye–conjugated secondary antibody (Alexa Fluor 488–conjugated rabbit IgG, 1:200 dilution, catalog no. A-11034; Life Technologies) was added and incubated for 30 minutes at room temperature. The nuclei was analyzed by incubating the cells for 10 minutes with Hoechst 33342 (1 μg/ml; Life Technologies). Finally, the slides were mounted with ProLong Gold Antifade Reagent (Life Technologies) and observed with fluorescence microscopy (Olympus). All images were imported into ImageJ Software (National Institute of Health) for quantitative image analysis.

3.5 Proteomic studies

3.5.1 Processing of protein samples for isobaric tags for relative and absolute quantification (iTRAQ) labeling

Proteomics based on mass spectrometry has emerged a powerful method to search for potential protein targets. As typical proteomic experiment, consist of extraction of proteins, their separation and identification by mass spectrometry.

This technique permits the analysis of 4 to 8 biological samples at the same time. The four reagents used in the iTRAQ 4-plex version are named 114, 115, 116 and 117. The eight reagents include these four and four additional reagents called 113, 118, 119 and 120. Each reagent is composed of a peptidic reactive group and an isobaric label consisting of a reporter group and an equilibrium group. For this, the labeling of the peptides is generated after digestion at the N-terminal end. The reactive group is derived from N-hydroxysuccinamide and reacts with the amino group of lysine residues and the N-terminal end of all peptides (136).

Human chondrocytes were transfected to induce defective autophagy (siCtrl and siAtg5) and processed for iTRAQ analysis as previously described (Calamia *et al.*, 2014). Briefly, protein from OA human chondrocytes was lysed using 6M urea/2% sodium dodecyl sulfate (SDS) buffer and then cleaned up by acetone precipitation. Protein pellets were dried in air and then resuspended in 25 ml Dissolution Buffer.

Then iTRAQ labeling was performed according to the supplier's instructions (ABSciex, Foster City, CA, USA). The samples were labeled as follows: 114;116 for siCTRL and 115;117 for siAtg5. Then, the iTRAQ-labeled peptides were mixed and desalted using reversed phase columns (Pierce C18 Spin Columns, Thermo Fisher Scientific, Rockford, IL, USA) prior to liquid chromatography coupled to mass spectrometry (LC-MS) analysis (137).

In the first phase, to each sample tube containing 50-100 µg of protein, we add 20 µl Dissolution Buffer and vortex the samples for 1 hour and then sonicate for 3 min. Next, add 1µl Denaturant kit, 2µl Reducent Reagent tube, mix well and incubate at 60 °C for one hour. After incubation time, add 1µl of Cysteine Blocking Reagent and incubate for 10 min. at room temperature. Afterward, we will begin the digestion with trypsin, for this we had to reconstitute a trypsin vial in the following proportion 10µl of

water + 4µl of trypsin (1µg / µl), and added to each sample 10µl (5µg): 20 enzyme: substrate) and incubate at 37 ° C overnight. Finally, the labeling of the proteins digested with iTRAQ Reagents takes place. We will add 70 µl of ethanol to each vial of iTRAQ which will then be transferred to one of the samples and incubate for 1 hour to label each vial with the different labels of 114, 115, 116 and 117. After the incubation time, we had centrifuged at 13000 rpm and checked the sample by the MS/MS to see that each sample contains the peaks corresponding to each label. We mixed the 4 vials and lyophilized the samples all night in the SpeebBack. To eliminate possible residues that may interfere with the technique, we washed it by column cleaning with Pierce® C18 Spin Columns. Once the samples are cleaned, freeze-dried and stored at -20ºC.

3.5.2 LC/MS/MS Analysis

The Sample tags are excised during tandem mass spectrometry (MS/MS). Each reporter tag produces different MS/MS signatures that can be detected as peaks of the m/z ratio. The relative intensity of the reporter group labels provides information about the relative abundance of the proteins in each sample. The equilibrium group maintains the total mass of the isobaric label constant. (138, 139).

The peptide mixture was firstly separated by high performance reversed-phase liquid chromatography (RP-LC) at basic pH (pH=10). The separation of the samples was carried out in HP 1200 system (Agilent Technologies, Santa Clara, CA, USA) using a reverse phase C18 Reverse-phase column (Zorbax extend C18, 100 3 2.1 mm id, 3.5 mm). The flow rate used is 0.2 ml/minute. Each fraction has been collected based on the UV intensity peaks (214 nm).Several fractions were pooled post-collection (FC203B fraction collector, Gilson, Middleton, WI, USA) based on the peak intensity of the UV trace, yielding a total of 60 samples per LC run.

Each fraction was dried in a vacuum concentrator and stored at -20ºC for the next step of analysis. The dried peptide fractions were dissolved in 0.1% trifluoroacetic acid (TFA) and 2% acetonitrile; 5 mL of this sample were injected onto a capillary trap column (0.5 3 2 mm, Michrom Bioresources, Auburn, CA, USA) at a flow rate of 15ml/minute. Peptides were desalted for 10 minutes and loaded onto a C18 column (Integrafit C18, ProteopepTMII, 75 mmid, 10.2 cm, 5 mm, 300A˚;New Objective,

Woburn, MA, USA) at a constant flow rate of 350 nl/minute to perform the separation. Then peptides were separated using linearly increasing concentration of acetonitrile in buffer B. The RP analytical column eluent was spotted onto a matrix-assisted laser desorption/ionization (MALDI TOF) sample plate using the Sun Collect MALDI Spotter/Micro Collector (SunChrom Wissenschaftliche Geräte GmbH, Germany) and analyzed by a 4800 mass spectrometer (AB Sciex). After the screening of all LC-MALDI sample positions in MS positive reflector mode, the fragmentation of automatically selected precursors was performed to generate fragment ions that provided sequence information for the peptide and reporter ions. The LC-MS analysis and the MS and MS/MS parameters have been extensively detailed previously for articular cartilage chondrocytesm (137, 140, 141).

3.5.3 Peptide Identification

Protein identification is usually performed by the peptide *mass fingerprint*. The peptide *mass fingerprint* identification of the protein corresponds to a mass spectrum (MS) corresponding to the peptides resulting from the enzymatic digestion of the protein. Many times the MS spectrum is not sufficient to identify the protein, whereby fragmentation of the peptides is proceeded to be obtained from fragments of a tandem mass spectrum of the protein (MS/MS). The spectra obtained by MS or MS/MS are transferred to a computer program with a database in which we can compare the spectra and identify the protein.(142)

Protein identification and quantification of proteins has been carried out using the program ProteinPilotTM software v.4.0 (ABSciex). Each MS/MS spectrum was searched in the Uniprot/Swissprot database for Homo sapiens. Search parameters within ProteinPilot were set with trypsin cleavage specificity; methyl methanethiosulfate (MMTS) modified cysteine as fixed modifications; biological modification ‘‘ID focus’’ settings, and a protein minimum confidence score of 95%. Thus, the identity of the protein from the analyzed peptide was confirmed, and the ratios of the peak areas of iTRAQ reporter ions were used to compare the relative abundance of the protein identified in the sample. The data were normalized based on error and background correction using Pro Group^{TM} algorithm (ABSciex). Only proteins identified with at

least 95% confidence, were considered for further analysis. Data were normalized for loading error by bias and the background correction was calculated using the Pro GroupTM algorithm (ABSciex). To determine the cutoff value for significant fold changes, coefficient of variation and cumulative frequency were calculated for the common proteins employing the R statistical package58. Using this tool, it was considered as statistically significant those changes with a p-value less than or equal to 0.05 and a ratio of 1.4. The data obtained in the ProteinPilot were exported to Microsoft Excel for further analysis (143).

3.5.4 Western blotting

Western blotting was performed with a chemiluminescence detection system. Protein from normal human chondrocytes was lysed using 6M urea/2% sodium dodecyl sulfate (SDS) buffer. Cell lysates were sonicated at 4°C, and protein concentrations were determined using a Pierce bicinchoninic protein assay kit kit (Pierce Biotechnology, Rockford, IL, USA). Then, protein extracts (20µg) were incubated with 4×laemmli Sample buffer solution (Bio-Rad, Hercules, CA, USA) and β-mercaptoethanol (Sigma-Aldrich), a reducing agent. The proteins were separated on 4–20% SDS–polyacrylamide gels and transferred to PVDF membranes (Bio-Rad, Hercules, CA, USA), blocked with 5% dry skimmed milk or 5% bovine serum albumin in Tris buffered saline–Tween (TBST), and blotted for 1 hour with rabbit polyclonal antibody specific for LC3 (1:1,000 dilution, catalog no. PM036; MBL International), with p-Akt (Ser473), with p–ribosomal protein S6 (1:2,000 dilution, catalog Nº. 4060 and 4858, respectively; Cell Signaling Technology), or with mouse antibody tubulin (1:2,000 dilution, catalog no. T9026; Sigma). The membranes were then incubated for 1 hour with horseradish peroxidase (HRP)–conjugated donkey anti-rabbit IgG or sheep antimouse IgG (1:5,000 dilution, catalog nos. NA934 and NA931, respectively; GE Healthcare). Afterward, the membranes were washed 3 times with TBST and developed using enhanced chemiluminescence substrate (Pierce Biotechnology, CA, USA). A summary of primary antibodies used in this study is detailed in Table 3.2

Table 3.2: Primary Antibodies used in WB studies.

Protein	Source	Clonality	MW (KDa)	Dilution	Supplier/Ref. Number
LC3	Rabbit	Polyclonal	16-18	1: 1000	MBL International/PM036
Atg5	Rabbit	Polyclonal	55	1:1000	Cell Signaling/8540
p-rpS6 (Ser 235/236)	Rabbit	Polyclonal	32	1:2000	Cell Signaling/4858
p-Akt (Ser473)	Rabbit	Polyclonal	60	1:2000	Cell Signaling/4060
Lamin A/C	Goat	Polyclonal	70	1:50	Santa cruz /6214
α-Tubulin	Mouse	Monoclonal	50	1:2000	Sigma-Aldrich®/ T9026
GAPDH	Mouse	Monoclonal	30	1:10000	Invitrogen

3.6 Genome editing studies in chondrocytes

3.6.1 Autophagy inhibition by silencing autophagy-related (ATG-5) with small interfering RNA

Primary normal human chondrocytes were transiently transfected with siRNA for ATG-5 (siATG-5, ID s18160; Ambion), an essential autophagy gene (90) using Lipofectamine 2000 (Life Technologies) as described previously (86, 144). Silencer negative control #1 siRNA (Ambion), containing a RNA scramble sequence was used as control.

The sense-strand sequence of the siRNA was 5-GCUAUAUCAGGAUGAGAUATT-3.

The transfected chondrocytes were then used for determination of mitochondrial membrane potential, ROS production analysis, Western blot analysis, proteomic screening by iTRAQ analysis and immunofluorescence.

3.6.2 Genetic deletion of Zmpste 24 by clustered regularly interspaced short palindromic repeats (CRISPR-Cas9) technology

Genome editing has recently emerged as a robust and efficient method to manipulate the genome with accuracy and precision. These technologies have apened opprotunities to study the functional consequences of genes and mutations relevant to disease.

The CRISPR/Cas technology comprises two components, a small guiding strand and the Cas9 nuclease, which recognizes and binds to the specific DNA site. The plasmid containing guiding RNA, PCMV-Cas9-GFP (**Figure 3.1**), was obtained from Sigma-Aldrich (Plasmid (V6-gRNA/CMV-Cas9 GFP; NM-005857; Zmpste24 Gene ID10269, HS0000322098). The target site is a 20 bp complementary to gRNA that targets to Zinc Metalloproteinase STE24 (Zmpste24) genomic sequence that was included into the plasmid. The sequence to target was 5'-GGCATCGCTGGACGCTTTGTGG- 3'.

The plasmid was replicated replication by heat shock transformation in DHLOβ competent bacteria were used, the plasmid was included within the bacterial genome by thermal shock. The amount of plasmid used was 20ng/µl. These bacteria were incubated

in super LB medium for 1 hour at 37 ° C. After that time, the bacteria were seeded in culture medium in superLB-Kanamycin selective medium (20 µg/µl) overnight at 37 ° C. A colony-forming unit (CFU) was picked and grown in LB medium for 24h at 37ºC and then, the DNA was isolated by the Maxi-prep technique following the manufacturer's instructions for the Qiagen Maxiprep kit.

TC28a2 human chondrocytes were cultivated in DMEM-F12 containing 10% FBS and 1% antibiotics in a humidified 5% CO2 at 37ºC. TC28a2 chondrocytes were cultivated to 60-80% confluence in 10 cm plates and transfected with the target vector (5µg) using Lipofectamine™ 2000 (Life Technologies, NY, USA) according to manufacturer´s instructions.

The positively transfected chondrocytes were selected by sorting. Isolated clones of Zmpste24-transfected chondrocytes were incubated in 96 well plates in increasing order for expansion. To confirm the mutation, we screen each clone by isolating genomic DNA and genotyping by using the following primers:

Forward: 5'-GCTCTGAAGGGACGAGTGTC-3';

Reverse: 5'-GTCCAGGAAAAGAGCAGCAC-3'.

PCR products were separated in 1% agarose gel, and the absence of Zmpste24 was confirmed by sequencing. A total of 3 mutated Zmpste24$^{-/-}$ clones were selected for functional analysis.

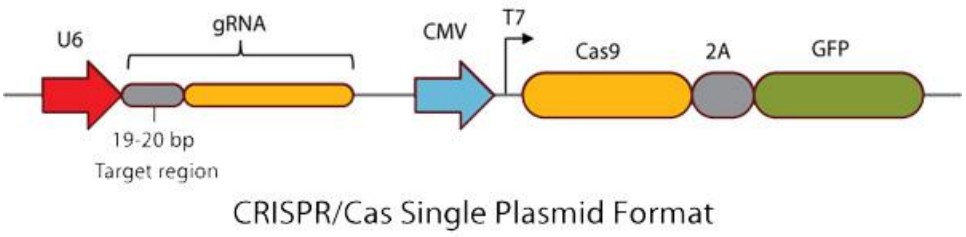

Figure 3.1: Schematic Plasmid of pCMV-Cas9-GFP cronstruction.

3.6.3 Gene expression analysis: RT-PCR and real-time PCR.

The analysis of mRNA expression consists of different steps: extraction of mRNA, polymerase chain reaction in reverse transcription (RT-PCR) and quantitative real-time polymerase chain reaction (qPCR).

RNA from our clones was extracted using the trizol technique. The trizol technique uses a complete reagent ready for the isolation of high quality RNA, being able to simultaneously extract RNA, DNA and protein from tissue samples or cell culture. The trizol reagent is a monophasic solution from phenol and guanidine isothiocyanate, which allows the RNA, DNA and proteins to be isolated in different phases. Due to the chemical properties of the reagent, trizol maintains RNA integrity through RNase inhibitors, while destroying cells and dissolving cellular components during homogenization of samples. After the homogenization of the sample, chloroform is added allowing the separation of the sample in different phases: aqueous where it is located in RNA, and organic phase and interface containing DNA and protein. The RNA from the aqueous phase is precipitated with isopropanol and subsequently washed to remove the impurities with 70% ethanol. The precipitate is resuspended in free RNase water. The quantification of the mRNA concentration obtained after the extraction was evaluated using spectrophotometric techniques (Nanodrop ND-1000) at 260nm and its purity was evaluated as a function of the absorbance ratio at 260nm and 280nm.

The extracted RNA permits the obtaining of introns-free DNA strand by the RT-PCR technique. Therefore, upon expression of this RT-PCR product, a messenger RNA (mRNA) consisting exclusively of exons might be generated. In conjunction with real-time PCR (qPCR), we can detect the amount of specific mRNA from small amounts of RNA cells.

Complementary DNA amplification (cDNA) was performed using the ThermoScrit ™ RT™ PCR System kit, where 1μg of RNA sample was transcribed. The cDNA synthesis consists of two phases, a first denaturing RNA where the RNA and primer are incubated for 5 min at 65 ° C; And a second step of cDNA synthesis consisting of three 10 min steps at 25 ° C, 50 min at 50 ° C and final step at 85 ° C for 5

min. Finally, the reaction is maintained at 4 ° C. Subsequently the DNA will be stored at -20 ° C after a 1:10 dilution in nuclease-free water until further use.

To complete the study of gene expression, the qPCR technique was carried out. In this way, we analyzed the expression and quantification of genes involved (Hs00797944_s1-MAP1LC3B; Cat Number 4331182, Life Technologies) and aging (Hs00153462_m1-LMNA; Cat Number: 4331182, Life Technologies). Actin B (ACTB) was used as the reference gene. The design of the different primers was carried out by the Primer 3 application.

The real-time amplification and quantification assay was performed on the Applied Biosystems 7300 Real-Time PCR System. Each sample was evaluated in triplicate in 96-well optical plates using 4.5 µl (10 ug) of cDNA from RT-PCR, 5 µl of Master Mix for Syber Green or TaqMan probes and 0.5 µl of primer 10 µM (Forward + Reverse). The conditions used were: incubation for 2 min at 50 ° C; 10 min at 95 ° C; Amplification of 40 cycles of 15 seconds at 95 ° C and 1 minute at 60 ° C; Followed by a dissociation cycle of 95 ° C for 15 seconds, 60 ° C for 20 seconds, 95 ° C for 15 seconds and 60 ° C for 15 seconds. Finally the samples are cooled to 4 ° C.

The fluorescence signal intensity emitted is proportional to the amount of amplified product, and therefore as a function of the amount of expression of the cDNA levels. The expression and quantification of the different genes was normalized based on our ACTB reference gene.

3.7 Consequences of Lamin A/C Accumulation in the Musculoskeletal System

3.7.1 Accelerated aging model: Zmpste24 Deficient Mice

To carry out this study, we used Zmpste24 deficient (KO) mice, since they produce a mutation in the processing of lamina A, which is interesting for the study of premature aging in the musculoskeletal system. The Zmpste24 KO mice were kindly provided by Dr. Carlos López-Otín (Universidad de Oviedo, Spain) and Animal experiments were conducted in accordance with the guidelines of the Committee on Animal Experimentation of Instituto de Investigación Biomédica de A Coruña (INIBIC)-Complejo Hospitalario Universitario de A Coruña (CHUAC), A Coruña, Spain.

The Zmpste24 KO mice exhibit phenotypic changes that accelerate the aging process in most tissues. These mice have different phenotypic characteristics with respect to the wild type or Zmpste24 heterozygous (HT). At birth, the Zmpste24 KO, whose genotype is $Zmpste24^{-/-}$, present the same phenotype like the rest of their siblings in the first weeks of ageing. As tim goes by, we can distinguish both genotypic classes by size and weight. Zmpste24 HT mice exhibit normal appearance at least until the first 12 months of life, but their Zmpste24 KO siblings at 4 months of age have a weaker, lost hair and weight aspect. This is because after weaning (21-30 days old) KO mice begin to gain weight in a slower way. They also present atrophy of the musculoskeletal system, presenting muscle weakness, and at approximately 6-8 weeks of age, develop kyphosis in the spine, as well as malnutrition. Over time, they begin to exhibit less mobility, and their hind legs are more arched at the time of walking, with greater tremor and unable to keep the bow upward as the wild and/or heterozygous phenotype. These mice have a lower half-life, presenting a lifespan of approximately 20 weeks, so due to animal welfare regulations we chose a point of slaughter at 18 weeks of age.

Zmpste24 KO mice are not fertile, so Zmpste24 HT were employed to form the colony. Zmpste24 HT mice do not have any alteration until approximately 15 months of age. To start the colony, two Zmpste24 HT female mice and two Zmpste24 HT male mice of three months of age were crossed to obtain the optimum number of KO and HT mice required for the study.

Once the mice are genotyped they are kept in colony until the time of sacrifice, approximately 18 weeks after their birth. From the sacrificed mice, both hind limbs will be collected from the femoral head, in addition to spine.

As mentioned, KO mice show obvious phenotypic alterations from 10-12 weeks, such as slower growth without weight gain and height, and although the causes of premature death are unknown, is likely due to cardiac changes (ref). For this reason, this animal model was classified as severe and therefore undergo periodic monitoring in which their overall appearance is evaluated and the mouse weight was evaluated weekly to note any observed abnormalities.

The body weight was monitored weekly for metabolic phenotype studies.

3.7.2 Animal Care

Because these mice are genetically engineered and more sensitive to environmental conditions than HT mice, we were very rigurous about their care and attention. The conditions of lodging, zootechnical and cares of the animals were carried out respecting the animal well-being, being and are collected in the **Table 3.3.**

Table 3.3: General conditions of mice accommodation.

Accommodation	Groups of max. 5 mice per cage
Bed of the cages	Sterilized absorbent material made from wood
Feeding	Feed for rodents of standard experimentation
Water	Tap water
Ventilation:	15 air renewal per hour
Temperature and Humidity	20 ° C and 24 ° C (± 1 ° C) and humidity of 55% (± 10%)
Light	Controlled artificial in cycles of 12 hours of light of 8 to 20 hours
Noise	Controlled
Health	Animal health and welfare strategy of the facility
Enrichment	Paper and cardboard inside the cage

To evaluate the general state of the mouse, we used a template with criteria of severity (**Apendix 2-Table 1**) that includes those clinical signs that are visibly perceived about its symptomatology with a score of 0 to 4.

Mice is programmed for slaughter at 18 weeks of age according to current regulations, one month before their life expectancy, to decrease the suffering and alterations caused by the mutation in the mice. On the other hand, if, during the follow-up, any of the mice has a score greater than or equal to 10 (**Appendix 2-Table 2**), they will be sacrificed to avoid suffering the animal.

This study has been approved by the ethical animal experimentation committee of the XXIAC, following Royal Decree 53/2013, which establishes the basic norms applicable for the protection of animals used in experimentation and other scientific purposes, including teaching. (145)

3.7.3 Mice Genotyping

For mice genotyping, we performed a DNA extraction from the tail tissue (small size) by using the QIAamp DNA Mini Kit (Quiagen). First, tissue was incubated with 180 µl of ATL buffer and 20µl of proteinase K at 56 °C with shaking until the tissue became completely lysed. Then, we added 200µl AL Buffe and mixed for 15 seconds and then incubated at 70°C for 10min. Next, we added 200µl of ethanol (96-100%) and place the sample in the QIAamp Mini spin column (2 ml collection tube) and centrifuge at 8000 rmp for 1min. Then, we transferred the column to a clean tube and add 500µl of AW1 Buffer and centrifuge again at 8000 rpm for 1 min. Afterwards, 500 µl of AW2Buffer was added and centriguged at 14000 rpm for 3min. Finally, we transfered our column to a clean tube of 1.5ml and carefully added 100µl of elution Buffer and then, the column was incubated for 5 min at room temperature and centrifuged. The eluted solution contained the DNA of each sample to evaluate the genotype by PCR.

3.7.3.1 PCR conditions for genotyping

The genotyping was performed by PCR by using the following primers and conditions shown in **Figure 3.2**.

Zmpste24_Forward: GCTGGCCTTGTTGCTGGAAT
Zmpste24_Reverse KO: CTTCCGGAGCGGATCTCAAA
Zmpste24_Reverse WT: GCTTCCTCCCTGAGCCAACC

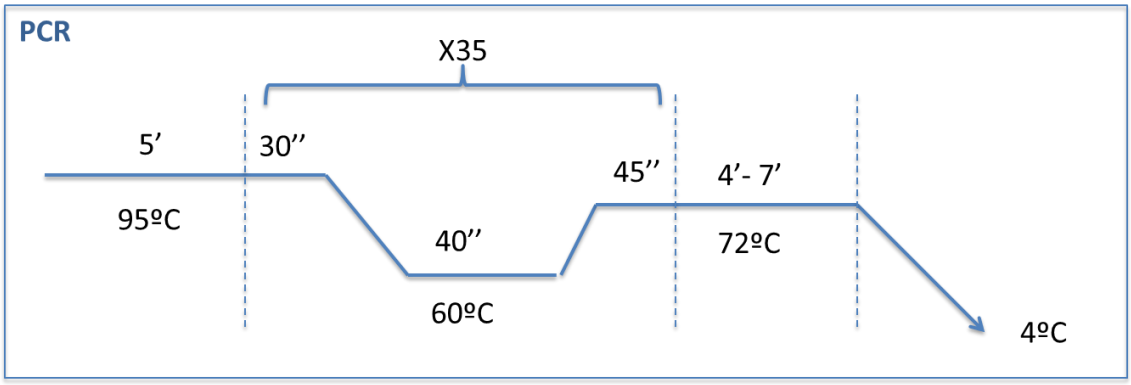

Figure 3.2: PCR program for Zmpste24 mice genotyping. The PCR program conditions was: one cycle of DNA denaturation, then a 35 cycles of DNA amplification, then one cycle of final elongation and finally a preservation of DNA at 4ºC.

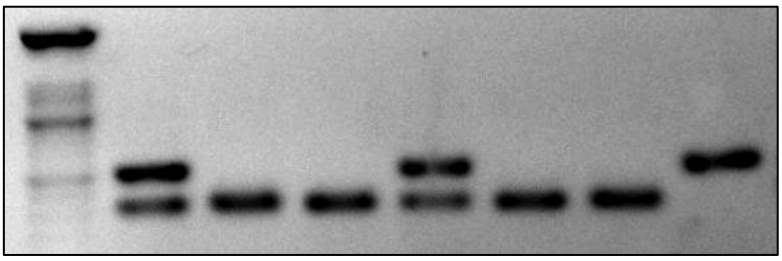

Figure 3.3: Representative example of Zmpste24 mice genotyping. A single band at 520pb correspond to Wild-type animals, a simple band at 303 pb correspond to Knock-out mice, so animals with two bands at 520 and 303 pb are Heterozygous mice.

3.8 Histological studies.

3.8.1 Tissue samples

Human Cartilage sections from healthy, aged cartilage and OA cartilage grade II-III and OA cartilage grade III-IV donors from University Hospital of A Coruña and The scrrips Research Institute in La Jolla, CA-USA, were employed for inmunohistochemical studies.

Mice were euthanized at 18 weeks of age, and the liver knee joints and spine were collected for analysis. Male and female mice were included in the study (Zmpste24 HT: 20 mice and Zmpste24 KO: 13 mice).

3.8.2 Immunohistochemistry for paraffin embedded samples.

Sections from paraffin-embedded joints were first deparaffinized in the xylene and rehydrated in graded ethanol and water. For antigen unmasking, sections in 10 mM sodium citrate buffer (pH 6.0) were heated in a microwave oven and kept at 80–85°C for 1.5 minutes. Slides were cooled for 20 minutes at room temperature after antigen unmasking. After washing with phosphate buffered saline (PBS), sections were blocked with 5% serum for 30 minutes at room temperature. Then, sections were incubated with antibodies for Lamin A/C (BM6000P, Acris Antibodies); pre-treatment EDTA; Dilution 1:50 overnight at 4°C. After washing with PBS, sections were incubated with biotinylated goat anti-mouse secondary antibody for 30 minutes at room temperature, and then incubated using Vectastain ABC-AP alkaline phosphatase (Vector Laboratories, Burlingame, CA) for 30 minutes. Slides were washed, and sections were incubated with 3,3´-diaminobenzidine (DAB) substrate for 3-10 minutes.

3.8.2.1 Quantification of Lamin A/C-positive cells

In human cartilage from healthy, aging and OA donors, the total number of Lamin A/C-positive cells was counted in three independent areas of each section (135). Results are expressed as the percentage of Lamin A/C-positive cells.

3.8.3 Safranin O / Fast Green Staining.

Mice tissue (joint and spine) were fixed in formalin for 24 hours, decalcified solution (Decalc™, HistoLab, 00601) for 6 hours, and then embedded in paraffin. Serial sagittal sections (4µm) were cut, stained with Safranin O-fast green. Safranin O is a cationic dyes that stain proteoglycans. Safranin O binds the carboxyl groups and sulfate groups (both negatively charged) which abound in the extracellular matrix of the articular cartilage

3.8.4 Hematoxylin-Eosin staining.

Hematoxylin is used in histology to stain the anionic (acid) components of the tissues, to which it gives a blue-purple coloration. It stains intensely the nuclei of the cells, since these contain nucleic acids rich in acid radicals. In contrast, eosin is an acidic compound whose property is based on its negative polarity, allowing it to bind to positively charged cellular constituents. It therefore colors cytoplasmic components and organelles, collagen and muscle fibers.

In the first time, the sample is stained with Harris hematoxylin (PANREAC 2539491612) for 5 minutes. After some time, a wash in tap water to turn the color and the samples are stained with eosin for 5 minutes.

3.8.5 Histologic analysis of joint cartilage in Zmpste24 mice

Mice knee joints from the three groups were harvested. The joints were fixed in formalin for 24 hours, decalcified solution (Decalc™, HistoLab, 00601) for 6 hours, and then embedded in paraffin. Serial sagittal sections (4µm) were cut, stained with Safranin O-fast green, and examined for histopathological changes using the OARSI semiquantitative scoring system (Glasson et al, 2010). In this system the scores are defined as follows: 0=normal cartilage, 0.5=loss of proteoglycan with a intact surface, 1=superficial fibrillation without loss of cartilage, 2=vertical clefts and loss surface lamina (any % or joint surface area), 3=vertical clefts/ erosion to the calcified layer lesion for 1–25% of the quadrant width, 4=lesion reaches the calcified cartilage for 25–

50% of the quadrant width, 5=lesion reaches the calcified cartilage for 50–75% of the quadrant width, 6=lesion reaches the calcified cartilage for >75% of the quadrant width.

3.8.5.1 Histologic analysis of bone changes in Zmpste24 mice

Subchondral bone in mouse knee joints was examined and scored using a grading system (17) that measures 3 parameters: subchondral bone thickening, number of trabeculae, and osteophyte formation, which were graded as normal (grade 0), mild (grade 1), moderate (grade 2), or severe (grade 3).

3.8.5.2 Histologic analysis of spine changes in Zmpste24 mice

Human and mouse samples were washed in phosphate buffered saline (PBS) and fixed using zinc buffered formalin (ZFix, Anatech) for 48 hours. After fixing, samples were decalcified in a Shandon TBD-2 decalcifier (Thermo Scientific) for 24 hours on a shaker, thoroughly washed with PBS and embedded in paraffin. 4-µm-thick sections were cut and stained with Safranin O-fast green. In mouse spines, histological analysis of C3/C4 and L4/L5 IVD was performed as follows. Degenerative changes in NP and AF were graded following *Masuda et al* (146) whereas changes in EP were scored according to the grading system described by *Boos et al* (147).

3.9 Statistical analysis

To compare means we will use Student's t or Mann Whitney test as appropriate after checking the normality of the quantitative variable with the Kolgomorov-Smirnov test. In general, the data sets follow a normal distribution. In the cases where the number of samples was too small to be tested accurately, we assumed the data follow a normal distribution. Statistically significant differences between 2 groups were determined by Student´s unpaired t-test. Statistically significant differences between multiple groups were determined analyzing variance (ANOVA) in conjunction with Tukey´s multiple comparison. Data are presented as the mean (lower level, upper level) (ll, ul) 95% confidence interval (CI). The data analysis and statistical interference was performed using Prism 5.0 software (GraphPad Software, La Jolla, CA, USA).

CHAPTER 4: RESULTS

CHAPTER 4.1 : TO STUDY THE EFFECTS OF DEFECTIVE AUTOPHAGY TO MITOCHONDRIAL FUNCTION USING PHARMACOLOGICAL AND GENETIC APPROACHES

4.1.1 Specific background

A common feature of aging-related diseases, such as osteoarthritis (OA), is the progressive accumulation of damaged macromolecules leading to cell dysfunction and death. Cellular homeostasis is dependent of intracellular mechanisms that maintain functional organelles and macromolecules required for cell survival and normal biosynthetic function (40). In tissues with a high rate of cell turnover, cellular constituents are continuously renewed. However, cartilage is a post-mitotic tissue with very low, barely detectable rate of cell replication. In fact, chondrocytes, the only cell type of adult articular cartilage, are capable of responding to structural changes in the surrounding cartilage matrix but the capacity of the adult articular chondrocyte to regenerate the normal cartilage matrix architecture is limited and declines with aging (19). Because cartilage homeostasis is disturbed in OA, leading to progressive extracellular matrix (ECM) destruction, identification of mechanisms of chondrocyte aging may create opportunities for preserving normal homeostasis and to prevent or delay chondrocytes death and cartilage structural damage.

Autophagy is a lysosome degradation pathway that is essential for cell survival, differentiation, development, and homeostasis. Autophagy serves as an adaptive role to protect organisms against diverse pathologies, including infections, cancer, neurodegeneration, and aging (21). Autophagy occurs at low basal levels in mammalian cells to perform homeostatic functions such as protein and organelle turnover. It is rapidly upregulated when intracellular nutrients or energy are required. Also, autophagy is activated when cells are undergoing structural remodeling such as during developmental transitions or to protect against oxidative stress or protein aggregate accumulation (80). Furthermore, genetic studies in mice support the importance of autophagy in many physiological and pathological events. In fact, loss of autophagy genes leads to neurodegeneration, cardiomyopathies, abnormalities in skeletal development and death (86, 87). Therefore, a better understanding of the autophagy mechanisms may lead to the discovery of new potential therapeutic targets for cell homeostasis regulation. In articular cartilage, which is characterized by a very low rate of cell turnover (19) autophagy would appear to be essential to maintain cellular integrity, function and survival, particularly during aging (148). Recent studies demonstrated that autophagy is a constitutively active and apparently protective process for the maintenance of articular cartilage homeostasis. By contrast, human OA and

aging-related and surgically induced OA in mice are associated with a reduction of autophagy regulators expression in articular cartilage. Furthermore, the reduction of these key regulators of autophagy is accompanied by increased apoptosis (37). These observations in cartilage are consistent with the notion that basal autophagic activity decreases with age, thus contributing to the accumulation of damaged macromolecules and susceptibility to aging-related cellular damage (94). Abnormal protein aggregation and formation of characteristic pathological structures are central features of such diseases (95, 96).

The role of mitochondria in OA is an area of research interest, and recent investigations have yielded novel and exciting discoveries. Indeed, mitochondrial dysfunction has been demonstrated in OA and is associated with an excessive reactive oxygen species (ROS) production (20). Furthermore, recent studies showed that mitochondrial dysfunction mediates several pathways involved in cartilage degradation (104). These include oxidative stress, deficiency of chondrocytes biosynthesis, up-regulated inflammation and increased chondrocyte death. In fact, OA chondrocytes show decreased activity in MRC complexes I, II, and III, which results in a reduction in the mitochondrial membrane potential and in ATP synthesis (149). Other reports indicate that decreased mitochondrial bioenergy reserve is a pathogenic factor in degenerative cartilage pathology (150, 151). Recently, a large body of evidence has shown that mitophagy, the selective autophagy degradation of mitochondria, is a critical quality control mechanism (152). Thus, this bulk, nonselective recycling system also has a vital role in mitochondrial homeostasis. Notably, defects in autophagy associated with human diseases are also linked to mitochondrial dysfunction (111, 114). Understanding the functional relationship between mitochondria and autophagy is critical for understanding the molecular mechanisms underlying aging-related diseases.

A current working model is that impaired autophagy results in a cell-damaging accumulation of dysfunctional mitochondria over time. These data indicate an interdependence of mitochondrial function and autophagy and raise the possibility that negative regulation of autophagy by dysfunctional mitochondria is a critical contributing factor in many aging-related diseases, such as OA. Here, we determine whether pharmacological activation of autophagy protects from induced mitochondrial dysfunction in normal human chondrocytes.

4.1.2 Material and methods

In this chapter, the following material and methods were used to study the influence of mitochondrial dysfunction in the Autophagy in human chondrocytes, as we described in the Material and Methods Section.

- **Cell Culture:** Immortal juvenile human chondrocytes (T/C-28A2) and Primary human chondrocytes were obtained and employed in this objective.
- **Reactives:** Oligomycin (Oligo, 10µg/ml) was employed to induce mitochondrial dysfunction. Rapamycin (10µM) and Torin 1 (50nM) were used to activate autophagy. Antimycin A (40µg/ml), Valinomycin (1µM), H_2O_2, (100µM) and TNFα+ActD (1µg/ml) were employed as positive controls for Mitochondrial dysfunction, ROS production and Cell Death by apoptosis, respectively.
- **Mitochondrial studies:**

  a. Mitochondrial Membrane Potential (Δψm): JC-1 and $DILC_1$ were used to quantified the Mitochondrial Membrane Potential.

  b. Reactive Oxygen Species Production: DCFH-DA and MitoSox were employed to evaluate and quantified the intracellular ROS, respectively.

  c. Cell Death Studies: To show the percentage of apoptosis or necrotic cells, Annexin-V and propidium iodide (PI) were used.
- **Autophagy Studies:** Autophagy was monitorized by determination of LC3 by Inmunofluorescence and WB). The influence of the mTOR pathway was investigated by WB.
- **Functional studies:** To study the importance of homeostasis maintenance to mitochondrial function, human chondrocytes were transfected with siRNA for Atg5, a key autophagy regulator, to knockdown the autophagy pathway.
- **Statistical analisys:** Statistically significant differences between 2 groups were determined by Student's t-test, while differences between multiple groups were determined analyzing ANOVA with Tukey's multiple comparison. The results are reported as the mean ± SEM. P values less than 0.05 were considered significant.

4.1.3 Results

4.1.3.1 Induction of mitochondrial dysfunction and cell death in human chondrocytes by inhibition of mitochondrial respiratory chain

Mitochondrial dysfunction has a negative influence on cell homeostasis by uncoupling the mitochondrial respiratory chain (MRC), increasing reactive oxygen species (ROS) production, and inducing cell death by apoptosis (153). Immortalized human chondrocytes T/C28a2 were treated with mitochondrial respiratory chain complex V inhibitor, Oligomycin (Oligo; 10 μg/ml), according previous studies (99, 154). The results indicated that mitochondrial dysfunction was induced by treatment with MRC inhibitor (**Figure 4.1A**), which significantly decreased $\Delta\psi m$ (Oligo: 41.74 ± 7.59, expressed as % vs. control; *p < 0.01 compared to control condition) (**Figure 4.1B**). These results are consistent with increased intracellular ROS production (25.7 % vs. control; *p < 0.001 compared to control condition) (**Figure 4.1C**), and mitochondrial superoxide generation (29.61 % vs. control; *p < 0.001 compared to control condition) (Figure 4.1D) at 5 minutes of treatment.

Moreover, increased cell death was observed at 14 hours, as shown by FACS analysis of Annexin-V (Control: 11.35 ± 1.735; Oligo: 25.37 ± 6.767, *p<0.05 vs. control) and Propidium iodide (Control: 15.34 ± 1.791; Oligo: 31.53 ± 2.61, *p<0.05 vs. control) (**Figure 4.2A-C**).

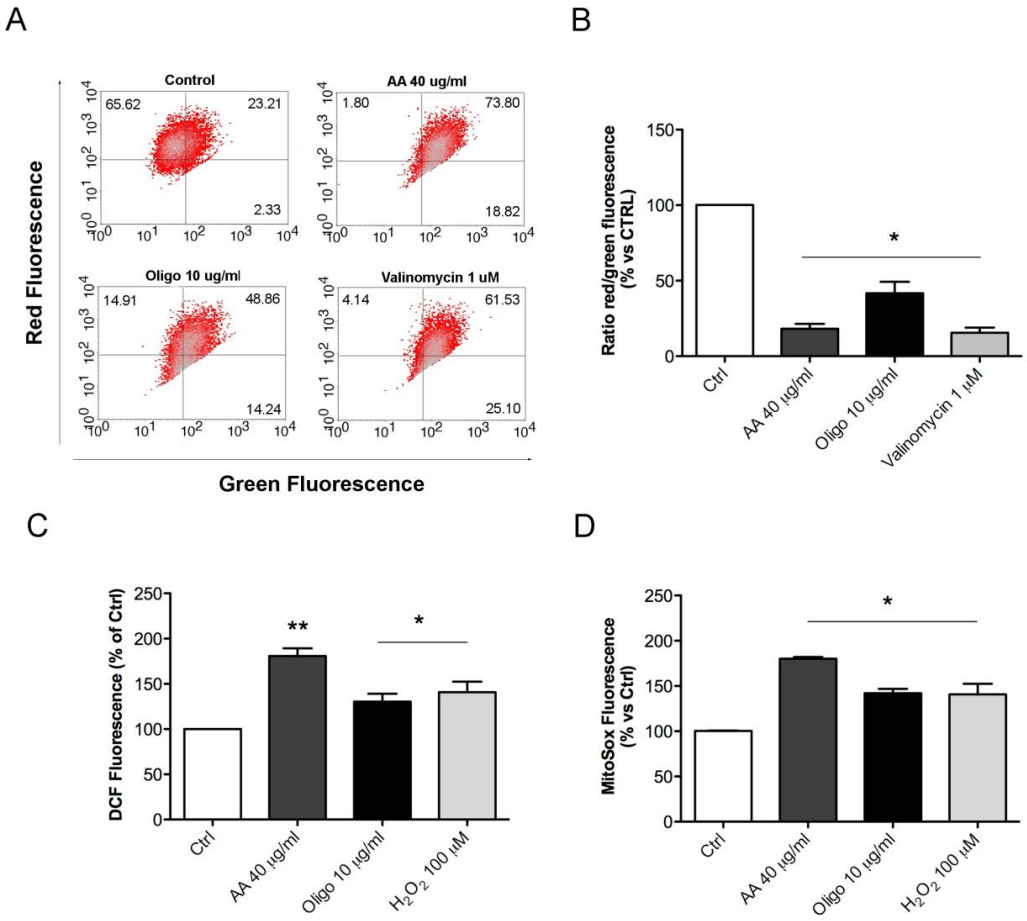

Figure 4.1: Inhibition of mitochondrial respiratory chain induces mitochondrial dysfunction in human chondrocytes. T/C-28a2 human chondrocytes were untreated (DMEM 2% FCS) or treated with Oligo 10 µg/ml for the indicated times. **A,** Mitochondrial membrane potential (Δψm) was analyzed by flow cytometry using JC-1 dye. A representative density plot for each condition at 6 hours is shown. **B,** Bar graph shows the Δψm expressed as Red/Green fluorescence ratio and $DilC_1$ fluorescence and represented as % vs. Ctrl at 6 hours post-treatment. Values are mean ± SEM of 7 individual experiments. *$p < 0.01$ versus for JC-1 dye and values are mean ± SEM of 3 individual experiments. *$p < 0.01$ versus Ctrl for $DilC_1$ dye. **C,** Quantitative analysis of intracellular ROS production by flow cytometry employing DCFH-DA dye at 5 minutes post-treatment. Values were expressed as percentage versus control condition at 5 minutes post-treatment. Values are mean ± SEM of 4 individual experiments. *$p < 0.01$ versus control. **D,** Quantitative analysis of mitochondrial superoxide by flow cytometry using MitoSox™ Red mitochondrial superoxide indicator. Values are mean ± SEM of 4 individual experiments. $p < 0.01$ versus control. Antimycin A (AA, 40 µg/ml), Valinomycin 1 µM and H_2O_2 100 µM were employed as positive controls for Mitochondrial dysfunction, Δψm and ROS production, respectively (*$p < 0.01$ versus control).

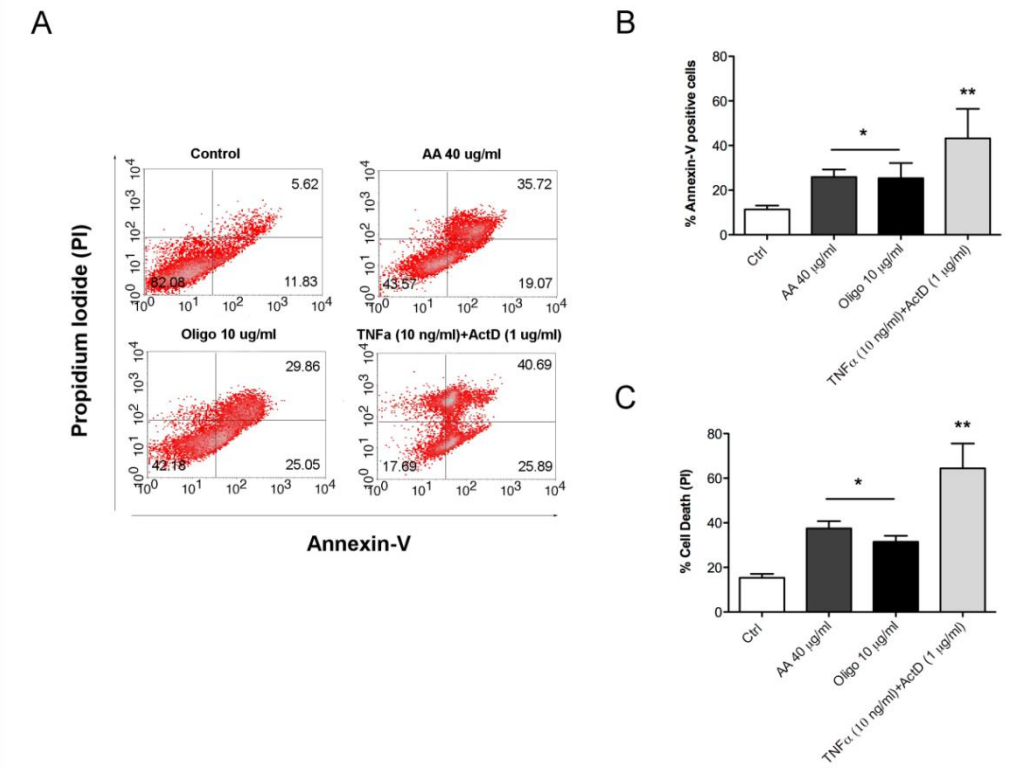

Figure 4.2: Inhibition of mitochondrial respiratory chain induces cell death by apoptosis in human chondrocytes. TC28a2 human chondrocytes were untreated (DMEM 2% CS) or treated with Oligo 10 µg/ml for 14 hours. Cell Death by apoptosis was analyzed by flow cytometry using annexin-V/propidium iodide dyes. **A,** A representative density plot for each condition at 14 hour is shown. **B,** Quantitative analysis of cell death induced by Oligo at 14 hours was performed by annexin-V and propidium iodide (PI) staining. Values were expressed as percentage versus control condition. Values are mean ± SEM of 5 individual experiments. *p < 0.01 versus control. Antimycin A (AA, 40 µg/ml) and TNFα (10 ng/ml) + ActD (1 µg/ml) were employed as positive control for Mitochondrial dysfunction and Cell Death by apoptosis, respectively (*p < 0.01 versus control; **p < 0.001 versus control).

4.1.3.2 Defective Autophagy in human chondrocytes with mitochondrial dysfunction

A common characteristic of aging-related pathologies is the accumulation of damaged macromolecules and organelles, such as mitochondria. As a consequence, the ability of cells to function normally and survive against stress stimuli is compromised. Autophagy is an essential homeostatic mechanism that regulates the elimination of damage macromolecules and promotes protection and cell survival.

To determine the activation and function of autophagy under mitochondrial dysfunction conditions, fluorescence-based detection of LC3 isoforms in TC28a2 cells was performed. Oligo treatment resulted in a significant reduction in the LC3 puncta, indicative of reduced autophagosome formation, compared to control condition at 14 hours (**Figure 4.3A, B**). Western blot analysis enables to detect LC3-I lipidation and conversion to LC3-II as a marker of autophagy activation and autophagosome formation (79). In response to Oligo treatment of normal human chondrocytes, the expression of LC3-II was increased at 24 hours after treatment, likely as an early response to stress, and then, decreased at 48 hours (**Figure 4.3C**).

These results demonstrate a decrease in autophagy activation as a response to mitochondrial dysfunction.

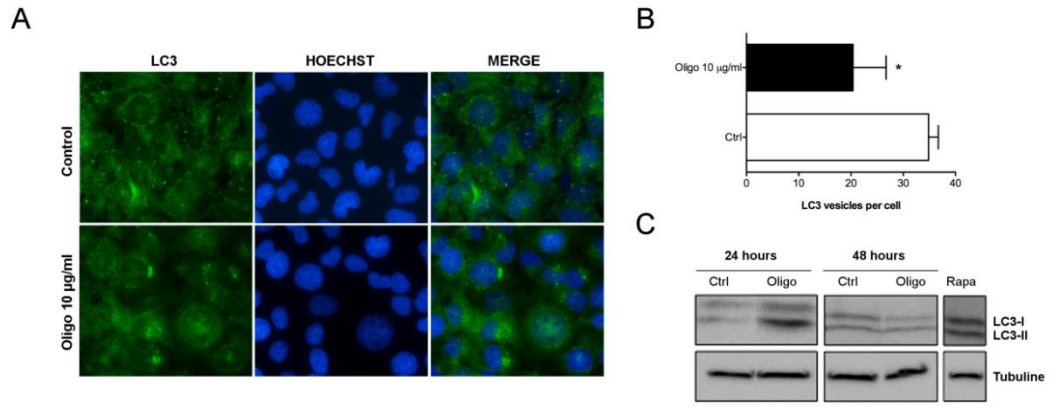

Figure 4.3: Autophagy is defective in human chondrocytes subjected to mitochondrial dysfunction. **A,** Fluorescence-based detection of LC3 in TC28a2 cells treated with Oligo 10 µg/ml for 14 hours reveals either diffuse cytoplasmic protein or puncta formation (vesicles), which reflects protein associated with autophagosomes. The number of punctate LC3 is associated with autophagosomes. Magnification 20x. **B,** Quantification of LC3 vesicles per cell in response to Oligo 10 µg/ml after 14 hours treatment. Values are mean ± SEM of 3 individual experiments. * = $P < 0.05$ vs. control. **C,** WB analysis was performed to detect autophagosome formation by lipidation of LC3-I to LC3-II, as a marker of autophagy activation, in normal human chondrocytes treated with Oligo 10 µg/ml at 24 and 48 hours.

4.1.3.3 Autophagy activation protects from mitochondrial dysfunction in human chondrocytes

To determine whether autophagy protects from mitochondrial dysfunction, autophagy was pharmacologically induced by using the mTORC1 selective inhibitor, Rapamycin (Rapa; 5, 10 μM) and the dual mTORC1 and mTORC2 inhibitor, Torin 1 (20, 50 nM). These inhibitors led to a significant concentration-dependent increase in the amount of LC3-II represented by LC3 puncta formation in the cytoplasm (*$p < 0.001$) (**Figure 4.4 A,B**). These data suggest that there are no differences in terms of autophagy activation when mTORC1 or mTORC2 isoforms are selectively inhibited.

Next, T/C28a2 human chondrocytes were pre-treated with Rapa (10 μM) or Torin 1 (50 nM) for 4 hours, followed by addition of Oligo (10μg/ml) for the indicated times. Rapa treatment induced an increase in the $\Delta\psi m$ (**Figure 4.3C**) and a significant decrease in the level of apoptosis induced by Oligo treatment (* $p < 0.05$) (**Figure 4.4 E,F**). However, we did not find any effect on ROS production (**Figure 4D**). By contrast, Torin 1 pre-treatment also significantly increased the $\Delta\psi m$ (* $p < 0.01$). This was accompanied by a significant decrease in ROS production and apoptosis (*$p < 0.05$). These results indicate a protective role of autophagy activation on mitochondrial dysfunction and a differential role of mTOR complex isoforms on ROS levels

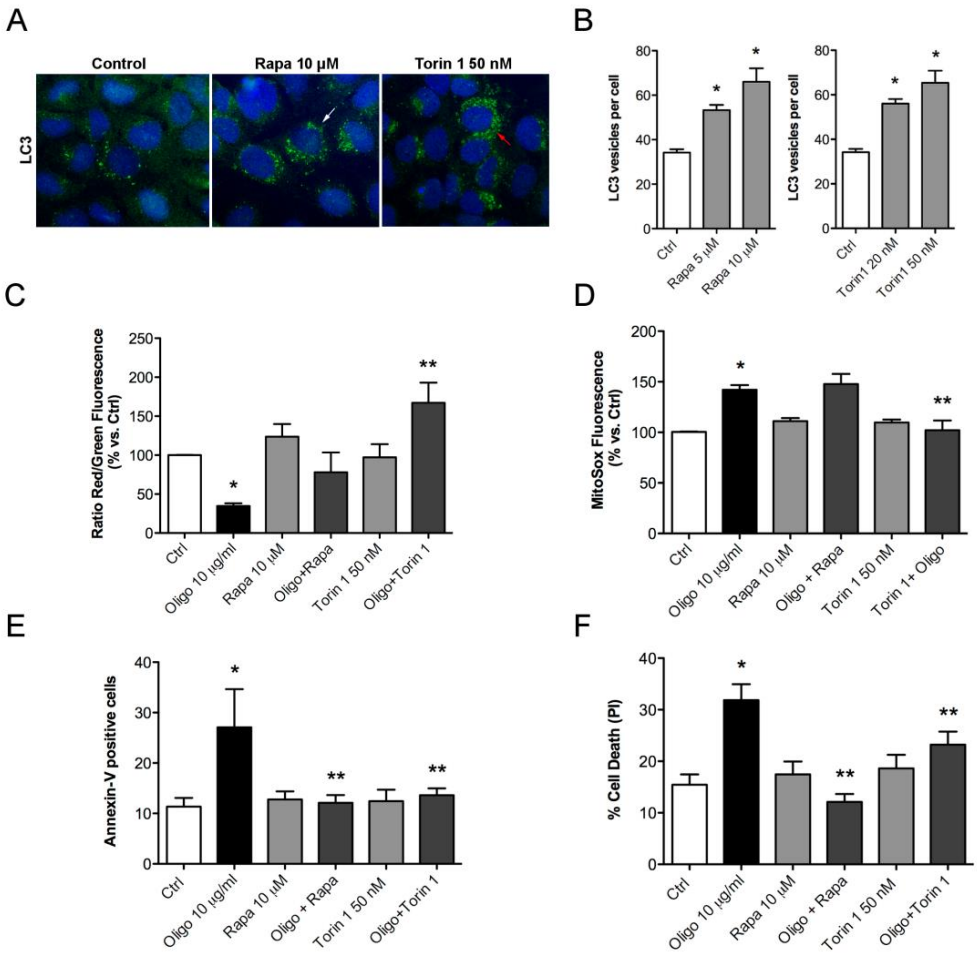

Figure 4.4: Autophagy activation protects from mitochondrial dysfunction in human chondrocytes. **A,** Fluorescence-based detection of LC3 in T/C28a2 human chondrocytes treated with Rapa 10 µM or Torin 1 50 nM during 14 hours. Magnification 40x. **B,** Quantification of LC3 vesicles per cell in response to Rapa or Torin 1 (20, 50 nM). Values are mean ± SEM of 3 individual experiments. * = $P < 0.01$ vs. control. T/C28a2 chondrocytes were pre-treated with Rapa 10 µM or Torin1 50 nM for four hours and then treated with Oligo 10 µg/ml. **C,** Statistical analysis of $\Delta\psi m$ expressed as Red/Green fluorescence ratio and represented as percentage versus control condition at 6 hours. Values are mean ± SEM of 4 individual experiments. * = $P < 0.01$ vs. control. **D,** Quantitative analysis of mitochondrial superoxide. Values were expressed as percentage versus control condition at 5 minutes post-treatment. Values are mean ± SEM of 3 individual experiments. * = $P < 0.01$ vs. control. **E,** Quantitative analysis of early apoptosis induced by Oligo at 14 hours. **F,** Quantitative analysis of late apoptosis induced by Oligo at 14 hours. Values were expressed as percentage versus control condition. Both values are mean ± SEM of 5 individual experiments. * = $P < 0.01$ vs. control.

4.1.3.4 Oligomycin-mediated mitochondrial dysfunction is dependent on Akt/mTOR pathway activation in human chondrocytes

To investigate the molecular components of oligomycin effect on autophagy, we studied Akt, mTOR and LC3, in normal human chondrocytes and in TC28a2 human chondrocytes. The results indicated that Oligo treatment induced phosphorylation of the serine/threonine kinase Akt, an upstream positive regulator of the mammalian target of rapamycin (mTOR), and the ribosomal protein S6 (rbS6), a direct and downstream target of mTOR (**Figure 4.5A**).

However, a differential role of Rapa and Torin 1 on Akt and rbS6 phosphorylation status was found. Torin 1 inhibited phosphorylation of Akt and rbS6 more potently than Rapa. These differences might be due to dual mTORC1 and mTORC2 Torin 1 inhibition and could explain the differential effects of Rapa and Torin 1 on mitochondrial dysfunction induced by Oligo. Moreover, analysis of LC3 expression indicated that Rapa and Torin 1 highly enhanced the LC3 puncta in response to Oligo treatment (**Figure 4.5B**).

These results suggest that Oligo is associated with an activation of Akt and mTOR signaling pathway in human chondrocytes that consequently reduces autophagy by blocking LC3-II formation.

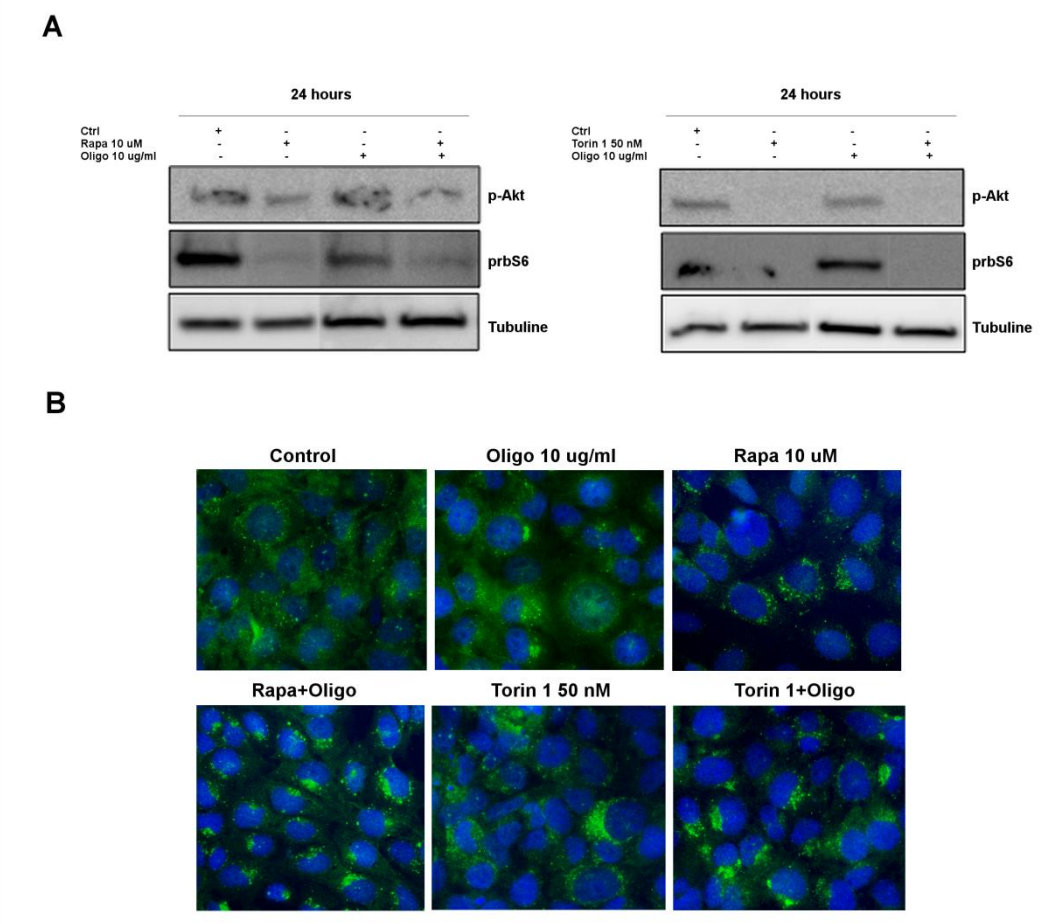

Figure 4.5: Oligomycin-mediated mitochondrial dysfunction is dependent on Akt/mTOR pathway activation in human chondrocytes. A, Normal human chondrocytes were untreated (DMEM 2% CS) or pretreated with Rapa 10 μM or Torin1 50 nM for four hours or treated with Oligo 10 μg/ml for 24 hours. Phosphorylation of Akt and ribosomal protein S6 (rbS6) was determined by Western blotting. **B,** Fluorescence-based detection of LC3 in T/C28a2 human chondrocytes untreated (DMEM 2% CS) or pretreated with Rapa 10 μM or Torin 1 50 nM for four hours or treated with Oligo 10 μg/ml for 14 hours. Magnification 20x.

4.1.3.5 Defective autophagy increases mitochondrial dysfunction in human chondrocytes

To determine the role of basal constitutive autophagy on mitochondrial function in human chondrocytes, we inhibited autophagy with siRNA for Atg5, which is essential for autophagosome formation and autophagy activation (155). Decreased Atg5 expression following siRNA treatment (**Figure 4.6A**) significantly induced mitochondrial dysfunction in human chondrocytes by decreasing the Δψm and increasing ROS production ($p < 0.05$) (**Figure 4.6B**). These data indicate an interdependence between mitochondrial function and autophagy.

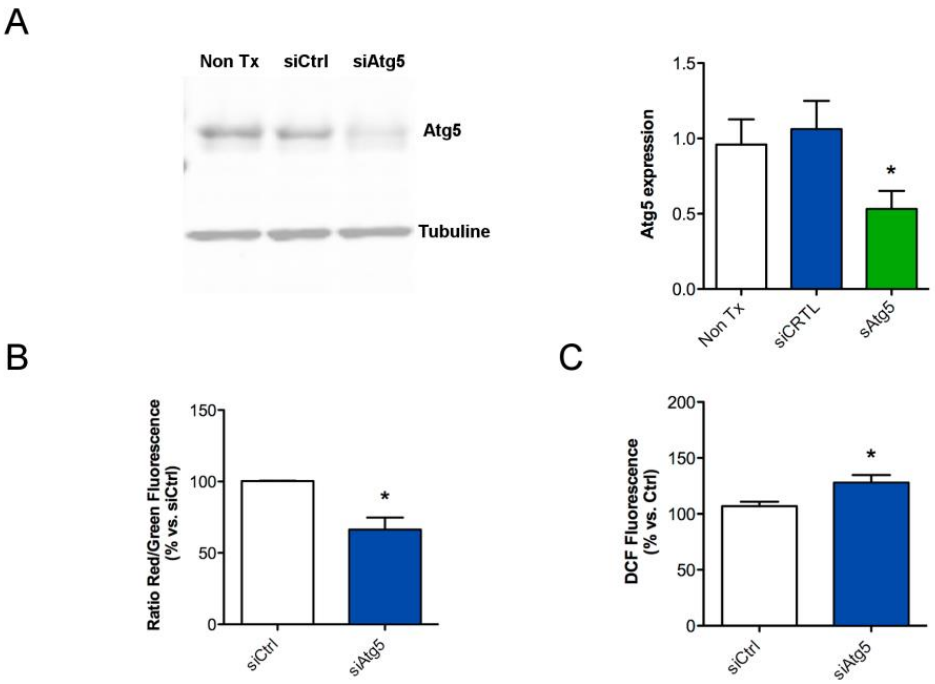

Figure 4.6: Defective autophagy induced by ATG5 siRNA increases mitochondrial dysfunction in human chondrocytes. Normal human chondrocytes were transfected with siCtrl or siAtg5 for 72 hours. **A,** The levels of Atg5 were determined by Western blotting. **B,** Bar graph show the statistical analysis of Δψm expressed as Red/Green fluorescence ratio and represented as percentage versus control condition at 72 hours posttransfection. Values are mean ± SEM of 3 individual experiments. * = $P < 0.05$ vs. control. **C,** Quantitative analysis of intracellular ROS production by Flow cytometry employing DCFH-DA dye at 72 hours post-transfection. Values are expressed as percentage versus control condition. Values are mean ± SEM of 3 independent experiments. * = $P < 0.05$ vs. control.

Overall, these results support the notion that identification of mechanisms of chondrocyte degeneration may create opportunities for preserving normal homeostasis and to prevent or delay chondrocytes death and cartilage structural damage (**Figure 4.7**).

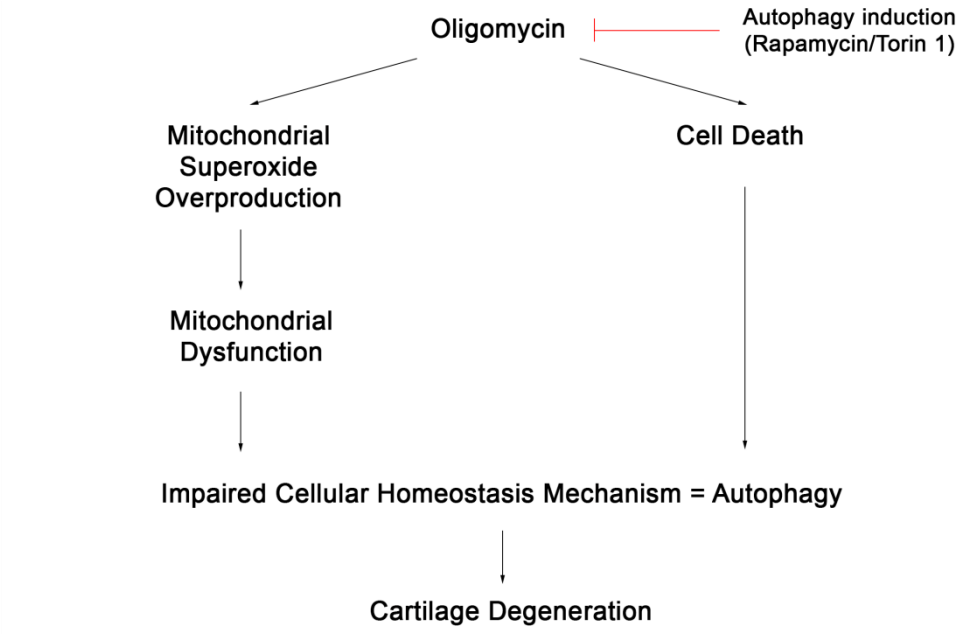

Figure 4.7: Flow chart for autophagy protective effect against mitochondrial dysfunction on human chondrocytes.

CHAPTER 4.2: TO IDENTIFY POTENTIAL TARGETS OF DEFECTIVE AUTOPHAGY ASSOCIATED WITH THE PATHOLOGY OF THE MUSCULOSKELETAL SYSTEM

Specific Background

We previously demonstrated that decreased autophagy is an early event that precedes joint damage in the pathogenesis of Osteoarthritis (OA)(156). A failure of cellular homeostasis mechanisms, such as autophagy, can cause extracellular matrix destruction, chondrocyte senescence, mitochondrial dysfunction and death, main features of cartilage pathogenesis. (62, 124, 157, 158)However, the specific targets that contribute to cartilage degeneration have not been completely identified.

Chondrocyte senescence has been highlighted as one of the major factor contributing to age-related changes in cartilage. (157). Since cartilage is a post-mitotic tissue with very low rate of cell turnover, (159) protecting chondrocyte function and viability is essential. In this sense, we previously shown that pharmacological activation of autophagy protects from chondrocyte loss and cartilage damage in cultured human chondrocytes, cartilage explants and in mice with experimental OA (40, 158, 160, 161).

To better delineate the role of autophagy in aging and OA, we examined the impact of compromised autophagy in the proteome of human chondrocytes with silenced Atg5, critical for autophagosome formation and autophagy activation. (144) Mice lacking Atg5 die whithin a day of birth, (162) whereas deletion of Atg5 in selected tissues promotes age-related abnormalities, such as neurodegeneration and OA (86, 163) To identify potential targets affecting autophagy regulation, we employed proteomics to perform a broad analysis of human chondrocytes. We found differential expression of proteins involved in the structural organization of the extracellular matrix and nucleus. Prelamin A/C, a nuclear protein implicated in premature cellular senescence, was upregulated under defective autophagy in human chondrocytes.

Nuclear lamins are intermediate filament proteins that are essential to maintain the structural properties of the nucleus. Lamins are involved in several nuclear processes including DNA replication, transcription and chromatin organization (164). In mammals, two major LMNA (A and C) and two major LMNB (B1 and B2) isoforms have been characterized (165). LMNA has been received a remarkable amount of attention because mutations on LMNA are associated with a variety of human diseases called laminophaties. These disorders are associated with cardiomyophaty, neuropathy

and premature aging (166). Hutchinson Gilford Progeria Syndrome (HPGS) is perhaps the most severe, and is characterized by defects in Lamin A maturation, resulting in acumulation of Prelamin A/C that leads to accelerated aging (167). Interestingly, Lamin A/C was found upregulated in OA cartilage, although the mechanism that regulates this alteration is still unknown (132).

The enzyme that mediates this process is Zn^{2+} membrane metalloprotease (Zmpste24). Zmpste24 plays a dual role in the maturation of Lamin A by participating in the elimination of the endoproteoytic AAX, and in the carboxymethylacion of the cysteine (130). Importantly, disruption in Zmpste24 cause failure in lamin A maturation, and in accumulation of prelamin A. This leads to the generation of abnormalities in nuclear architecture, that eventually lead to accelerated aging. In this sense, disruption of Z24 caused severe growth retardation and premature death. Therefore, Z24 deficient mice provide an ideal mouse model to study the impact of aging in the musculoskeletal system.

Since age is a risk factor strongly correlated with OA (168) and decreased basal autophagy activity, (156) efforts to identify and establish the role of the targets regulating these processes are necessary to find ways to prevent cartilage aging and degeneration.

4.2.2 Specific Material and methods

In this chapter, the following experimental procedures, were employed to identify and validate potential targets of autophagy related with aging and OA, as we described in the Material and Methods Section.

- **Cell Culture:** OA human cartilage was obtained from patients undergoing knee replacement (mean ± SD**;** 76,75 ± 3,30 years, n=2). OA human chondrocytes were transiently transfected with small interference RNA (siRNA) for Atg5 100 nM using Lipofectamine™ 2000. The sense strand sequence of the siRNA was 5'-GCUAUAUCAGGAUGAGAUATT-3'. The transfected chondrocytes were then collected and used for iTRAQ analysis. Immortal juvenile human chondrocytes (T/C-28A2) were employed for validation studies.
- **Human Cartilage Samples:** Articular cartilage sections from healthy donors (mean ± SD, 28,5 ± 3,53, n=2), aged cartilage (mean ± SD, 75,33 ± 10,34, n=6), OA cartilage grade II-III (mean ± SD, 54,75 ± 6,29, n=4) and OA cartilage grade III-IV (mean ± SD, 65,33 ± 14,15, n=4) were employed for inmunohistochemical studies.
- **Proteomic Studies:** Proteomic screening was performd by isobaric tags for relative and absolute quantification (iTRAQ) labeling to identify targets regulating autophagy in human chondrocytes with defective autophagy.
- **Validation Studies:** Upregulation of Lamin A/C, the identified target by proteomic screening under defective autophagy conditions, was validated in human chondrocytes and healthy, aging and OA human cartilage by Inmunofluorescence, Western Blotting and Immunohistochemistry, respectively.
- **Functional studies:**

  In vitro:

a. **Clustered regularly interspaced short palindromic repeats (CRISPR-Cas9) technology:** The Genetic deletion of Zmpste24 was performed in T/C28a2 human chondrocytes by CRISPR-Cas9 knockdown to evaluate the role of Lamin A/C up-regulation on chondrocyte homeostasis.

b. **Quantification of cell death by apoptosis, determination of mitochondrial membrane potential (Δψm) and quantification of ROS production:** To

investigate the role of Lamin A/C accumulation on OA phenotype in human chondrocytes.

c. ***In Vivo:***

   a. **Mutant Mice:** Zmpste24 KO mice were employed to evaluate the consequences of aging in the musculoskeletal system.

   b. **Phenotypic studies:** Body weight, cartilage changes, bone changes and spine degeneration were evaluated to investigate the role of Lamin A/C accumulation on Musculoskeletal system.

Statistical analysis: Statistically significant differences between 2 groups were determined by Student's t-test, while differences between multiple groups were determined analyzing ANOVA with Tukey's multiple comparison. The results are reported as the mean ± SEM. P values less than 0.05 were considered significant.

4.2.3 Results

4.2.3.1 Identification of differentially regulated proteins in autophagy deficient human chondrocytes

Autophagy is reduced in articular cartilage of elderly and OA patients (37, 156). To identify the key proteins regulated when autophagy is compromised, we silenced Atg5 in primary human chondrocytes. Atg5 is essential for autophagosome formation and represents a critical checkpoint (144). We hypothesize that proteins exhibiting altered expression in Atg5-knockdown chondrocytes might be potential regulators of cartilage homeostasis. Lysates from siCtrl and siAtg5 chondrocytes were subjected to iTRAQ labeling and on-line 2D LC/MS/MS analysis as described in the Materials and Methods section.

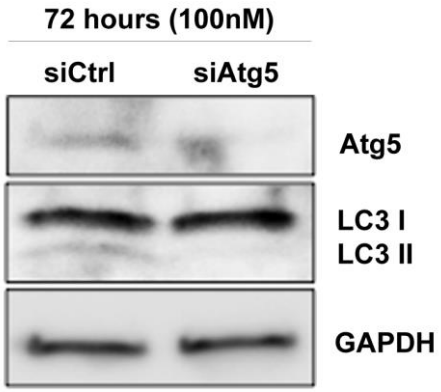

Figure 4.8: Defective autophagy induced by ATG5 siRNA in human chondrocytes. OA human chondrocytes were transfected with siCtrl or siAtg5 for 72 hours. **A,** The levels of Atg5 and LC3 were determined by Western blotting.

We identified 487 proteins in human chondrocytes (**Appendix 3: Table 3**). Interestingly, 24 proteins were significantly modulated ($p<0.05$) in siAtg5 chondrocytes compared to siCtrl (**Table 1**). Proteins involved in cytoskeleton organization, collagen catabolism, oxidative stress, and aging pathways were differentially regulated. From this set, 11 proteins were significantly down-regulated and 13 were significantly up-regulated. For follow up studies, we decided to focus on Prelamin A/C, a nuclear protein implicated in cell senescence, significantly upregulated. Alterations in Lamin A and C cause cellular senescence, and mutations in the LMNA gene have been correlated with degenerative disorders and accelerated aging in humans (166).

Table 1. Identification of regulated proteins in autophagy deficient human chondrocytes by iTRAQ analysis (siAtg5 vs. siCtrl)

Accession #	Name	Symbol	Peptides	Ratio*	pValue	Ratio*	pValue	Location	Function
Q15149	Plectin	PLEC	130	0.3945	0	0.6545	0.0217	Cyto.	ECM organization
P12111	Collagen alpha-3 (VI) chain	COL6A3	122	0.6194	0.0487	0.3373	0	Cyto.	ECM organization
P21333	Filamin-A	FLNA	90	0.302	0	0.6368	0.0298	Cyto.	Cytos. organization
P35579	Myosin-9	MYH9	68	0.4529	0	0.7516	0.0412	Cyto.	Cytos. organization
P14618	Pyruvate kinase isoenzymes M1/M2	PKM2	58	0.6138	0.0159	0.7244	0.0413	Cyto.	Glycolisis
P12814	Alpha-actinin-1	ACTN1	44	0.6081	0.0046	0.6607	0.0367	Cyto.	ECM organization
P02545	Prelamin A/C	LMNA	44	1.4588	0.0413	1.4859	0.044	Nucl.	Estruct. organization
Q00610	Clathrin heavy chain 1	CLTC	36	0.3981	0.0001	0.6546	0.005	Cyto.	Protein Transport
P08758	Annexin A5	ANXA5	35	2.8054	0.0001	1.5276	0.0011	Cyto.	Protein Transport
P07900	Heat shock protein HSP90-alpha	HSP90A1	27	0.6855	0.0019	0.8710	0.0496	Cyto.	Stress response
Q14764	Major vault protein	MVP	25	0.6081	0.0061	0.7516	0.0491	Cyto.	Protein transport
P04179	Superoxide dismutase [Mn], mitochondrial	SOD2	25	1.8880	0.0379	2.0317	0.0346	Mito.	Stress response
P36222	Chitinase-3-like protein 1	CHI3L1	24	1.7219	0.0017	1.2246	0.0273	ECM	Inflammatory response
P06576	ATP synthase subunit beta, mitochondrial	ATP5B	23	1,8030	0.0064	1.4588	0.0234	Mito.	ATP synthesis
O60701	UDP-glucose 6-dehydrogenase	UGDH	21	0.5210	0.0113	0.7178	0.0416	Cyto.	Synthesis GAGs
Q9NZM1	Myoferlin	MYOF	19	0.6918	0.0448	0.6982	0.0435	Memb.	Phospholipid binding
P09601	Heme oxygenase 1	HMOX1	16	2.2284	0	1.3305	0.0420	ER	Apoptosis
O43852	Calumenin	CALU	15	2.8576	0.001	2.1677	0.0026	ER	Calcium binding
P37802	Transgelin-2	TAGLN2	14	1.7539	0.0487	2.0701	0.0314	Exo.	Actin filament binding
P67936	Tropomyosin alpha-4 chain	TPM4	14	1.5560	0.0091	1.6596	0.010	Cyto.	Calcium binding
P62805	Histone H4	HIST1H4A	13	1.5560	0.027	1.3305	0.0668	Nucl.	DNA binding
Q96D15	Reticulocalbin-3	RCN3	10	2.4210	0.0032	1.7219	0.0449	ER	Calcium binding
P19105	Myosin regulatory light chain 12A	MYL12A	8	1.7061	0.0731	2.1677	0.0144	Cyto.	Calcium binding
P16070	CD44 antigen	CD44	6	1.2474	0.0595	1.5136	0.0268	Memb.	Cell adhesion

 # Protein accession number according to SwissProt database

*** Average iTRAQ ratios that represent the relative protein abundance in siAtg5 vs. siCtrl chondrocytes, calculated by protein pilot 3.0 Software. (p value ≤ 0.05 was accepted).**

4.2.3.2 Defective autophagy increases Lamin A/C accumulation in human chondrocytes

Genetic knockdown of Atg5 in TC28a2 human chondrocytes reduced the expression of LC3, the main marker for autophagosome formation and autophagy activation. This reduction was correlated with an increase in Lamin A/C expression (**Figure 4.9 A and B**). Immunofluorescence detected increased Lamin A/C localization in the nuclear membrane of chondrocytes in response to defective autophagy (**Figure 4.9C**). We reasoned that nuclear lamina component Lamin A/C might play a role in articular cartilage aging due to abnormal accumulation.

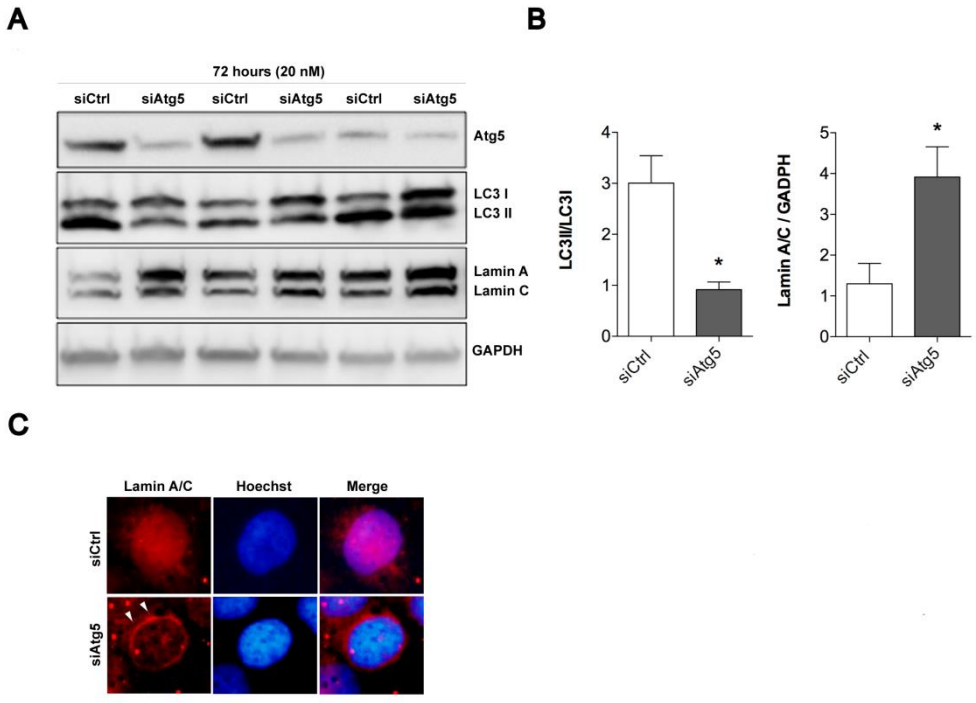

Figure 4.9: Defective autophagy increases Lamin A/C accumulation in human chondrocytes. A, Western blot analysis to detect Atg5, autophagosome formation by lipidation of LC3 I to LC3 II and Lamin A/C expression in TC28a2 human chondrocytes under defective autophagy conditions (siCtrl versus siAtg5). **B,** Densitometric analysis of ratio of LC3II/LC3I, and Lamin A/C. GAPDH was employed as a loading control. Values are mean ± SEM of three repeated observations. LC3 II/LC3I: *p < 0.01 versus siCtrl; Lamin A/C: *p < 0.05 versus siCtrl. **C,** Fluorescence-based detection of Lamin A/C in TC28a2 chondrocytes under defective autophagy (siAtg5 versus siCtrl). Scale bar 10µm. Lamin A/C expression was localize in the nuclear membrane: white arrows.

4.2.3.3 Increased of expression of nuclear Lamin A/C in human aging cartilage

Alterations in Lamin A/C cause cellular senescence in humans, and mutations in LMNA gene are correlated with degenerative disorders, referred to as laminopathies (169). We evaluated the expression of Lamin A/C in human aged cartilage and found increased expression in aged cartilage compared to healthy cartilage. We observed a strong expression of Lamin A/C in the nuclear membrane of the chondrocytes. However, the expression in the healthy cartilage was diffuse and only few cells show positive immunoreactivity (**Figure 4.10 A and B**). These results indicate that aging chondrocytes highly express markers of cellular senescence from the nuclear lamina, and support further investigations of the role of Lamin A/C in cartilage.

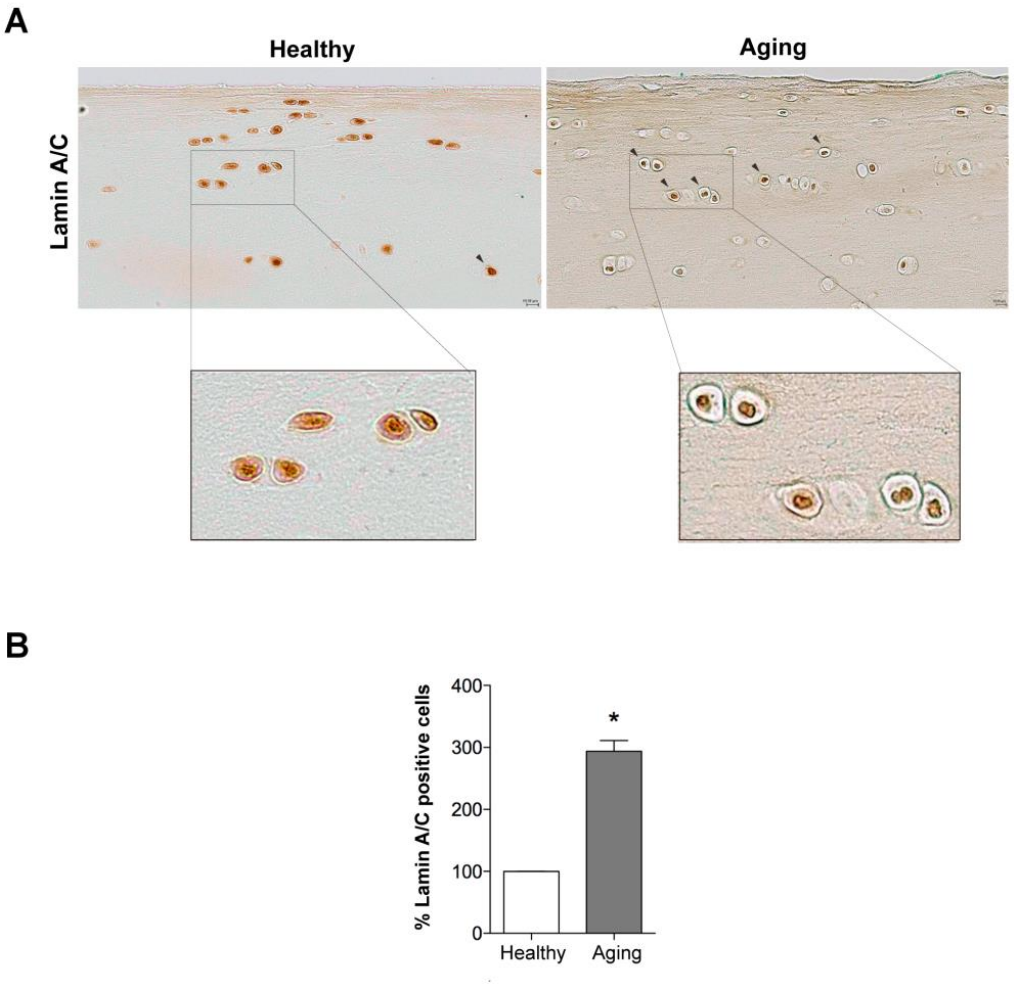

Figure: 4.10: Increased Lamin A/C expression in aging cartilage. A, Human cartilage from healthy and aged patients were employed. Lamin A/C expression was evaluated and quantified by immunohistochemistry. Magnification: 40x. Scale bar 100µm**. B,** Quantitative analysis of Lamin A/C-positive cells. Total cell number in three fields and Lamin A/C-positive cells were counted. Values are the means ± SEM of 6 independent human cartilage donors sections. *p<0.0001 versus healthy cartilage.

4.2.3.4 Lamin A/C accumulation in osteoarthritic cartilage

To investigate the association between chondrocyte senescence by Lamin A/C accumulation and OA, we evaluated the expression in OA human cartilage by immunohistochemistry. The results showed increased Lamin A/C expression in OA cartilage compared to healthy cartilage. Indeed, cartilage with different grades of OA severity expressed differential abundance of Lamin A/C. We found a significant increase in Lamin A/C-positive cells in mild and severe cartilage pathology, even in grade IV OA cartilage where the superficial zone is particularly compromised. Consistent with abnormalities often observed in laminopathies, chondrocytes positive for Lamin A/C in severe OA samples showed irregular nuclear architecture which may cause cellular fragility (**Figure 4.11 A and B**).

These results suggest a direct relationship between Lamin A/C regulation and cartilage degeneration that occurs in OA progression.

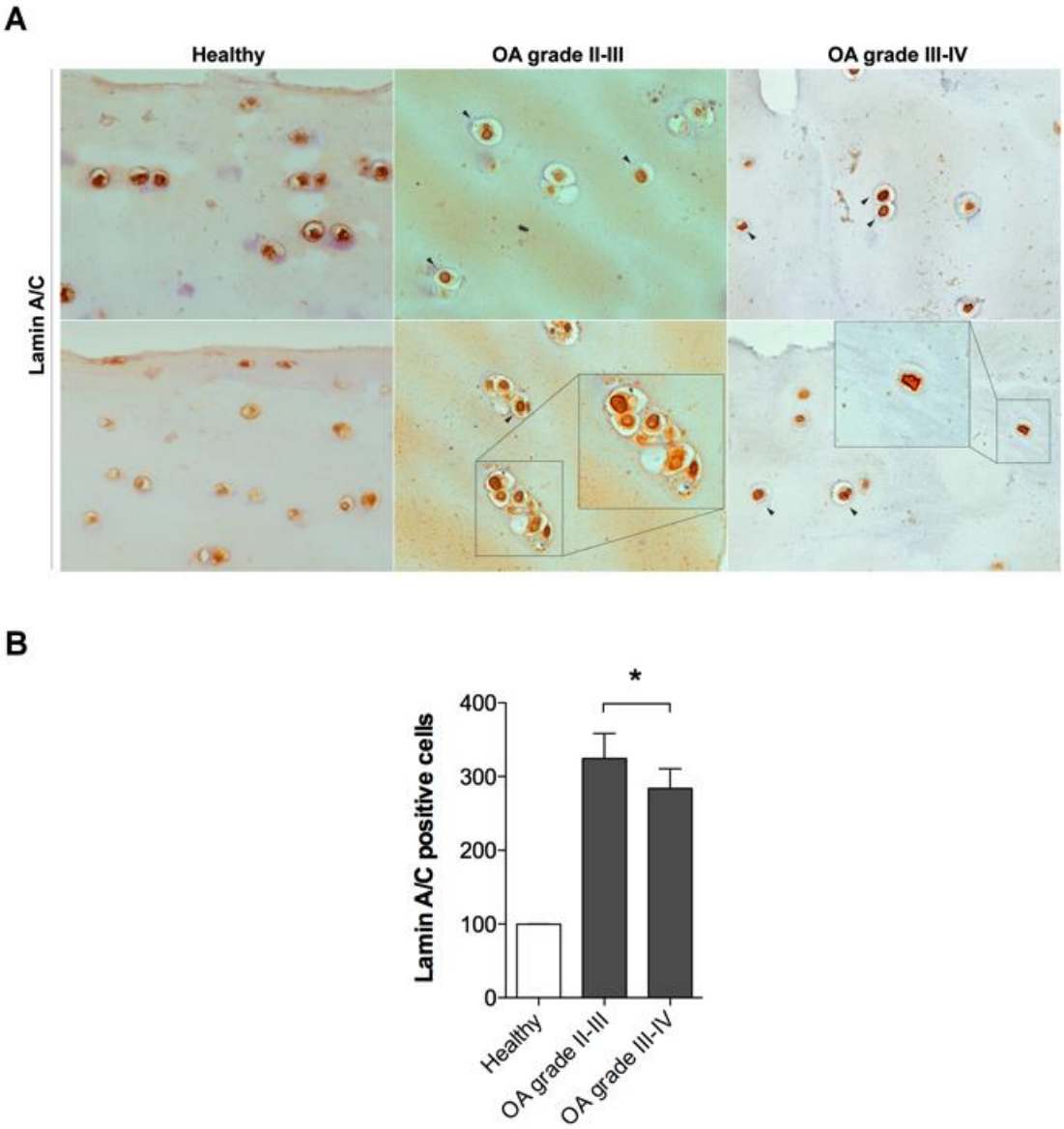

Figure: 4.11. Lamin A/C expression is increased in OA cartilage. Cartilage sections from healthy (n=2), OA grade II-III cartilage (n=4) and OA grade III-IV cartilage (n=4) were analysed by immunohistochemistry for Lamin A/C. Magnification: 40x. Scale bar 100µm**. B,** Quantitative analysis of Lamin A/C-positive cells. Total cell number in three fields and Lamin A/C-positive cells were counted. Values are mean ± SEM. *p<0.01 versus healthy cartilage.

4.2.3.5 Lamin A/C disrupts chondrocyte homeostasis in human chondrocytes

To determine the role of Lamin A/C on the autophagy pathway, we performed an *in vitro* premature aging model by genetic deletion of Zinc Metalloproteinase STE24 (Zmpste24) via CRISPR-Cas9 technology in TC28a2 chondrocytes. Zmpste24 (Z24) plays a critical role in Lamin maturation. Genetic deletion of Z24 accelerates the ageing process due to accumulation of Prelamin A, which leads to nuclear abnormalities and Lamin A/C alterations (170).

In this sense, the genetic reduction of Z24 in human chondrocytes significantly reduced the expression levels of Lamin A and LC3 (**Figure 4.12A**). Importantly, protein studies confirmed that genetic deletion of Z24, increased Prelamin A/C expression and reduced autophagy by decreasing the ratio between LC3II and LC3I (**Figure 4.12B**). Moreover, this reduction in autophagy was correlated with an increase in chondrocyte death by apoptosis in $Z24^{-/-}$ chondrocytes compared to wild type (WT) chondrocytes (**Figure 4C and D**).

These results suggest that deficient autophagy is associated with increased senescence and disruption of homeostasis in human articular cartilage.

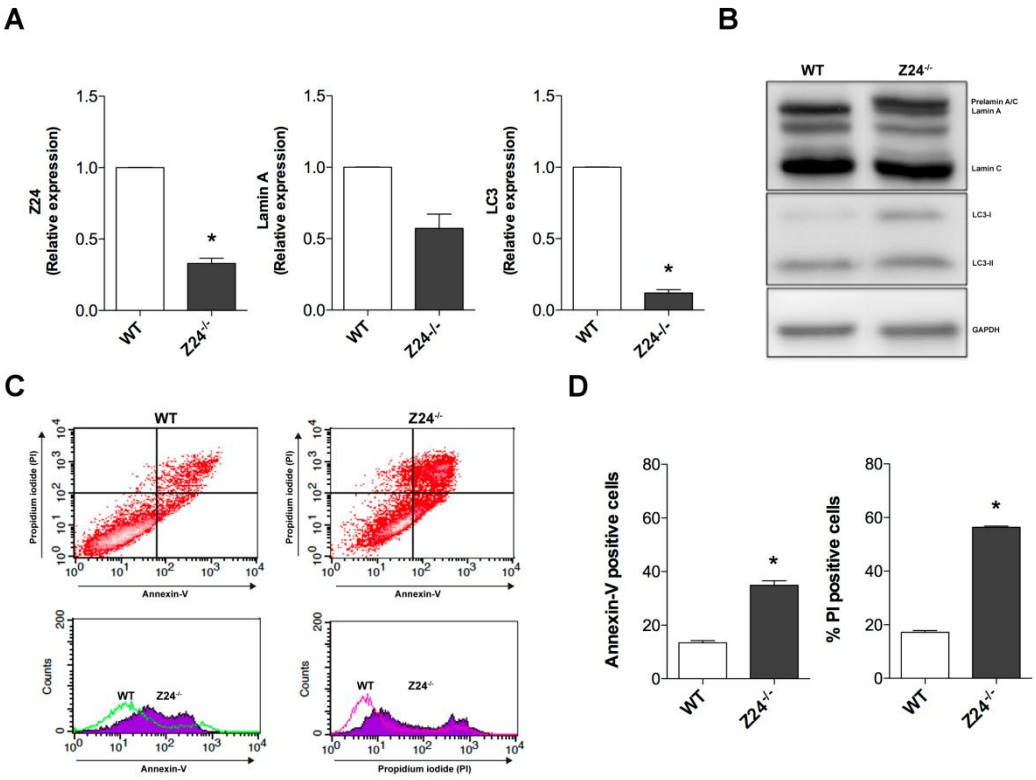

Figure 4.12: Upregulation of Lamin A/C expression reduced autophagy in human chondrocytes. A, Relative expression of Zmpste24 (Z24), Lamin A and LC3 in wild type (WT) and Z24$^{-/-}$ TC28a2 human chondrocytes. Values are mean ± SEM of two repeated observations for duplicate. Z24: *p < 0.01 versus WT; Lamin A: p = 0.0523; LC3: *p < 0.001 versus WT. **B,** Western Blot analysis to detect Prelamin A/C and lipidation of LC3 I to LC3 II in WT and Z24$^{-/-}$ TC28a2 human chondrocytes. **C,** Flow cytometry determination of early apoptosis by Annexin-V staining, and late apoptosis by propidium iodide (PI) staining in WT and Z24$^{-/-}$ TC28a2 human chondrocytes. **D,** Quantitative analysis of chondrocyte death by Annexin-V and PI staining. Values are mean ± SEM of three repeated observations. Annexin-V: *p < 0.001 versus WT; PI: * p < 0.0001 versus WT.

4.2.3.6 Increased mitochondrial dysfunction in accelerated ageing chondrocytes

Mitochondria plays a key role in aging-related diseases, such as OA(20). To establish the connection between aging, chondrocyte homeostasis and mitochondrial function, we employed Z24$^{-/-}$ human chondrocytes. Our results showed a significant increase in the mitochondrial superoxide production (**Figure 4.13A**) and a significant decrease in the mitochondrial membrane potential in Z24$^{-/-}$ chondrocytes compared to WT chondrocytes (**Figure 4.13B**). Taking together, these results demonstrated that accelerated ageing is associated to defective autophagy, chondrocyte death by apoptosis, and mitochondrial dysfunction, all main features of OA disease.

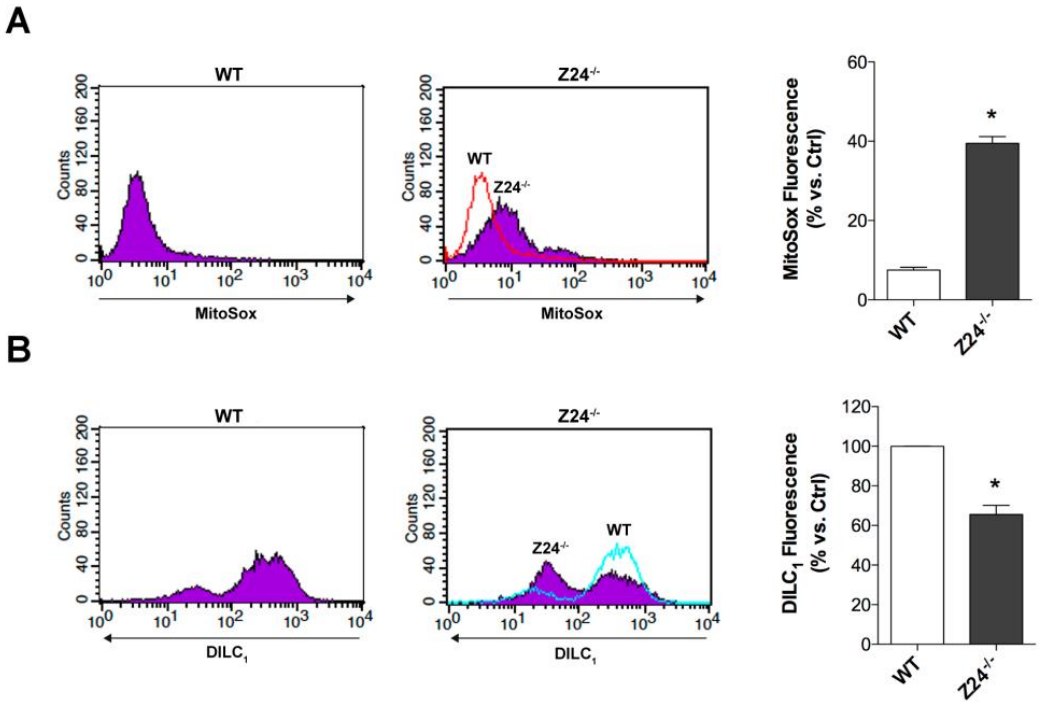

Figure: 4.13. Increased mitochondrial dysfunction in accelerated ageing chondrocytes. A, Quantitative analysis of mitochondrial superoxide using MitoSox red dye in wild type (WT) and Z24$^{-/-}$ TC28a2 human chondrocytes. Values are mean ± SEM of three repeated observations. *p < 0.0001 versus WT. **B,** Analysis of mitochondrial membrane potential (Δψm) using $DILC_1$ dye in wild type (WT) and Z24$^{-/-}$ TC28a2 human chondrocytes. Expression of Δψm as $DILC_1$ fluorescence (percentage of Ctrl). Values are mean ± SEM of three repeated observations. *p < 0.0001 versus WT.

4.2.3.7 Zmpste24 deficient mice as a model of accelerated aging in musculoskeletal system

The Zmpste24 deficient mice (*Zmpste24*$^{-/-}$) show phenotypic changes that accelerate the aging process in most tissues (17). At birth, *Zmpste24*$^{-/-}$ mice are similar to the heterozygous siblings (*Zmpste24*$^{+/-}$) and seemed healthy, until four weeks of age, approximately. Successively, the *Zmpste24*$^{-/-}$ mice might be distinguished from *Zmpste24*$^{+/-}$ in size and body weight. After 4 weeks of age, the growth rate was reduced and the mice stopped to grow. As shown in **Figure 4.14 A**, the size of *Zmpste24*$^{-/-}$ mice is smaller than *Zmpste24*$^{+/-}$ (*Zmpste24*$^{+/-}$: 26.29 ± 0.8841 g, N=21; *Zmpste24*$^{-/-}$: 13.77 ± 0.8098 g, N=13), indicating that the body weight of *Zmpste24*$^{-/-}$ mice is aproximately 50% less than the *Zmpste24*$^{+/-}$: mice **(Figure 4.14B)**. Body weight of males and females was also evaluated with no significance differences found within sex **(Figure 4.14C)**.

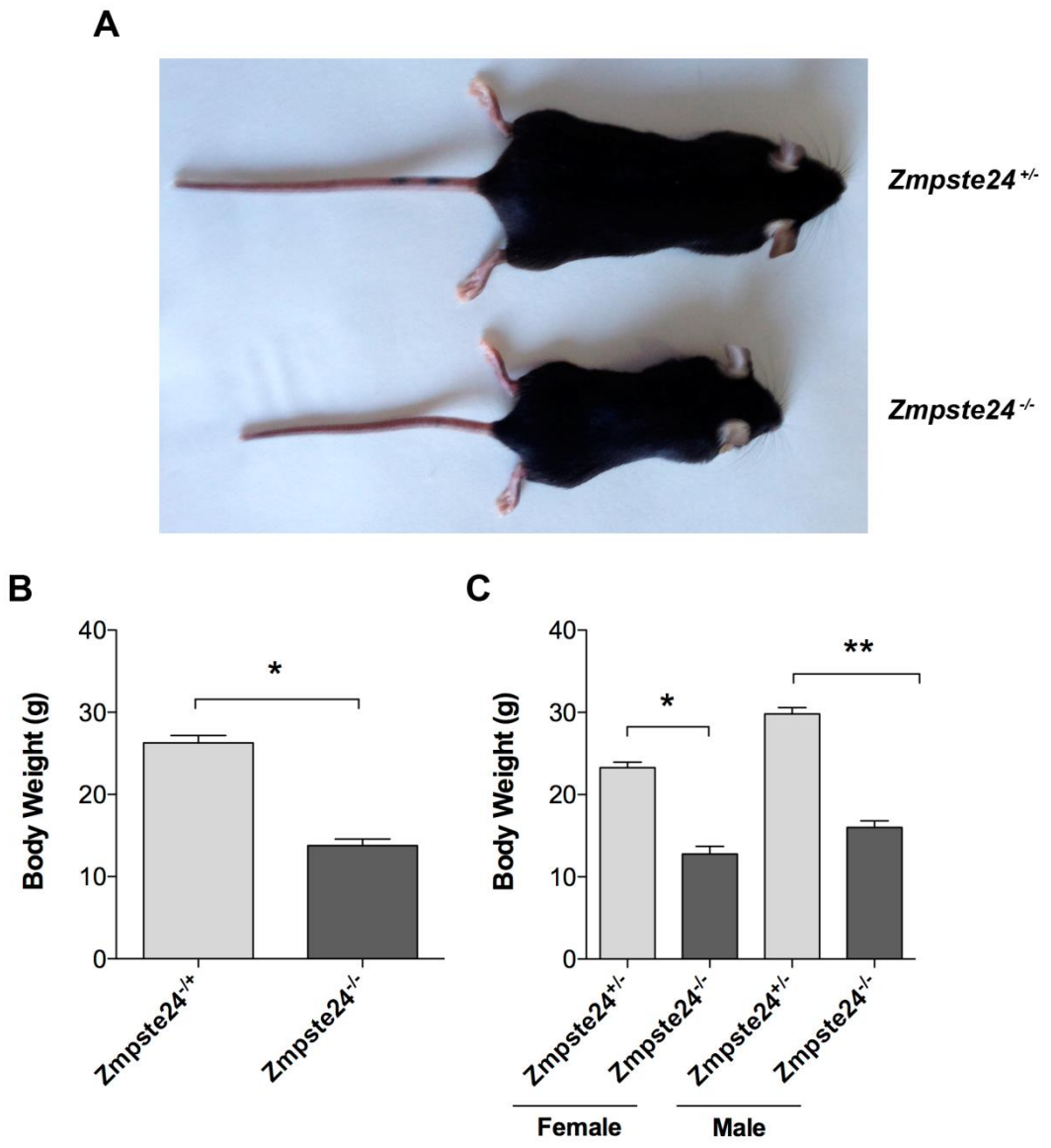

Figure: 4.14. Phenotypic changes of Zmpste24 deficient mice. A, Image of two littermates of *Zmpste24*$^{+/-}$ and *Zmpste24*$^{-/-}$ mice at 20 weeks of age. **B,** Statistical analysis of body weight of *Zmpste24*$^{+/-}$ and *Zmpste24*$^{-/-}$ mice, *p < 0.0001 versus *Zmpste24*$^{+/-}$. **C,** Statistical analysis of body weight of *Zmpste24*$^{+/-}$ and *Zmpste24*$^{-/-}$ mice distributed by sex; *p < 0.0001 versus female *Zmpste24*$^{-/+}$ and *p < 0.0001 versus male *Zmpste24*$^{-/+}$.

4.2.3.8 Aging-associated histopathological changes in Zmpste 24 deficient mice joint tissues

Aging represents the major risk factor for OA and progress has been made in characterizing the phenotype of aging-related changes in cartilage extracellular matrix and in cartilage cells. However, this analysis remains incomplete, and the mechanisms and pathways responsible for such changes are poorly defined.

Here, we investigated the role of lamin A/C on joint damage by employing an accelerated aging model, the *Zmpste24*$^{-/-}$ mice. Surprisingly, we did not found any histological changes in joint cartilage **(Figure 4.15 A and B)**, although cartilage is the tissue with the highest prevalence of aging-related pathological changes, probably because this accelerated aging model is too short to develop evident changes in the joint cartilage. Because OA is a whole-joint disorder, synovium and bone were also evaluated. The analysis of synovial inflammation indicated that there is no synovitis associated with lamin A/C accumulation (Data not shown). Interestingly, we found significant differences in bone integrity after evaluation. The results showed a significant reduction in the subchondral bone thickening and in the trabeculae bone. Furthermore, we found that the bone was very osteoporotic and fragil **(Figure 4.15C).**

Our histological analysis of joint indicates evidence of pathological damage in the bone of *Zmpste24*$^{-/-}$ mice, without any defect in joint cartilage or synovium.

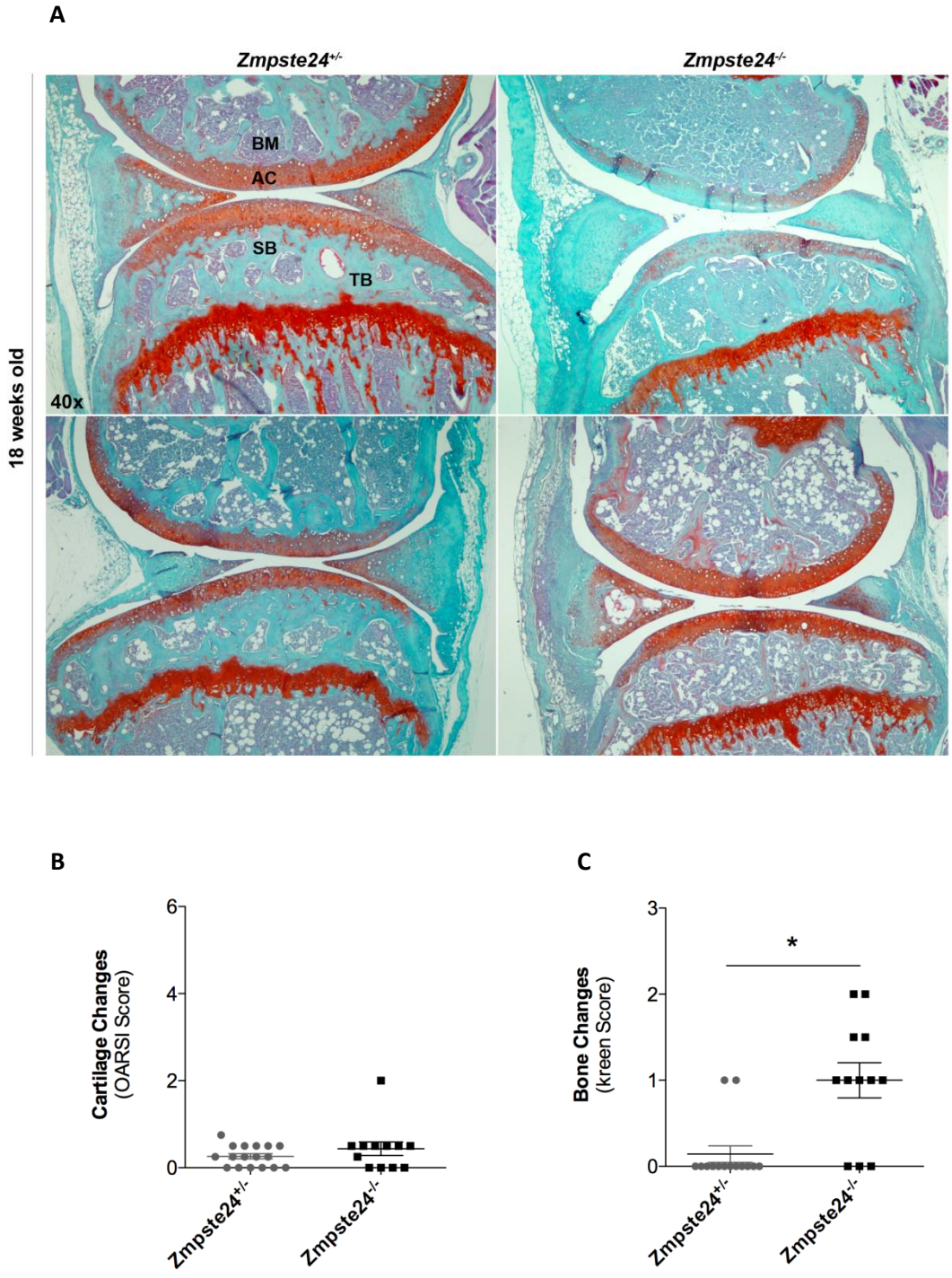

Figure 4.15: Aging-associated histopathologic changes in Zmpste24 deficient mice joint tissues. A, Knee joints obtained from Zmpste24+/- and Zmpste24-/- mice at 18 weeks of age were analyzed. Representative images of knee joints stained with Safranin O. Original magnification 40x. **B**, Scoring of cartilage changes (Zmpste24+/-, n=17; Zmpste24-/-, n=12). **C**, Quantification of bone changes (Zmpste24+/-, n=14; Zmpste24-/-, n=12). Values are the mean ± SEM, *p < 0.001 versus Zmpste24+/- mice.

4.2.3.9 Accelerated aging induces intervertebral disc degeneration in Zmpste24 mice

Because intervertebral disc degeneration (IVD) is also an important feature in aging-related diseases, we evaluated the spine. We collected the spines at 20 weeks for histological analysis to compare *Zmpste24*$^{-/-}$ mice and *Zmpste24*$^{+/-}$. To determine the aging-related pattern of cervical and lumbar spines, sections were stained with Safranin-O/Fast green and Hematoxylin-Eosin, respectively. The results indicated that *Zmpste24* $^{-/-}$ mice exhibited histological changes that are characteristic of IVD degeneration in cervical and lumbar spine compared to *Zmpste24*$^{+/-}$. These changes included a disruption of the Nucleus Pulposus (NP) and Annulus Fibrosus (AF) borders, associated with a reduction in NP size. Furthermore, we found ruptured fibers and a disorganization of AF and an apparent loss of proteoglycan staining and some ossification in the EP. In addition, these changes were more severe in male mice than in female mice **(Figure 4.16)**. In addition, these changes included decreased cellularity in the NP, AF and EP in *Zmpste24*$^{-/-}$ mice compared to *Zmpste24*$^{+/-}$ mice. These differences in cellularity were also higher in male mice than in females **(Figure 4.17)**.

These results indicate that the abnormal accumulation of Lamin A/C is associated with age-related degeneration in the IVD, and this phenotype was more severe in male mice.

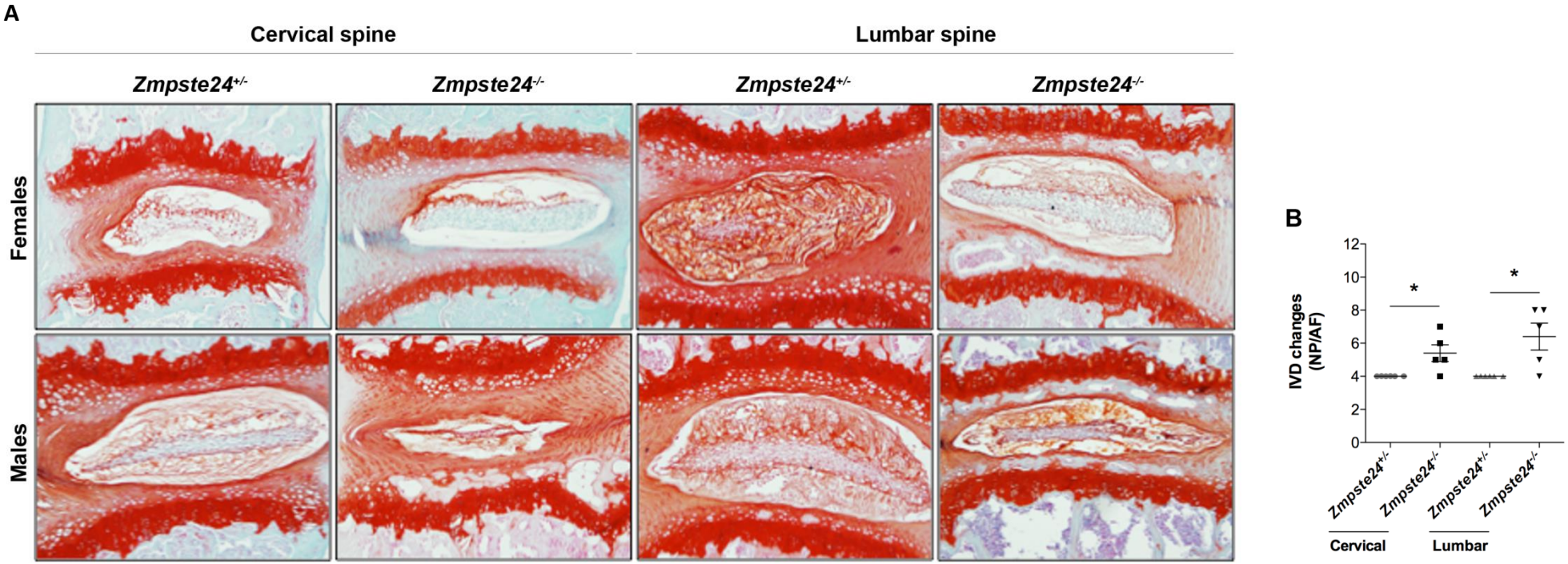

Figure 4.16: Accelerated aging induces intervertebral disc degeneration (IVD) in *Zmpste24* mice. A, Spines obtained from*Zmpste24*$^{+/-}$ and *Zmpste24*$^{-/-}$ mice at 18 weeks of age were analyzed. Representative images of spine (cervical and lumbar) stained with Safranin O. Magnification 40x. **B,** Quantification of IVD changes in cervical and lumbar spine (*Zmpste24*$^{+/-}$, n=6; *Zmpste24*$^{-/-}$, n=6). Values are the mean ± SEM; Cervical spine: *p < 0.05 versus *Zmpste24*$^{+/-;}$; Lumbar spine: *p < 0.01 versus *Zmpste24*$^{+/-}$ mice. Lumbar: *p < 0.05 versus *Zmpste24*$^{+/-;}$ Cervical: *p < 0.01 versus *Zmpste24*$^{+/-}$.

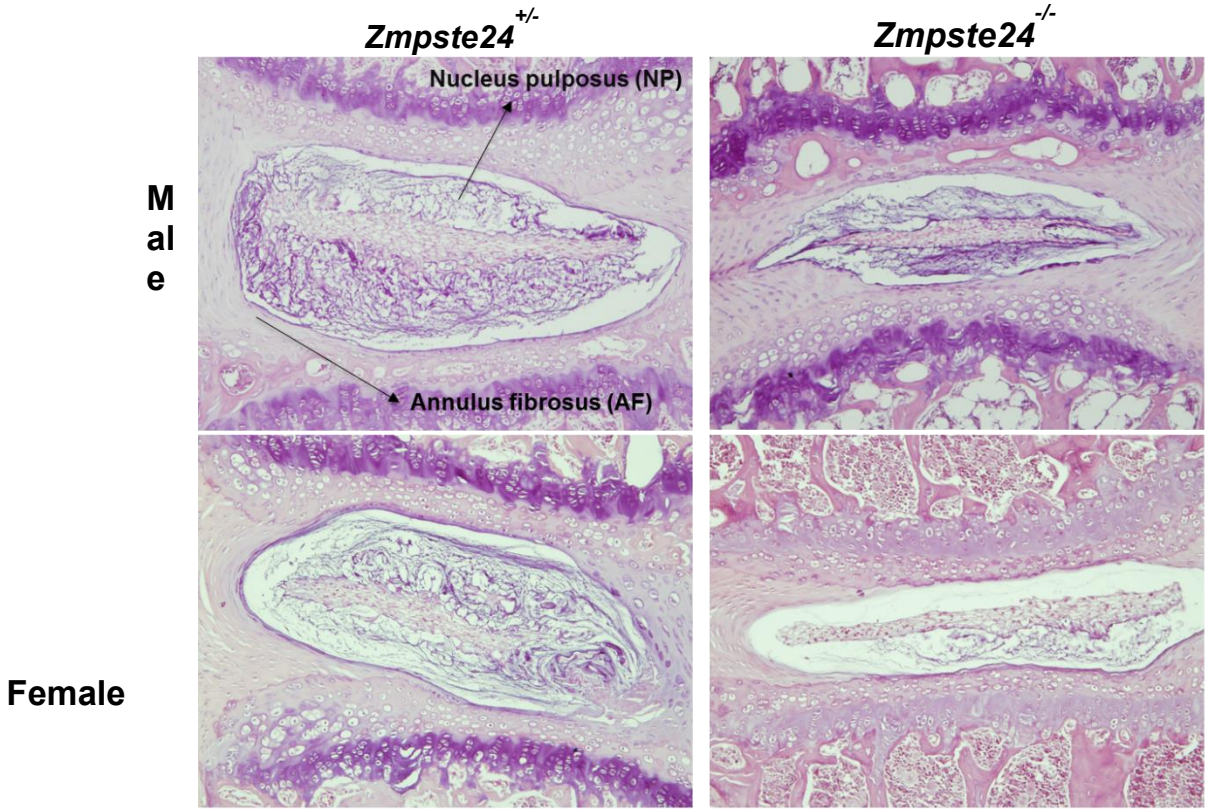

Figure 4.17: Loss of cellularity in Intervertebral disc in accelerated aging mice. Representative pictures of loss of cellularity in spine from males and females *Zmpste24*$^{-/-}$ and *Zmpste2*$^{+/-}$ mice by Hematoxilin- Eosin staining. Magnification 20x.

CHAPTER 5: DISCUSSION

5.1 To study the effects of defective autophagy to mitochondrial function using pharmacological and genetic approaches

Defective autophagy and mitochondrial dysfunction are features of aging-related cartilage degeneration (20, 37). However, the interdependence of these critical cellular homeostasis mechanisms in the pathogenesis of cartilage degeneration has not been directly investigated.

The data from the present study indicate that autophagy activation protects against mitochondrial dysfunction in human chondrocytes. Autophagy is an essential cellular homeostasis mechanism that functions not only by adjusting to variations in nutrient supply, but also by removing dysfunctional organelles and macromolecules, such as mitochondria (155), which have been observed in OA cartilage (104). The critical role of autophagy in chondrocytes and cartilage function is illustrated by the presence of deficient autophagy activity in experimental and spontaneous aging-associated OA models. In this regard, manifestations of autophagy defects are often linked to cell dysfunction and cell death (63). Cellular dysfunction leads to tissue and organ failure and can manifest as aging-associated degenerative disease (171, 172). Conversely, pharmacologic augmentation of autophagy protects against cell dysfunction and disease and, in model organisms, extends lifespan (172) and health (173, 174). We previously demonstrated that autophagy activation protects against mechanical damage in cultured cartilage explants and in mice with experimental OA (62, 160). These findings support the notion that mechanisms that can induce repair of cellular damage are critical for chondrocyte homeostasis.

The mitochondrial respiratory chain oxidizes nutrients to generate the energy molecule ATP. An abnormal production of ROS during the oxidative phosphorylation process can cause harm and may eventually cause cell death (175). In human chondrocytes, the oxygen supply is gradually reduced across the different zones of articular tissue (20), which most likely result in a tight regulation of the number and function of mitochondria to maintain cellular energy homeostasis. Nevertheless, data on adaptation of chondrocytes to oxygen needs by regulating mitochondrial density and function are limited.

In the present study, we investigated autophagy as a critical mechanism for maintaining mitochondrial function in human articular chondrocytes. We used oligomycin, a mitochondrial respiratory chain complex V inhibitor, to induce

mitochondrial dysfunction in human chondrocytes. The respiratory capacity of chondrocytesis compromised in OA articular cartilage due to defects in mitochondrial coupling efficiency (149). Oligomycin reduces electron flow through the electron transport chain, although not completely, due to mitochondrial uncoupling (176). Because of this defect in the respiratory capacity of chondrocytes in OA, we tried to mimic the mitochondrial dysfunction by using oligomycin, an inhibitor of the ATP synthase that blocks the inducible proton leak but not the basal uncoupling capacity. On the other hand, mitochondrial respiratory chain inhibitors such as antimycin A, a complex III inhibitor, have irreversible effects by binding to cytochrome c reductase. The subsequent disruption of the proton gradient and ATP synthesis by antimycin A results in the formation of high levels of superoxide and a dramatic loss of mitochondrial coupling efficiency (176), which likely potently affects the respiratory capacity of chondrocytes.

The effects of oligomycin we observed were consistent with those from previous studies (99, 153).

Under conditions where oligomycin induced significant mitochondrial dysfunction in chondrocytes, the basal level of autophagy was reduced, which indicates that partial inhibition of mitochondrial respiratory chain is sufficient to disrupt autophagy. Furthermore, we found an early activation of autophagy at 24 hours in response to mitochondrial dysfunction, followed by a clear and sustained reduction at 48 hours. We hypothesize that autophagy activation may protect against cell damage as a compensatory mechanism. However, when prolonged stress exceeds cellular compensation, autophagy may not be able to maintain the cellular balance, and ultimately, the presence of toxic molecules may lead to cell death (177).

A major regulator of autophagy is mTOR. To determine whether autophagy activation protects against mitochondrial dysfunction, autophagy was activated by rapamycin, a selective inhibitor of mTORC-1, and by torin 1, a dual inhibitor of mTORC-1 and mTORC-2.

Rapamycin has been shown to induce autophagy in a variety of cell types (178, 179), including articular chondrocytes and cartilage, which prevents cartilage damage in

vivo (62, 160). Our study is the first to demonstrate that torin 1 activates autophagy in human chondrocytes in a manner similar to that of rapamycin.

We evaluated the effects of oligomycin in mTOR signaling. Interestingly, oligomycin has stimulatory effects in articular chondrocytes, activating phosphorylation at the Ser235/236 residue of the ribosomal protein S6, a downstream target of mTOR activated with growth and proliferation (180). We also investigated Akt protein kinase, an upstream mTOR regulator activated by growth and survival factors (180). Our data indicate that oligomycin induces Akt phosphorylation at residue Ser473, which is an indication that mTORC-2 is directly regulated when mitochondrial ATP synthase is pharmacologically inhibited. Taken together, our evidence indicates that oligomycin decreases autophagy in an Akt/mTOR-dependent manner in human chondrocytes, which might result in reduced cell growth and may partly explain the cartilage degradation observed in OA.

In summary, our study is the first to demonstrate that autophagy is a protective mechanism in human chondrocytes with mitochondrial dysfunction. Our observations suggest that autophagy plays an important role in the protection of chondrocytes from oxidative stress and support the idea that pharmacologic interventions that target autophagy may prevent cartilage degradation.

Furthermore, we provide evidence of a direct link between mitochondrial function and autophagy regulation in cartilage, which may lead to new therapeutic strategies for aging-related musculoskeletal disorders such as OA.

5.2 To identify potencial targets of defective autophagy associated with the pathology of the musculoskeletal system

Autophagy regulation in cells has been recognized as a paradigm-shifting in our molecular understanding of disease (181). Alterations in autophagy contribute to the progression of various rheumatic diseases, including OA, where chondrocytes within articular cartilage show decreased autophagy, leading to cell death and degeneration (182). We previously demonstrated that some of the consequences of autophagy deficiency in human chondrocytes are associated to oxidative stress and mitochondrial dysfunction (158). However, the potential targets regulating the link between autophagy and cartilage homeostasis are still unknown.

Here, we performed a proteomic analysis to identify the biological processes and proteins relevant to the homeostatic state of human chondrocytes. We carried out a comparative analysis and protein quantification through incorporation of stable isotopes (iTRAQ) in Atg5-deficient primary human chondrocytes. Our list of protein explains many biological processes and mechanisms present in articular cartilage, including nuclear structure, cytoskeleton organization, collagen catabolism, oxidative stress, and aging. Interestingly, upregulation of Prelamin A/C indicated that nuclear structural components might be implicated in cell senescence. Increased accumulation of Lamin A is observed in OA chondrocytes and cartilage(132, 183). We therefore propose Lamin A/C accumulation as a inherent alteration related to chondrocyte senescence and OA progression.

We observed Lamin A/C accumulation in the nuclear membrane and reduced LC3 expression in Atg5-deficient human chondrocytes, which indicates that nuclear lamina components play a key role in articular cartilage aging. Lamin A/C accumulation is primarily observed not only in human aged cartilage but in OA cartilage. Indeed, Lamin A/C-positive cells are apparent in mild and severe cartilage, even in grade IV OA cartilage where the superficial zone is particularly compromised. These results suggest a direct relationship between Lamin A/C regulation and OA progression.

To explore the molecular mechanism of this association, we deleted Zmpste24, that accelerates the ageing process due to accumulation of Prelamin A in tissues and leads to nuclear abnormalities and Lamin A/C alterations m (170). Zmpste24, a metalloprotease, is required for the proteolytic clevages during Lamin A maturation.

[33] Mutations in Zmpste24 gene cause nuclear abnormalities that lead to accelerated-aging human syndromes, such as Hutchinson-Gilford Progeria Syndrome (HGPS) (116, 170, 184). Interestingly, Prelamin A accumulation enhance aging phenotype in hMSCs (185). However, the role of Prelamin A/C in premature aging chondrocytes has not been established yet. Deletion of Zmpste24 by CRISPR-Cas9 in human chondrocytes significantly reduced the expression of Prelamin A/C and decreased LC3II/LC3I ratio. The presence of accumulated Prelamin A/C under autophagy defects could ultimately lead to senescence of chondrocytes. Pathways otherwise intact in cartilage might be altered, for example in the premature aging phenotype of chondrocytes, such as the dysregulation of autophagy under starvation conditions that occurs in joint aging.

Because mitochondria plays a key role in the aging process, we explored whether premature aging in chondrocytes influence mitochondrial function. Indeed, accumulation of Prelamin A in human chondrocytes is associated with increased oxidative damage and mitochondrial dysfunction. These results are consistent with previous studies where deletion of Zmpste24 elevates ROS production and induces depolarization of mitochondrial membrane potential in human fibroblasts (186). Similarly, Zmpste24 deficient mice are associated with mitochondrial dysfunction, but more importantly, fibroblasts from HGPS patients showed alterations in the mitochondrial function (187, 188). These results highlight the notion that mitochondrial function is altered during aging in articular cartilage.

Our data collectively establish that autophagy is a key factor for the accumulation of Prelamin A in chondrocytes, inducing a premature aging phenotype which ultimately results in a clear decrease in cartilage functional capacity *in vivo.* In this human experimental model of premature aging, the aged phenotype is clearly exacerbated when autophagy is impaired. Our results are similar to those observed in both mice and patients where the presence of progerin induce aging,(189, 190) indicating the value of our model to the study of late onset of cartilage aging.

Ultimately, the identification of a relevant role of nuclear lamins in the aging of human chondrocytes and cartilage might provide the basis to explore the therapeutic potential of manipulating this pathway in OA.

CHAPTER 6: CONCLUSIONS

1. **To study the effects of defective autophagy to mitochondrial function using pharmacological and genetic approaches:**

   1.1. Mitochondrial dysfunction and cell death by apoptosis in human chondroytes were induced by inhibition of mitochondrial respiratory chain complex V by Oligomycin.

   1.2. Autophagy is defective in human chondrocytes with mitochondrial dysfunction.

   1.3. Pharmacological activation of autophagy by Rapamycin and Torin1 protects from mitocondrial dysfunction in human chondrocytes.

   1.4. AKT/mTOR pathway is critical for mitochondrial dysfunction of human chondrocytes.

   1.5. Defective autophagy by genetic deletion of Atg5, a key autophagy regulator, increases mitochondrial dysfunction in human chondrocytes.

2. **To identify potencial targets of defective autophagy associated with the pathology of the musculoskeletal system**

   2.1. Among the proteins detected, a number of 24 differentially regulated proteins were found in autophagy deficient primary human chondrocytes.

   2.2. Proteins differentially regulated in defective autophagy human chondrocytes are implicated in key cellular processes, such as, structural organization, protein transport, stress response, and calcium metabolism of chondrocytes.

   2.3. Defective autophagy increases Lamin A/C expression, a nuclear protein implicated in the structural organization and involved in the aging process, in human chondrocytes.

   2.4. Accumulation of Lamin A/C is observed in human aging cartilage and is directly correlated with OA severity.

   2.5. Accumulation of Lamin A/C, by genetic deletion of *Zmpste24* in human chondrocytes, disrupts chondrocyte homeostasis in conditions of accelerated aging associated to cell death by apoptosis and mitochondrial dysfunction.

   2.6. In mice with accelerated aging as a result of Lamin A/C accumulation, bone changes in mice joint were observed. Intervertebral disc degeneration (IVD) in

cervical and lumbar spine is also affected, and together might contribute to the pathology of the musculoskeletal system in mice.

CHAPTER 7: REFERENCES

1. Manuel Llusá Pérez AM, D. Ruano. Manual y atlas fotográfico de anatomía del aparato locomotor2004.
2. Buckwalter JA MH, Grodzinsky AJ Articular cartilage and osteoarthritis. Instructional course lectures. 2005;54:465-80.
3. Khan IM RS, Williams R, Dowthwaite GP, Oldfield SF, Archer CW. The development of synovial joints. Current topics in developmental biology (2007) 79: 1-36.

4. J. JIMENEZ-CASTELLANOS BALLESTEROS; CARLOS JAVIER CATALINA HERRERA; AMPARO CARMONA BONO. Anatomia Humana General 2008.
5. Blanco IS. Manual SERMEF de rehabilitación y medicina física. Ed Médica Panamericana. 2006:857.
6. Newell N, Little JP, Christou A, Adams MA, Adam CJ, Masouros SD. Biomechanics of the human intervertebral disc: A review of testing techniques and results. Journal of the mechanical behavior of biomedical materials. 2017;69:420-34.
7. Weber KT, Jacobsen TD, Maidhof R, Virojanapa J, Overby C, Bloom O, et al. Developments in intervertebral disc disease research: pathophysiology, mechanobiology, and therapeutics. Current reviews in musculoskeletal medicine. 2015;8(1):18-31.
8. Martel-Pelletier J BC, Pelletier JP, Roughley PJ Cartilage in normal and osteoarthritis conditions. . Best practice & research Clinical rheumatology. 2008;22:351-84.
9. Reumatología SEd. Artrosis. Fisiopatología, Diagnostico y Tratamiento. 2010

10. Buckwalter JA MH, Grodzinsky AJ Articular cartilage and osteoarthritis. Instructional course lectures 2005;54:465-80.
11. D E. Collagen of articular cartilage. Arthritis research. 2002;4:30-5.
12. Camarero-Espinosa S R-RB, Foster EJ, Weder C Articular cartilage: from formation to tissue engineering. Biomaterials science. 2016;4:734-67.

13. Sophia Fox AJ BA, Rodeo SA The basic science of articular cartilage: structure, composition, and function. Sports health. 2009;1:461-8.
14. Dudhia J (2005) Aggrecan aaaiac. Aggrecan, aging and assembly in articular cartilage. . Cellular and molecular life sciences 2005;CMLS 62:2241-56.
15. D H. Proteoglycans and more--from molecules to biology. International journal of experimental pathology 2009;90:575-86.
16. Houard X, Goldring MB, Berenbaum F. Homeostatic mechanisms in articular cartilage and role of inflammation in osteoarthritis. Current rheumatology reports. 2013;15(11):375.
17. (2001) RP. Articular cartilage and changes in arthritis: noncollagenous proteins and proteoglycans in the extracellular matrix of cartilage. . Arthritis research. 2001;2:342-7.
18. Faye H Chen KTRaRST. Nature Clinical Practice Rheumatology 2006;2:373-82.
19. MB G. Update on the biology of the chondrocyte and new approaches to treating cartilage diseases. Best practice & research Clinical rheumatology. 2006;20:1003-25.

20. Blanco FJ, Rego I, Ruiz-Romero C. The role of mitochondria in osteoarthritis. Nature reviews Rheumatology. 2011;7(3):161-9.
21. Goldring MB, Goldring SR. Osteoarthritis. Journal of cellular physiology. 2007;213(3):626-34.

22. Strobel S LM, Wendt D, Schenk AD, Candrian C, Lindberg RL, Moldovan F, Barbero A, Martin I. Anabolic and catabolic responses of human articular chondrocytes to varying oxygen percentages. Arthritis research & therapy. 2010; 12: R34.

23. Lee RB UJ. Evidence for a negative Pasteur effect in articular cartilage. The Biochemical journal of Medical Genetics. 1997; 321 (Pt 1):95-102.

24. Goldring MB, Birkhead JR, Suen LF, Yamin R, Mizuno S, Glowacki J, et al. Interleukin-1 beta-modulated gene expression in immortalized human chondrocytes. The Journal of clinical investigation. 1994;94(6):2307-16.
25. Alwin Prem Anand A, Gowri Sankar S, Kokila Vani V. Immortalization of neuronal progenitors using SV40 large T antigen and differentiation towards dopaminergic neurons. Journal of cellular and molecular medicine. 2012;16(11):2592-610.
26. Finger F, Schorle C, Zien A, Gebhard P, Goldring MB, Aigner T. Molecular phenotyping of human chondrocyte cell lines T/C-28a2, T/C-28a4, and C-28/I2. Arthritis and rheumatism. 2003;48(12):3395-403.
27. Matta C, Zakany R. Calcium signalling in chondrogenesis: implications for cartilage repair. Frontiers in bioscience (Scholar edition). 2013;5:305-24.
28. Jiang Y, Tuan RS. Origin and function of cartilage stem/progenitor cells in osteoarthritis. Nature reviews Rheumatology. 2015;11(4):206-12.
29. Loeser RF, Goldring SR, Scanzello CR, Goldring MB. Osteoarthritis: a disease of the joint as an organ. Arthritis and rheumatism. 2012;64(6):1697-707.
30. Altman RD, Gold GE. Atlas of individual radiographic features in osteoarthritis, revised. Osteoarthritis and cartilage / OARS, Osteoarthritis Research Society. 2007;15 Suppl A:A1-56.
31. Kraus VB, Blanco FJ, Englund M, Karsdal MA, Lohmander LS. Call for standardized definitions of osteoarthritis and risk stratification for clinical trials and clinical use. Osteoarthritis and cartilage / OARS, Osteoarthritis Research Society. 2015;23(8):1233-41.
32. Villanueva I, Guzmán MM, Toyos FJ, Ariza R, Navarro F. Sensibilidad y especificidad de los criterios OARSI de mejoría para artrosis: el efecto de la utilización de tres diferentes medidas de dolor. Revista Española de Reumatología. 2003;30(3):105-9.
33. Felson DT LR, Dieppe PA, Hirsch R, Helmick CG, Jordan JM, Kington RS, Lane NE, Nevitt, MC ZY, Sowers M, McAlindon T, Spector TD, Poole AR, Yanovski SZ, Ateshian G, Sharma L,, Buckwalter JA BK, Fries JF Osteoarthritis: new insights. Part 1: the disease and its risk factors. Annals of internal medicine. 2000;133:635-46.

34. AM M. Osteoarthritis year in review 2015: biology. Osteoarthritis and cartilage / OARS, Osteoarthritis Research Society. 2016;24:21-6

35. Goldring MB, Berenbaum F. Emerging targets in osteoarthritis therapy. Current opinion in pharmacology. 2015;22:51-63.
36. Bijlsma JW BF, Lafeber FP Osteoarthritis: an update with relevance for clinical practice. . Lancet. 2011;377:2115-26.
37. Carames B, Taniguchi N, Otsuki S, Blanco FJ, Lotz M. Autophagy is a protective mechanism in normal cartilage, and its aging-related loss is linked with cell death and osteoarthritis. Arthritis and rheumatism. 2010;62(3):791-801.
38. Hunter DJ, Le Graverand MP, Eckstein F. Radiologic markers of osteoarthritis progression. Current opinion in rheumatology. 2009;21(2):110-7.

39. Goldring MB, Marcu KB. Epigenomic and microRNA-mediated regulation in cartilage development, homeostasis, and osteoarthritis. Trends in molecular medicine. 2012;18(2):109-18.
40. Lotz MK, Carames B. Autophagy and cartilage homeostasis mechanisms in joint health, aging and OA. Nature reviews Rheumatology. 2011;7(10):579-87.
41. Carames B, Lopez-Armada MJ, Cillero-Pastor B, Lires-Dean M, Vaamonde C, Galdo F, et al. Differential effects of tumor necrosis factor-alpha and interleukin-1beta on cell death in human articular chondrocytes. Osteoarthritis and cartilage / OARS, Osteoarthritis Research Society. 2008;16(6):715-22.
42. Vaamonde-Garcia C, Riveiro-Naveira RR, Valcarcel-Ares MN, Hermida-Carballo L, Blanco FJ, Lopez-Armada MJ. Mitochondrial dysfunction increases inflammatory responsiveness to cytokines in normal human chondrocytes. Arthritis and rheumatism. 2012;64(9):2927-36.
43. Martel-Pelletier J, Barr AJ, Cicuttini FM, Conaghan PG, Cooper C, Goldring MB, et al. Osteoarthritis. Nature reviews Disease primers. 2016;2:16072.
44. Sandell LJ AT. Articular cartilage and changes in arthritis. An introduction: cell biology of osteoarthritis. Arthritis research. 2001;3:107-13.
45. Lories RJ LF. The bone-cartilage unit in osteoarthritis. Nature reviews Rheumatology. 2011;7:43-9.
46. Li YS, Xiao WF, Luo W. Cellular aging towards osteoarthritis. Mechanisms of ageing and development. 2016.
47. Velasquez MT KJ. teoarthritis: another component of metabolic syndrome? . Metabolic syndrome and related disorders. 2010;8:295-305.
48. Musumeci G AF, Szychlinska MA, Di Rosa M, Castrogiovanni P, Mobasheri A. Osteoarthritis in the XXIst century: risk factors and behaviours that influence disease onset and progression. International journal of molecular sciences. 2015;16:6093-112.

49. DT F. Identifying different osteoarthritis phenotypes through epidemiology. Osteoarthritis and cartilage. 2010;18:601-4.
50. Castaneda S R-BJ, Largo R, Herrero-Beaumont G. Osteoarthritis: a progressive disease with changing phenotypes. Rheumatology. 2014;53: 1-3

51. Blanco FJ. Osteoarthritis: something is moving. Reumatologia clinica. 2014;10(1):4-5.
52. Zhuo Q, Yang W, Chen J, Wang Y. Metabolic syndrome meets osteoarthritis. Nature reviews Rheumatology. 2012;8(12):729-37.
53. Lane NE BK, Hawker G, Peeva E, Schreyer E, Tsuji W, Hochberg MC OARSI-FDA initiative: defining the disease state of osteoarthritis. Osteoarthritis and cartilage 2011;19:478-82

54. Cooper C, Adachi JD, Bardin T, Berenbaum F, Flamion B, Jonsson H, et al. How to define responders in osteoarthritis. Current medical research and opinion. 2013;29(6):719-29.
55. Uyen-Sa D. T. Nguyen YZ, , Yanyan Zhu, Jingbo Niu, MD,, BZ, ScD, Piran Aliabadi, MD, and David T. Felson, MD, MPH. Increasing Prevalence of Knee Pain and Symptomatic Knee Osteoarthritis. Ann Intern Med. 2011;155(11):725–32.
56. Allen KD, Golightly YM. State of the evidence. Current opinion in rheumatology. 2015;27(3):276-83.
57. Loza E, Lopez-Gomez JM, Abasolo L, Maese J, Carmona L, Batlle-Gualda E, et al. Economic burden of knee and hip osteoarthritis in Spain. Arthritis and rheumatism. 2009;61(2):158-65.

58. Meijer AJ, Codogno P. Autophagy: Regulation and role in disease. Critical Reviews in Clinical Laboratory Sciences. 2009;46(4):210-40.
59. Glick D, Barth S, Macleod KF. Autophagy: cellular and molecular mechanisms. The Journal of pathology. 2010;221(1):3-12.
60. Cuervo AM, Macian F. Autophagy, nutrition and immunology. Molecular aspects of medicine. 2012;33(1):2-13.
61. Ravikumar B, Sarkar S, Davies JE, Futter M, Garcia-Arencibia M, Green-Thompson ZW, et al. Regulation of mammalian autophagy in physiology and pathophysiology. Physiological reviews. 2010;90(4):1383-435.
62. Carames B, Hasegawa A, Taniguchi N, Miyaki S, Blanco FJ, Lotz M. Autophagy activation by rapamycin reduces severity of experimental osteoarthritis. Annals of the rheumatic diseases. 2012;71(4):575-81.
63. Rubinsztein DC, Marino G, Kroemer G. Autophagy and aging. Cell. 2011;146(5):682-95.
64. Thorburn A. Apoptosis and autophagy: regulatory connections between two supposedly different processes. Apoptosis : an international journal on programmed cell death. 2008;13(1):1-9.
65. Abounit K ST, McCauley RB Autophagy in mammalian cells. World journal of biological chemistry. 2012;3:1-6.
66. Yoshimori T YA, Moriyama Y, Futai M, Tashiro Y Bafilomycin A1, a specific inhibitor of vacuolar-type H(+)-ATPase, inhibits acidification and protein degradation in lysosomes of cultured cells. . The Journal of biological chemistry. 1991;266:17707-12.
67. Yang Z HJ, Geng J, Nair U, Klionsky DJ (2006) Atg22 recycles amino acids to link the degradative and recycling functions of autophagy. Molecular biology of the cell. 2006;17:5094-104.
68. Mizushima N YT, Ohsumi Y The role of Atg proteins in autophagosome formation. Annual review of cell and developmental biology. 2011;27:107-32.
69. Kobayashi S. Choose Delicately and Reuse Adequately: The Newly Revealed Process of Autophagy. Biological & pharmaceutical bulletin. 2015;38(8):1098-103.
70. Funderburk SF WQ, Yue Z The Beclin 1-VPS34 complex--at the crossroads of autophagy and beyond. . Trends in cell biology. 2010;20:355-62.
71. Reggiori F, Komatsu M, Finley K, Simonsen A. Autophagy: more than a nonselective pathway. International journal of cell biology. 2012;2012:219625.
72. Mizushima N, Kuma A, Kobayashi Y, Yamamoto A, Matsubae M, Takao T, et al. Mouse Apg16L, a novel WD-repeat protein, targets to the autophagic isolation membrane with the Apg12-Apg5 conjugate. Journal of cell science. 2003;116(Pt 9):1679-88.
73. Nakatogawa H, Ichimura Y, Ohsumi Y. Atg8, a ubiquitin-like protein required for autophagosome formation, mediates membrane tethering and hemifusion. Cell. 2007;130(1):165-78.
74. Kabeya Y, Mizushima N, Ueno T, Yamamoto A, Kirisako T, Noda T, et al. LC3, a mammalian homologue of yeast Apg8p, is localized in autophagosome membranes after processing. The EMBO journal. 2000;19(21):5720-8.
75. Fujita N, Itoh T, Omori H, Fukuda M, Noda T, Yoshimori T. The Atg16L complex specifies the site of LC3 lipidation for membrane biogenesis in autophagy. Mol Biol Cell. 2008;19(5):2092-100.
76. Geng J, Klionsky DJ. The Atg8 and Atg12 ubiquitin-like conjugation systems in macroautophagy. 'Protein modifications: beyond the usual suspects' review series. EMBO reports. 2008;9(9):859-64.

77. Hanada T, Noda NN, Satomi Y, Ichimura Y, Fujioka Y, Takao T, et al. The Atg12-Atg5 conjugate has a novel E3-like activity for protein lipidation in autophagy. The Journal of biological chemistry. 2007;282(52):37298-302.
78. Debnath JKJ. Autophagy at the crossroads of catabolism and anabolism. Nature Reviews Molecular Cell Biology. 2015;16:461–72
79. Mizushima N, Yoshimori T, Levine B. Methods in mammalian autophagy research. Cell. 2010;140(3):313-26.
80. Levine B, Kroemer G. Autophagy in the pathogenesis of disease. Cell. 2008;132(1):27-42.
81. Albert V, Hall MN. mTOR signaling in cellular and organismal energetics. Current opinion in cell biology. 2015;33:55-66.
82. Hung CM, Garcia-Haro L, Sparks CA, Guertin DA. mTOR-dependent cell survival mechanisms. Cold Spring Harbor perspectives in biology. 2012;4(12).
83. Benjamin D, Colombi M, Moroni C, Hall MN. Rapamycin passes the torch: a new generation of mTOR inhibitors. Nature reviews Drug discovery. 2011;10(11):868-80.
84. Jacinto E, Loewith R, Schmidt A, Lin S, Ruegg MA, Hall A, et al. Mammalian TOR complex 2 controls the actin cytoskeleton and is rapamycin insensitive. Nature cell biology. 2004;6(11):1122-8.
85. Thoreen CC, Kang SA, Chang JW, Liu Q, Zhang J, Gao Y, et al. An ATP-competitive mammalian target of rapamycin inhibitor reveals rapamycin-resistant functions of mTORC1. The Journal of biological chemistry. 2009;284(12):8023-32.
86. Hara T, Nakamura K, Matsui M, Yamamoto A, Nakahara Y, Suzuki-Migishima R, et al. Suppression of basal autophagy in neural cells causes neurodegenerative disease in mice. Nature. 2006;441(7095):885-9.
87. Mizushima N, Klionsky DJ. Protein turnover via autophagy: implications for metabolism. Annual review of nutrition. 2007;27:19-40.
88. Mobasheri A, Vannucci SJ, Bondy CA, Carter SD, Innes JF, Arteaga MF, et al. Glucose transport and metabolism in chondrocytes: a key to understanding chondrogenesis, skeletal development and cartilage degradation in osteoarthritis. Histology and histopathology. 2002;17(4):1239-67.
89. Cuervo AM, Bergamini E, Brunk UT, Dröge W, Ffrench M, Terman A. Autophagy and Aging: The Importance of Maintaining "Clean" Cells. Autophagy. 2005;1(3):131-40.
90. Sasaki H, Takayama K, Matsushita T, Ishida K, Kubo S, Matsumoto T, et al. Autophagy modulates osteoarthritis-related gene expression in human chondrocytes. Arthritis and rheumatism. 2012;64(6):1920-8.
91. Zhang Y, Vasheghani F, Li YH, Blati M, Simeone K, Fahmi H, et al. Cartilage-specific deletion of mTOR upregulates autophagy and protects mice from osteoarthritis. Annals of the rheumatic diseases. 2015;74(7):1432-40.
92. Shapiro IM, Layfield R, Lotz M, Settembre C, Whitehouse C. Boning up on autophagy. Autophagy. 2014;10(1):7-19.
93. Charlier E, Relic B, Deroyer C, Malaise O, Neuville S, Collee J, et al. Insights on Molecular Mechanisms of Chondrocytes Death in Osteoarthritis. International journal of molecular sciences. 2016;17(12).
94. Cuervo AM, Dice JF. Age-related decline in chaperone-mediated autophagy. The Journal of biological chemistry. 2000;275(40):31505-13.
95. Martinez A, Portero-Otin M, Pamplona R, Ferrer I. Protein targets of oxidative damage in human neurodegenerative diseases with abnormal protein aggregates. Brain pathology. 2010;20(2):281-97.

96. Lee JY, Nagano Y, Taylor JP, Lim KL, Yao TP. Disease-causing mutations in parkin impair mitochondrial ubiquitination, aggregation, and HDAC6-dependent mitophagy. The Journal of cell biology. 2010;189(4):671-9.
97. Bohensky J, Terkhorn SP, Freeman TA, Adams CS, Garcia JA, Shapiro IM, et al. Regulation of autophagy in human and murine cartilage: hypoxia-inducible factor 2 suppresses chondrocyte autophagy. Arthritis and rheumatism. 2009;60(5):1406-15.
98. Bratic A, Larsson NG. The role of mitochondria in aging. The Journal of clinical investigation. 2013;123(3):951-7.
99. Cillero-Pastor B, Carames B, Lires-Dean M, Vaamonde-Garcia C, Blanco FJ, Lopez-Armada MJ. Mitochondrial dysfunction activates cyclooxygenase 2 expression in cultured normal human chondrocytes. Arthritis and rheumatism. 2008;58(8):2409-19.
100. Green DR, Reed JC. Mitochondria and Apoptosis. Science. 1998;281(5381):1309-12.
101. Ross PL, Huang YN, Marchese JN, Williamson B, Parker K, Hattan S, et al. Multiplexed protein quantitation in Saccharomyces cerevisiae using amine-reactive isobaric tagging reagents. Molecular & cellular proteomics : MCP. 2004;3(12):1154-69.
102. Chinnery P, Howell N, Andrews R, Turnbull D. Clinical mitochondrial genetics. Journal of Medical Genetics. 1999;36(6):425-36.
103. Loeser RF, Collins JA, Diekman BO. Ageing and the pathogenesis of osteoarthritis. Nature reviews Rheumatology. 2016;12(7):412-20.
104. Maneiro E, Martin MA, de Andres MC, Lopez-Armada MJ, Fernandez-Sueiro JL, del Hoyo P, et al. Mitochondrial respiratory activity is altered in osteoarthritic human articular chondrocytes. Arthritis and rheumatism. 2003;48(3):700-8.
105. Griffiths LA, Flatters SJL. Pharmacological Modulation of the Mitochondrial Electron Transport Chain in Paclitaxel-Induced Painful Peripheral Neuropathy. The Journal of Pain. 2015;16(10):981-94.
106. Lopez-Armada MJ, Carames B, Martin MA, Cillero-Pastor B, Lires-Dean M, Fuentes-Boquete I, et al. Mitochondrial activity is modulated by TNFalpha and IL-1beta in normal human chondrocyte cells. Osteoarthritis and cartilage / OARS, Osteoarthritis Research Society. 2006;14(10):1011-22.
107. Frantz M, Wipf P. Mitochondria as a target in treatment. Environmental and molecular mutagenesis. 2010;51(5):462-75.
108. Dequeker J LF. The history of osteoarthritis osteoarthrosis. Ann Rheum Dis. 2008;67:5-10.
109. Benedek, TG. When did "osteo--arthritis" become osteoarthritis? J Rheumatol. 1999;26(6):1374-6.
110. Ashrafi G, Schwarz TL. The pathways of mitophagy for quality control and clearance of mitochondria. Cell death and differentiation. 2013;20(1):31-42.
111. Wallace DC. A mitochondrial paradigm of metabolic and degenerative diseases, aging, and cancer: a dawn for evolutionary medicine. Annual review of genetics. 2005;39:359-407.
112. Galluzzi L, Kepp O, Trojel-Hansen C, Kroemer G. Mitochondrial control of cellular life, stress, and death. Circulation research. 2012;111(9):1198-207.
113. Gavriilidis C, Miwa S, von Zglinicki T, Taylor RW, Young DA. Mitochondrial dysfunction in osteoarthritis is associated with down-regulation of superoxide dismutase 2. Arthritis and rheumatism. 2013;65(2):378-87.
114. Mizushima N, Levine B, Cuervo AM, Klionsky DJ. Autophagy fights disease through cellular self-digestion. Nature. 2008;451(7182):1069-75.

115. Portal-Nunez S, Esbrit P, Alcaraz MJ, Largo R. Oxidative stress, autophagy, epigenetic changes and regulation by miRNAs as potential therapeutic targets in osteoarthritis. Biochemical pharmacology. 2016;108:1-10.
116. Lopez-Otin C, Blasco MA, Partridge L, Serrano M, Kroemer G. The hallmarks of aging. Cell. 2013;153(6):1194-217.
117. Benderdour M, Martel-Pelletier J, Pelletier JP, Kapoor M, Zunzunegui MV, Fahmi H. Cellular Aging, Senescence and Autophagy Processes in Osteoarthritis. Current aging science. 2015;8(2):147-57.
118. Li Y, Wei X, Zhou J, Wei L. The age-related changes in cartilage and osteoarthritis. BioMed research international. 2013;2013:916530.
119. Mobasheri A, Matta C, Zakany R, Musumeci G. Chondrosenescence: definition, hallmarks and potential role in the pathogenesis of osteoarthritis. Maturitas. 2015;80(3):237-44.
120. Huang W, Ao P, Li J, Wu T, Xu L, Deng Z, et al. Autophagy Protects Advanced Glycation End Product-Induced Apoptosis and Expression of MMP-3 and MMP-13 in Rat Chondrocytes. BioMed research international. 2017;2017:6341919.
121. Hui W, Young DA, Rowan AD, Xu X, Cawston TE, Proctor CJ. Oxidative changes and signalling pathways are pivotal in initiating age-related changes in articular cartilage. Annals of the rheumatic diseases. 2016;75(2):449-58.
122. Lotz M, Loeser RF. Effects of aging on articular cartilage homeostasis. Bone. 2012;51(2):241-8.
123. Heidari B. Knee osteoarthritis prevalence, risk factors, pathogenesis and features: Part I. Caspian journal of internal medicine. 2011;2(2):205-12.
124. Hwang HS, Kim HA. Chondrocyte Apoptosis in the Pathogenesis of Osteoarthritis. International journal of molecular sciences. 2015;16(11):26035-54.
125. Salminen A, Kaarniranta K. Regulation of the aging process by autophagy. Trends in molecular medicine. 2009;15(5):217-24.
126. Johnson SC, Rabinovitch PS, Kaeberlein M. mTOR is a key modulator of ageing and age-related disease. Nature. 2013;493(7432):338-45.
127. Lamming DW, Ye L, Sabatini DM, Baur JA. Rapalogs and mTOR inhibitors as anti-aging therapeutics. The Journal of clinical investigation. 2013;123(3):980-9.
128. Loeser RF. Aging and osteoarthritis. Current opinion in rheumatology. 2011;23(5):492-6.
129. Barrowman J, Hamblet C, Kane MS, Michaelis S. Requirements for efficient proteolytic cleavage of prelamin A by ZMPSTE24. PloS one. 2012;7(2):e32120.
130. Young SG, Meta M, Yang SH, Fong LG. Prelamin A farnesylation and progeroid syndromes. The Journal of biological chemistry. 2006;281(52):39741-5.
131. Cenni V, Capanni C, Columbaro M, Ortolani M, D'Apice MR, Novelli G, et al. Autophagic degradation of farnesylated prelamin A as a therapeutic approach to lamin-linked progeria. European journal of histochemistry : EJH. 2011;55(4):e36.
132. Attur M, Ben-Artzi A, Yang Q, Al-Mussawir HE, Worman HJ, Palmer G, et al. Perturbation of nuclear lamin A causes cell death in chondrocytes. Arthritis and rheumatism. 2012;64(6):1940-9.
133. McCulloch K, Litherland GJ, Rai TS. Cellular senescence in osteoarthritis pathology. Aging cell. 2017.
134. Chang J, Wang W, Zhang H, Hu Y, Wang M, Yin Z. The dual role of autophagy in chondrocyte responses in the pathogenesis of articular cartilage degeneration in osteoarthritis. International journal of molecular medicine. 2013;32(6):1311-8.
135. Taniguchi N, Carames B, Ronfani L, Ulmer U, Komiya S, Bianchi ME, et al. Aging-related loss of the chromatin protein HMGB2 in articular cartilage is linked to

reduced cellularity and osteoarthritis. Proceedings of the National Academy of Sciences of the United States of America. 2009;106(4):1181-6.
136. Luo R, Zhao H. Protein quantitation using iTRAQ: Review on the sources of variations and analysis of nonrandom missingness. Statistics and its interface. 2012;5(1):99-107.
137. Calamia V, Mateos J, Fernandez-Puente P, Lourido L, Rocha B, Fernandez-Costa C, et al. A pharmacoproteomic study confirms the synergistic effect of chondroitin sulfate and glucosamine. Scientific reports. 2014;4:5069.
138. Rauniyar N, Yates JR, 3rd. Isobaric labeling-based relative quantification in shotgun proteomics. Journal of proteome research. 2014;13(12):5293-309.
139. Paul D, Kumar A, Gajbhiye A, Santra MK, Srikanth R. Mass spectrometry-based proteomics in molecular diagnostics: discovery of cancer biomarkers using tissue culture. BioMed research international. 2013;2013:783131.
140. Calamia V, Rocha B, Mateos J, Fernandez-Puente P, Ruiz-Romero C, Blanco FJ. Metabolic labeling of chondrocytes for the quantitative analysis of the interleukin-1-beta-mediated modulation of their intracellular and extracellular proteomes. Journal of proteome research. 2011;10(8):3701-11.
141. Fernández-Puente P, Mateos J, Fernández-Costa C, Oreiro N, Fernández-López C, Ruiz-Romero C, et al. Identification of a Panel of Novel Serum Osteoarthritis Biomarkers. Journal of proteome research. 2011;10(11):5095-101.
142. Di Girolamo F, Lante I, Muraca M, Putignani L. The Role of Mass Spectrometry in the "Omics" Era. Current organic chemistry. 2013;17(23):2891-905.
143. Lourido L, Calamia V, Mateos J, Fernández-Puente P, Fernández-Tajes J, Blanco FJ, et al. Quantitative Proteomic Profiling of Human Articular Cartilage Degradation in Osteoarthritis. Journal of proteome research. 2014;13(12):6096-106.
144. Kuma A HM, Matsui M, et al. The role of autophagy during the early neonatal starvation period. Nature 2004;432:1032–6.
145. PRESIDENCIA MDL. Boletin Oficial del estado. 2013;34.
146. Masuda K, Aota Y, Muehleman C, Imai Y, Okuma M, Thonar EJ, et al. A novel rabbit model of mild, reproducible disc degeneration by an anulus needle puncture: correlation between the degree of disc injury and radiological and histological appearances of disc degeneration. Spine. 2005;30(1):5-14.
147. Boos N, Weissbach S, Rohrbach H, Weiler C, Spratt KF, Nerlich AG. Classification of age-related changes in lumbar intervertebral discs: 2002 Volvo Award in basic science. Spine. 2002;27(23):2631-44.
148. Komatsu M, Waguri S, Ueno T, Iwata J, Murata S, Tanida I, et al. Impairment of starvation-induced and constitutive autophagy in Atg7-deficient mice. The Journal of cell biology. 2005;169(3):425-34.
149. Blanco FJ, Lopez-Armada MJ, Rego I. Mitochondria and chondrocytes: role in osteoarthritis. BIOMEDICAL AND HEALTH RESEARCH-COMMISSION OF THE EUROPEAN COMMUNITIES THEN IOS PRESS. 2007;70:192.
150. Tomita M, Sato EF, Nishikawa M, Yamano Y, Inoue M. Nitric oxide regulates mitochondrial respiration and functions of articular chondrocytes. Arthritis and rheumatism. 2001;44(1):96-104.
151. Carlo MD, Jr., Loeser RF. Increased oxidative stress with aging reduces chondrocyte survival: correlation with intracellular glutathione levels. Arthritis and rheumatism. 2003;48(12):3419-30.
152. Youle RJ, Narendra DP. Mechanisms of mitophagy. Nature reviews Molecular cell biology. 2011;12(1):9-14.

153. Ruiz-Romero C, Calamia V, Mateos J, Carreira V, Martinez-Gomariz M, Fernandez M, et al. Mitochondrial dysregulation of osteoarthritic human articular chondrocytes analyzed by proteomics: a decrease in mitochondrial superoxide dismutase points to a redox imbalance. Molecular & cellular proteomics : MCP. 2009;8(1):172-89.
154. Cillero-Pastor B, Rego-Perez I, Oreiro N, Fernandez-Lopez C, Blanco FJ. Mitochondrial respiratory chain dysfunction modulates metalloproteases -1, -3 and -13 in human normal chondrocytes in culture. BMC musculoskeletal disorders. 2013;14:235.
155. Mizushima N. Physiological functions of autophagy. Current topics in microbiology and immunology. 2009;335:71-84.
156. Caramés B OM, Kiosses WB, et al. . The relationship of autophagy defects to cartilage damage during joint aging in a mouse model. . Arthritis & rheumatology. 2015;67:1568-76.
157. Loeser RF CJ, Diekman BO. Ageing and the pathogenesis of osteoarthritis. . Nature reviews Rheumatology. 2016;12:412–20.
158. Lopez de Figueroa P, Lotz MK, Blanco FJ, Carames B. Autophagy activation and protection from mitochondrial dysfunction in human chondrocytes. Arthritis & rheumatology. 2015;67(4):966-76.
159. RF LMaL. Effects of aging on articular cartilage homeostasis. . Bone 2012;51:241–8.
160. Caramés B TN, Seino D, et al. Mechanical injury suppresses autophagy regulators and pharmacologic activation of autophagy results in chondroprotection. Arthritis and rheumatism. 2012;64:1182–92.
161. Ribeiro M LdFP, Nogueira-Recalde U, et al. Diabetes-accelerated experimental osteoarthritis is prevented by autophagy activation. Osteoarthritis and cartilage / OARS, Osteoarthritis Research Society. 2016;pii:S1063-458430170-4.
162. Yoshii SR KA, Akashi T, et al. Systemic Analysis of Atg5-Null Mice Rescued from Neonatal Lethality by Transgenic ATG5 Expression in Neurons. Dev Cell. 2016;Dev Cell.
163. Bouderlique T VK, Newton PT, et al. Targeted deletion of Atg5 in chondrocytes promotes age-related osteoarthritis. Annals of the rheumatic diseases. 2016;75:627–31.
164. Dittmer TA, Misteli T. The lamin protein family. Genome biology. 2011;12(5):222.
165. Dechat T, Adam SA, Taimen P, Shimi T, Goldman RD. Nuclear lamins. Cold Spring Harbor perspectives in biology. 2010;2(11):a000547.
166. Osorio FG, Varela I, Lara E, Puente XS, Espada J, Santoro R, et al. Nuclear envelope alterations generate an aging-like epigenetic pattern in mice deficient in Zmpste24 metalloprotease. Aging cell. 2010;9(6):947-57.
167. Kane MS, Lindsay ME, Judge DP, Barrowman J, Ap Rhys C, Simonson L, et al. LMNA-associated cardiocutaneous progeria: an inherited autosomal dominant premature aging syndrome with late onset. American journal of medical genetics Part A. 2013;161A(7):1599-611.
168. Shen T, Alvarez-Garcia O, Li Y, Olmer M, Lotz MK. Suppression of Sestrins in aging and osteoarthritic cartilage: dysfunction of an important stress defense mechanism. Osteoarthritis and cartilage / OARS, Osteoarthritis Research Society. 2017;25(2):287-96.
169. Gibbs-Seymour I, Markiewicz E, Bekker-Jensen S, Mailand N, Hutchison CJ. Lamin A/C-dependent interaction with 53BP1 promotes cellular responses to DNA damage. Aging cell. 2015;14(2):162-9.

170. Marino G, Ugalde AP, Fernandez AF, Osorio FG, Fueyo A, Freije JM, et al. Insulin-like growth factor 1 treatment extends longevity in a mouse model of human premature aging by restoring somatotroph axis function. Proceedings of the National Academy of Sciences of the United States of America. 2010;107(37):16268-73.
171. Shibata M, Lu T, Furuya T, Degterev A, Mizushima N, Yoshimori T, et al. Regulation of intracellular accumulation of mutant Huntingtin by Beclin 1. The Journal of biological chemistry. 2006;281(20):14474-85.
172. Harrison DE, Strong R, Sharp ZD, Nelson JF, Astle CM, Flurkey K, et al. Rapamycin fed late in life extends lifespan in genetically heterogeneous mice. Nature. 2009;460(7253):392-5.
173. Pan T, Rawal P, Wu Y, Xie W, Jankovic J, Le W. Rapamycin protects against rotenone-induced apoptosis through autophagy induction. Neuroscience. 2009;164(2):541-51.
174. Spilman P, Podlutskaya N, Hart MJ, Debnath J, Gorostiza O, Bredesen D, et al. Inhibition of mTOR by rapamycin abolishes cognitive deficits and reduces amyloid-beta levels in a mouse model of Alzheimer's disease. PloS one. 2010;5(4):e9979.
175. Kanki T, Klionsky DJ. The molecular mechanism of mitochondria autophagy in yeast. Molecular microbiology. 2010;75(4):795-800.
176. Vander Heiden MG, Chandel NS, Williamson EK, Schumacker PT, Thompson CB. Bcl-xL regulates the membrane potential and volume homeostasis of mitochondria. Cell. 1997;91(5):627-37.
177. Xiong N, Xiong J, Jia M, Liu L, Zhang X, Chen Z, et al. The role of autophagy in Parkinson's disease: rotenone-based modeling. Behavioral and brain functions : BBF. 2013;9:13.
178. Shigemitsu K, Tsujishita Y, Hara K, Nanahoshi M, Avruch J, Yonezawa K. Regulation of translational effectors by amino acid and mammalian target of rapamycin signaling pathways. Possible involvement of autophagy in cultured hepatoma cells. The Journal of biological chemistry. 1999;274(2):1058-65.
179. Sabers CJ, Martin MM, Brunn GJ, Williams JM, Dumont FJ, Wiederrecht G, et al. Isolation of a protein target of the FKBP12-rapamycin complex in mammalian cells. The Journal of biological chemistry. 1995;270(2):815-22.
180. Laplante M, Sabatini DM. mTOR signaling in growth control and disease. Cell. 2012;149(2):274-93.
181. Ohsumi Y. Historical landmarks of autophagy research. Cell research. 2014;24(1):9-23.
182. Rockel JS, Kapoor M. Autophagy: controlling cell fate in rheumatic diseases. Nature reviews Rheumatology. 2016;12(9):517-31.
183. Ruiz-Romero C, Carreira V, Rego I, Remeseiro S, Lopez-Armada MJ, Blanco FJ. Proteomic analysis of human osteoarthritic chondrocytes reveals protein changes in stress and glycolysis. Proteomics. 2008;8(3):495-507.
184. Capell BC, Olive M, Erdos MR, Cao K, Faddah DA, Tavarez UL, et al. A farnesyltransferase inhibitor prevents both the onset and late progression of cardiovascular disease in a progeria mouse model. Proceedings of the National Academy of Sciences of the United States of America. 2008;105(41):15902-7.
185. Infante A, Gago A, de Eguino GR, Calvo-Fernandez T, Gomez-Vallejo V, Llop J, et al. Prelamin A accumulation and stress conditions induce impaired Oct-1 activity and autophagy in prematurely aged human mesenchymal stem cell. Aging. 2014;6(4):264-80.
186. Sieprath T, Corne TD, Nooteboom M, Grootaert C, Rajkovic A, Buysschaert B, et al. Sustained accumulation of prelamin A and depletion of lamin A/C both cause

oxidative stress and mitochondrial dysfunction but induce different cell fates. Nucleus (Austin, Tex). 2015;6(3):236-46.
187. Peinado JR, Quiros PM, Pulido MR, Marino G, Martinez-Chantar ML, Vazquez-Martinez R, et al. Proteomic profiling of adipose tissue from Zmpste24-/- mice, a model of lipodystrophy and premature aging, reveals major changes in mitochondrial function and vimentin processing. Molecular & cellular proteomics : MCP. 2011;10(11):M111.008094.
188. Rivera-Torres J, Acin-Perez R, Cabezas-Sanchez P, Osorio FG, Gonzalez-Gomez C, Megias D, et al. Identification of mitochondrial dysfunction in Hutchinson-Gilford progeria syndrome through use of stable isotope labeling with amino acids in cell culture. Journal of proteomics. 2013;91:466-77.
189. Baek JH, Schmidt E, Viceconte N, Strandgren C, Pernold K, Richard TJ, et al. Expression of progerin in aging mouse brains reveals structural nuclear abnormalities without detectible significant alterations in gene expression, hippocampal stem cells or behavior. Human molecular genetics. 2015;24(5):1305-21.
190. Cao K, Blair CD, Faddah DA, Kieckhaefer JE, Olive M, Erdos MR, et al. Progerin and telomere dysfunction collaborate to trigger cellular senescence in normal human fibroblasts. The Journal of clinical investigation. 2011;121(7):2833-44.

CHAPTER 8: SUPPLEMENTAL DATA

Appendix 1: Resumen en lengua castellana

La osteoartrosis (OA) es la enfermedad articular más común, y el envejecimiento representa uno de sus principales factores de riesgo. La relación entre el envejecimiento y el desarrollo de la OA no se conoce en detalle, pero es evidente que los cambios relacionados con el envejecimiento en el sistema músculo-esquelético contribuyen a la progresión, y se acompañan por otros factores de riesgo como los factores mecánicos, genéticos o la mala alineación de la articulación. Recientemente se ha avanzado en la caracterización de las vías patogénicas más relevantes, Sin embargo, estas investigaciones no han permitido definir los mecanismos y vías responsables de tales cambios en relación con los mecanismos implicados en el envejecimiento del cartílago articular. Una posible estrategia sería dirigir las intervenciones terapéuticas hacia las etapas iniciales de la patología artrósica, sin embargo, los mecanismos que conducen a estos cambios tempranos no están bien caracterizados.

Una característica común en las patologías relacionadas con el envejecimiento, como la osteoartritis (OA), es la progresiva acumulación de macromoléculas dañadas que provocan daño celular y finalmente el deterioro de los tejidos.

La autofagía es un proceso de degradación lisosomal esencial para la supervivencia celular, la diferenciación, el desarrollo y la homeostasis. La autofagía desempeña un mecanismo fundamental para proteger a los organismos frente a diversas patologías, como las infecciones, el cáncer, la neurodegeneración, las enfermedades del corazón, y el envejecimiento, mediante la eliminación de moléculas dañadas. La característica morfológica más importante de este proceso es la formación de vesículas con doble membrana, denominadas autofagosomas. Los componentes moleculares del proceso de autofagía, son los genes ATG, que fueron identificados por primera vez en levaduras, sin embargo la mayoría de las proteínas implicadas en este proceso tienen sus homólogos en eucariotas superiores. En este sentido Atg1, Atg6, Atg8 (ULK1, Beclin1 y LC3 en mamíferos, respectivamente) y Atg5 son cuatro de los principales reguladores de la vía de la autofagía. Finalmente, la formación y expansión de los autofagosomas requiere dos sistemas de conjugación de proteínas que implican a Atg5 y LC3.

Además, la autofagía se activa cuando las células están experimentando una remodelación estructural, como en las transiciones de desarrollo o para proteger a las células contra los efectos del estrés oxidativo, las infecciones o la acumulación de

agregados proteicos mutados. De hecho, la pérdida de genes autofagía da lugar a procesos de neurodegeneración, cardiomiopatías, anormalidades en el desarrollo y la muerte. Por lo tanto, un mejor entendimiento de los mecanismos de la autofagía puede ayudar al descubrimiento de nuevas dianas terapéuticas para la regulación de la homeostasis celular.

El cartílago articular está caracterizado por una baja tasa de renovación celular, la autofagía parece ser esencial para mantener la integridad celular, la función y la supervivencia. Además, mientras que la autofagía esta alterada en diversos modelos y tejidos con el envejecimiento, esto no ha sido investigado en el cartílago articular. Hemos demostrado que existe una disminución de autofagía en cartílago y condrocitos de pacientes de edad avanzada y con OA. Estas observaciones en el cartílago son consistentes con otros tejidos donde la actividad de autofagía basal disminuye con la edad, lo que contribuye a la acumulación de macromoléculas y a un daño celular relacionado con el envejecimiento.

Por otro lado, otros estudios han descrito alteraciones en la respuesta de este proceso a los cambios hormonales en el envejecimiento. En particular, los efectos del estrés oxidativo sobre la vía del receptor de señalización de la insulina parecen jugar un papel crítico en la disminución de la autofagía en los organismos envejecidos. La red de señalización que implica a los factores de longevidad como SIRT1, mTOR, FoxO3, NF-kB y p53 regulan la autofagía y podrían tener un papel en el proceso de envejecimiento. En concreto, mTOR y NF-kB son represores de la vía de la autofagía en virtud de las señales de entrada de estrés y de inflamación, mientras que SIRT1, es un factor de resistencia al estrés y de longevidad; y FoxO3, un importante regulador del metabolismo celular, la proliferación y la resistencia al estrés, mejoran la autofagía.

Durante la última década, la importancia de la mitocondria en la biología celular ha sido enfatizada por la evidencia de que alteraciones en proteínas mitocondriales pueden causar algunas enfermedades humanas. Estas modificaciones pueden conducir a importantes disfunciones celulares que contribuyen a fallos neurológicos, como las enfermedades de Alzheimer, Parkinson y Huntington, diabetes tipo 2, enfermedades cardiovasculares, o diversos síndromes neuromusculares y algunos procesos de envejecimiento.

La comprensión de la relación funcional entre las mitocondrias y la autofagía es fundamental para el entendimiento de los mecanismos moleculares que subyacen a las enfermedades relacionadas con el envejecimiento. En este sentido, existen evidencias que apuntan a una interdependencia entre la función mitocondrial y la autofagía y plantean la posibilidad de que la regulación negativa de la autofagía por las mitocondrias disfuncionales es un factor que contribuye en el desarrollo de muchas enfermedades relacionadas con el envejecimiento, como la OA.

Las intervenciones farmacológicas actuales son insuficientes, puesto que sólo abordan el dolor crónico y no existe ninguna terapia modificadora de la enfermedad. La prevalencia de OA aumenta directamente con la edad y es la causa más común de discapacidad crónica en los adultos mayores. A día de hoy, no existe ninguna aproximación terapéutica para el tratamiento del envejecimiento del cartílago. Una posible estrategia sería dirigir las intervenciones terapéuticas hacia las etapas iniciales de la patología artrósica, sin embargo, los mecanismos que conducen a estos cambios tempranos no están bien caracterizados.

Nuestra hipótesis se centra en la búsqueda de dianas que nos indiquen los fallos en la homeostasis celular, aquellos defectos en la autofagía que conducen a la disfunción celular y en consecuencia a la muerte, iniciando así, el proceso de degradación del cartílago característico de la OA.

"*Una reducción en la autofagía durante el proceso de envejecimiento, contribuye a la acumulación de orgánulos y proteínas dañadas, produciendo un fallo en el mecanismo de homeostasis en el cartílago, contribuyendo al desarrollo de OA"*

Nuestra propuesta se basa en resultados previos donde demostramos la pérdida de función del proceso de autofagía en el cartílago y condrocitos humanos de pacientes con OA y de edad avanzada. Creemos que estos hallazgos proporcionan una oportunidad única para estudiar el envejecimiento del cartílago a través de la regulación del proceso de autofagía como mecanismo fundamental del envejecimiento del cartílago articular, y al mismo tiempo explorar el potencial terapéutico para prevenir farmacológicamente la senescencia y activar la autofagía.

Nuestro objetivo principal ha sido investigar el papel de la autofagía en la disfunción mitocondrial en el cartílago articular, e identificar dianas para el futuro

desarrollo de terapias farmacológicas para prevenir, retrasar o incluso revertir la artrosis.

Para ello hemos dividido el trabajo en dos objetivos principales:

1. Estudiar los efectos de la pérdida de la función de autofagía sobre la función mitocondrial en condrocitos normales.
2. Identificar potenciales dianas en el contexto de una disminución de autofagía en el proteína de condrocitos humanos y validar el efecto de la autofagía sobre el envejecimiento en un modelo murino.

Para la realización del primer objetivo empleamos condrocitos humanos inmortalizados procedentes de la línea celular TC28a2 y condrocitos humanos procedentes de cultivo primario de donantes sanos donde se realizaron dos abordajes experimentales diferentes: En el primero se indujo una disfunción mitocondrial farmacológica, empleando Oligomicina (Oligo, 10 μg/ml), un inhibidor del complejo V de la cadena respiratoria mitocondrial (CRM) y posteriormente analizamos su efecto sobre el mecanismo celular de autofagía. Los resultados obtenidos indicaron que la Oligo provocó una disfunción mitocondrial en los condrocitos humanos, representado por una disminución significativa del potencial de membrana mitocondrial ($\Delta\psi m$). Estos resultados fueron consistentes con un incremento significativo en la producción de especies reactivas del oxígeno (ROS) y en la muerte celular por apoptosis a las 12 h. El siguiente paso fue evaluar cuál es el efecto de la disfunción mitocondrial sobre la autofagía. Para ello se evaluó la expresión de LC3, el marcador más importante de activación de autofagía que indica la formación de autofagosomas y la activación del proceso de autofagía. Lo resultados indicaron la reducción significativa de la expresión de LC3 en respuesta a Oligomicina a las 12 horas. Para evaluar si la autofagía regula la disfunción mitocondrial, los condrocitos fueron pre-tratados durante 4 horas con dos activadores farmacológicos de autofagía, Rapamicina 10 μM y Torin 1 50 nM. Finalizado el tiempo de preincubación las células fueron tratadas con Oligomicina solo o en combinación con los activadores de autofagía durante 12 horas. Los resultados obtenidos indicaron que la activación farmacológica de autofagía tuvo un efecto protector frente a la disfunción mitocondrial provocada por la oligomicina. El tratamiento con los inductores de autofagía Rapamicina y Torin1 incrementaron el

Δψm, disminuyeron la producción de ROS y redujeron la muerte celular. Estos resultados sugieren un efecto protector de la activación de autofagía sobre la disfunción mitocondrial inducida por la inhibición de la CRM. El segundo abordaje planteó estudiar cómo una disminución de autofagía puede afectar a la función mitocondrial de los condrocitos. Para disminuir la autofagía, empleamos la tecnología siARN dirigida a Atg5, un gen indispensable para la translocación y activación de LC3-I a LC3-II, presente en la doble membrana de los autofagosomas. Los resultados obtenidos mediante estudios de expresión de proteínas, indicaron una disminución en la expresión de Atg5 y de LC3-II. Los resultados han indicado que la disminución de autofagía provocó una mayor predisposición a un daño mitocondrial traducido por una disminución significativa del potencial de membrana y un incremento en la producción de ROS.

Para llevar a cabo la identificación de dianas potenciales en caso de una disminución de autofagía en condrocitos humanos, hemos empleado la misma tecnología que en nuestro primer objetivo, el silenciamiento génico mediante tecnología siRNA para Atg5. Una vez bloqueado el proceso de autofagía, se aisló la proteína total de cada condición (siCTRL y siAtg5) y se realizó la técnica proteómica iTRAQ (isobaric tags for relative and absolute quantification) acoplada con 2D LC/MS/MS. La identificación y la cuantificación de proteínas se realizó mediante la utilización del software Protein Pilot v4.0. Cada espectro obtenido en el MS/MS es procesado en la base de datos Uniprot/Swissprot para la especie Homo Sapiens.

Mediante el empleo de dicha técnica se identificaron un total de 487 proteínas, de las cuales 24 están moduladas o alteradas. La prelamina-A/C, precursora de la lamina A/C esta significativamente sobreexpresada en los tres donantes con respecto al control. Esta proteína es de gran interés, ya que la lamina A/C está implicada en la senescencia prematura de la célula, por lo que resulta de gran interés para el estudio del envejecimiento del condrocito en OA.

Estos resultados indican que cuando el proceso de autofagía esta disminuído o bloqueado, hay un incremento en la expresión de proteínas relacionadas con el envejecimiento y la muerte celular, indicando que la autofagía juega un papel importante en la regulación de los procesos de supervivencia celular.

Para la validación de estos resultados, se utilizará la línea de condrocitos inmortalizada Tc28a2 transfectada para el bloqueo del gen Atg5. Mediante la técnica de Western blot se evaluarán los niveles de nuestras proteínas de interés para la autofagía (atg5 y LC3) y envejecimiento (Lamina A/C). La expresión de lamina A/C será también evaluada mediante Inmunofluorescencia. Paralelamente, se empleó cartílago procedente de pacientes humanos y se evaluó mediante técnicas histológicas la expresión de estos marcadores (LC3, Lamina A/C) en cartílago humano procedentes de cartílago procedente de donantes sin patología (normal) vs. Cartílago envejecido vs. Cartílago OA.

Posteriormente, para observar el efecto sobre la autofagía en condrocitos con envejecimiento prematuro, hemos utilizado la tecnología de edición genética CRIPSPR/Cas9 para el gen de la metaloproteasa STE24 (Zmpste24), un gen importante para el proceso de maduración correcta de la lamina A/C. Estos estudios confirmaron que una delección de Zmpste 24 produce un incremento de acumulación de prelamin A/C, así como una reducción de la autofagía mediante western-Blot. Además, esta reducción de autofagía fue correlacionada con un incremento de muerte celular en células con envejecimiento prematuro (Zmpste $24^{-/-}$).

Para evaluar la importancia de la autofagía en el envejecimiento en el cartílago, utilizamos un modelo in vivo de ratones que tienen sobreexpresada la lamina A/C. Para ello empleamos un modelo murino que presenta una mutación en el gen Zmpste24 causando envejecimiento prematuro en ratones homocigóticos. Esto es debido a que estos ratones presentan una acumulación de "farnesylated lamin A precursor" producida por la mutación en el gen Zmpste24, lo que ocasiona un mal procesado de la lamina A/C a progerina, convirtiéndola en una herramienta de gran utilidad para el estudio del envejecimiento.

Se evaluaron los cambios fenotípicos comparando ratones con fenotipo Wild tipo (Zmpste$24^{-/+}$) que no tiene alterado el gen frente a ratones Zmpste$24^{-/-}$ que si presentan mutación para el gen. Los ratones fueron sacrificados a los 4 meses de edad y se obtuvieron las rodillas de los ratones para evaluar el daño en el cartílago.

Estos ratones nos han permitido iniciar los estudios articulares para el estudio de la autofagía durante el envejecimiento. Para ello se utilizaron tinciones histológicas (Safranina O-Fast Green y hematoxilina-Eosina), que permitieron evaluar la

degradación del cartílago mediante la deformación y desgaste del mismo, así como la perdida de proteoglicanos. Los resultados han permitido demostrar una diferencia en el hueso de articulaciones de rodilla, así como diferencias significativas en columna vertebral, donde hemos podido observar una degeneración del disco intervertebral, causado por un estrechamiento del *nucleus pulposus* y desorganización de *annulus fibrosus*.

En conclusión, hemos podido comprobar que la disfunción mitocondrial juega un papel fundamental en el proceso de envejecimiento en el cartílago artrósico, pero que una activación farmacológica de la autofagía por rapamicina tiene un efecto condroprotector sobre el cartílago articular humano. Por otro lado, la inhibición de autofaxía incrementa la expresión de lamina A/C, implicada en el proceso de envejecimiento. Por lo que, una acumulación de lamina por mutación del gen zmpste24, altera la homeostasis celular acelerando el envejecimiento asociado con la muerte celular. En el caso de ratones con un envejecimiento prematuro, hemos podido observar un aumento de la patología musculoesquelética causado por cambios en el hueso articular y cambios en el cartílago a nivel intervertebral.

Appendix 2: Total proteins identified in defect autophagy in chondrocytes.

Table 8.1: Identification of 487 regulated proteins in autophagy deficient human chondrocytes by iTRAQ analysis (siAtg5 vs. siCtrl)

Total	% Cov (95)	Accession	Name	Peptides (95%)	DONOR 1 115:114	PVal 115:114	DONOR 2 117:116	PVal 117:116
141,25	48,9	P21333	Filamin-A	90	0,302	0	0,6368	0,0298
21,23	47,6	P09601	Heme oxygenase 1 OS	16	2,2284	0	1,3305	0,042
96,2	33,3	P35579	Myosin-9 OS	68	0,4529	0	0,7516	0,0412
215,09	43,8	Q09666	Neuroblast differentiation-associated protein AHNAK OS	140	0,5445	0	1,3183	0,0018
39,44	75,3	P08758	Annexin A5	35	2,8054	0,0001	1,5276	0,0011
229,01	31,3	Q15149	Plectin OS	130	0,3945	0	0,6545	0,0217
60,19	20,4	Q00610	Clathrin heavy chain 1 OS	36	0,3981	0,0001	0,6546	0,005
22,67	51,1	O43852	Calumenin OS	15	2,8576	0,001	2,1677	0,0026
27,01	46,2	P36222	Chitinase-3-like protein 1 OS	24	1,7219	0,0017	1,2246	0,0273
42,29	36,1	P07900	Heat shock protein HSP 90-alpha OS	27	0,6855	0,0019	0,871	0,0496
14,1	30,8	Q96D15	Reticulocalbin-3 OS	10	2,421	0,0032	1,7219	0,0449
55,2	68	P06733	Alpha-enolase OS	56	0,597	0,0037	1,0471	0,4455
61,66	45,3	P12814	Alpha-actinin-1 OS	44	0,6081	0,0046	0,6607	0,0367

38,46	34,6	Q14764	Major vault protein OS	25	0,6081	0,0061	0,7516	0,0491
30,92	44,6	P06576	ATP synthase subunit beta, mitochondrial OS	23	1,803	0,0064	1,4588	0,0234
24,09	45,6	P67936	Tropomyosin alpha-4 chain OS	14	1,556	0,0091	1,6596	0,01
28,74	41,1	O60701	UDP-glucose 6-dehydrogenase OS	21	0,521	0,0113	0,7178	0,0416
26,54	10,1	P02751	Fibronectin OS	16	0,6138	0,0125	1,0186	0,7646
14,28	22,7	Q15084	Protein disulfide-isomerase A6 OS	12	1,4322	0,0156	1,0864	0,891
64,73	66,5	P14618	Pyruvate kinase isozymes M1/M2 OS	58	0,6138	0,0159	0,7244	0,0413
13,96	52,4	P62805	Histone H4 OS	13	1,556	0,027	1,3305	0,0668
46,17	36,4	P11216	Glycogen phosphorylase, brain form OS	30	0,6194	0,0285	0,787	0,28
41,29	32,5	P12109	Collagen alpha-1(VI) chain OS	32	1,4997	0,0315	0,3873	0
8,19	11,9	Q02818	Nucleobindin-1 OS	4	2,421	0,0318	1,3062	0,6913
17,7	2,2	Q14204	Cytoplasmic dynein 1 heavy chain 1 OS	7	0,4831	0,0379	0,5754	0,1018
21,45	52,3	P04179	Superoxide dismutase [Mn], mitochondrial OS	25	1,888	0,0379	2,0137	0,0346
17,57	41,6	P05388	60S acidic ribosomal protein P0 OS	10	0,7516	0,0394	0,9376	0,5738
48,23	47,3	P02545	Lamin-A/C OS	44	1,4588	0,0413	1,4859	0,044
46,89	42,8	P08133	Annexin A6 OS	27	0,6427	0,0435	0,8166	0,2732
11,12	37,6	P04792	Heat shock protein beta-1 OS	10	1,4723	0,0435	1,0666	0,7161
36,88	11,9	Q9NZM1	Myoferlin OS	19	0,6918	0,0448	0,6982	0,0435

40,97	64,8	P00558	Phosphoglycerate kinase 1 OS	36	0,6427	0,0448	0,879	0,8106
38,86	51,1	P30101	Protein disulfide-isomerase A3 OS	34	1,6749	0,0449	1,2589	0,231
10,04	24,7	P50914	60S ribosomal protein L14 OS	6	1,3183	0,0457	0,9817	0,755
32,18	35,1	Q07065	Cytoskeleton-associated protein 4 OS	21	1,3932	0,0475	1,1169	0,6495
24,01	50	P10915	Hyaluronan and proteoglycan link protein 1 OS	17	1,9231	0,048	0,4966	0,005
13,16	14,5	O60506	Heterogeneous nuclear ribonucleoprotein Q OS	8	0,7047	0,0481	0,955	0,7378
145,01	31,7	P12111	Collagen alpha-3(VI) chain OS	122	0,6194	0,0487	0,3373	0
16,33	49,8	P37802	Transgelin-2 OS	14	1,7539	0,0487	2,0701	0,0314
9,27	6,6	P16070	CD44 antigen OS	6	1,2474	0,0595	1,5136	0,0268
20,09	16,7	Q7KZF4	Staphylococcal nuclease domain-containing protein 1 OS	12	0,7727	0,0679	0,9727	0,9665
55,02	46,6	P11021	78 kDa glucose-regulated protein OS	50	1,1695	0,0689	1,0666	0,2321
7,16	12,6	P52209	6-phosphogluconate dehydrogenase, decarboxylating OS	4	0,7112	0,0703	0,863	0,4981
11,97	51,5	P19105	Myosin regulatory light chain 12A OS	8	1,7061	0,0731	2,1677	0,0144
15,83	16,3	P52272	Heterogeneous nuclear ribonucleoprotein M OS	9	0,6427	0,0732	1,2706	0,3011
18,33	28	Q6NZI2	Polymerase I and transcript release factor OS	14	1,7865	0,0752	1,4859	0,2672
9,85	39,4	P02511	Alpha-crystallin B chain OS	5	1,5136	0,079	0,8872	0,2035
19,65	19,2	P19338	Nucleolin OS	14	1,556	0,0805	1,3428	0,2667
8,12	33,7	Q99584	Protein S100-A13 OS	5	1,8707	0,0813	1,4997	0,216

30,82	15,3	Q9P2E9	Ribosome-binding protein 1 OS	17	0,9036	0,0821	0,9817	0,7784
16	45,1	P08865	40S ribosomal protein SA OS	9	2,0137	0,0833	1,0375	0,7219
12,02	35,3	Q01995	Transgelin OS	9	1,5276	0,0872	1,3428	0,1741
14,01	20,6	Q13838	Spliceosome RNA helicase BAT1 OS	9	0,5546	0,0884	0,9204	0,776
38,74	30	P13639	Elongation factor 2 OS	21	0,7178	0,0891	0,7447	0,1828
15,02	22,7	Q16658	Fascin OS	8	0,597	0,0906	0,7586	0,3041
8	3,6	P07814	Bifunctional aminoacyl-tRNA synthetase OS	4	0,7586	0,0946	0,9727	0,8022
10	64,4	P07108	Acyl-CoA-binding protein OS	7	1,5704	0,0955	1,556	0,1374
14,7	22,5	P61158	Actin-related protein 3 OS	8	0,912	0,0971	0,929	0,2983
6,25	18,5	P52907	F-actin-capping protein subunit alpha-1 OS	5	0,7586	0,0973	1,0765	0,5069
6,11	7,8	P07602	Proactivator polypeptide OS	4	2,2491	0,0978	2,0701	0,0569
9,07	7,1	Q05682	Caldesmon OS	5	1,2474	0,0989	1,1588	0,2237
4,33	2,8	O94925	Glutaminase kidney isoform, mitochondrial OS	2	0,8472	0,1056	0,9727	0,6636
11,32	15,5	P36578	60S ribosomal protein L4 OS	6	0,6918	0,1227	0,7586	0,2342
28,02	46,2	P50454	Serpin H1 OS	20	1,3305	0,1297	0,6546	0,3148
85,13	29,8	P24821	Tenascin OS	56	0,8241	0,1317	0,7447	0,3361
5,11	7,2	Q10471	Polypeptide N-acetylgalactosaminyltransferase 2 OS	3	0,8241	0,132	0,8872	0,5144
7,3	29,1	P62277	40S ribosomal protein S13 OS	4	1,556	0,1363	1,0568	0,5625

10,73	29,9	P29692	Elongation factor 1-delta OS	7	1,2023	0,1385	0,9727	0,7896
8,84	19,4	Q15019	Septin-2 OS	6	1,6293	0,1416	1,2706	0,5134
8,05	14,3	Q12907	Vesicular integral-membrane protein VIP36 OS	4	0,871	0,1443	1,0186	0,7604
75,24	53,5	O43707	Alpha-actinin-4 OS	56	0,6486	0,1454	0,955	0,8077
6,08	5,1	P35606	Coatomer subunit beta' OS	3	0,7311	0,1498	0,8472	0,4093
10,04	3	Q13813	Spectrin alpha chain, brain OS	5	0,8872	0,1519	1,0765	0,1294
9,01	22,8	P78417	Glutathione S-transferase omega-1 OS	6	0,5649	0,1533	1,1912	0,6023
24,89	48,2	P23284	Peptidyl-prolyl cis-trans isomerase B OS	21	1,3932	0,1538	1,1803	0,4481
5,27	7,7	Q96QK1	Vacuolar protein sorting-associated protein 35 OS	5	0,6194	0,156	0,955	0,6938
4,65	15,3	O15173	Membrane-associated progesterone receptor component 2 OS	3	1,0864	0,1619	1	0,8031
32,95	46,4	P00338	L-lactate dehydrogenase A chain OS	20	0,8091	0,1629	0,8551	0,2656
18,05	18,5	P07686	Beta-hexosaminidase subunit beta OS	9	1,4859	0,1641	1,0471	0,2642
9,79	13,5	Q9UHD8	Septin-9 OS	6	0,8551	0,1649	0,9727	0,7742
11,89	28,1	P40926	Malate dehydrogenase, mitochondrial OS	8	0,52	0,1658	0,9638	0,7814
20,01	20,8	P13797	Plastin-3 OS	11	0,7047	0,1684	0,9817	0,9388
5	17,2	P61313	60S ribosomal protein L15 OS	4	0,7244	0,1739	0,631	0,1135
19,01	18,4	P40939	Trifunctional enzyme subunit alpha, mitochondrial OS	10	0,7516	0,1793	0,8395	0,5471
29,08	20,2	P22314	Ubiquitin-like modifier-activating enzyme 1 OS	21	0,7244	0,182	0,929	0,5697

6,97	47,9	P69905	Hemoglobin subunit alpha OS	10	1,556	0,1859	1,1169	0,6807
11,88	57	P09382	Galectin-1 OS	16	0,8017	0,187	1,1272	0,3819
15,3	16,2	Q06210	Glucosamine--fructose-6-phosphate aminotransferase [isomerizing] 1 OS	8	0,4786	0,188	0,9462	0,4656
9,77	6,7	P63010	AP-2 complex subunit beta OS	5	0,6252	0,1906	0,6427	0,1439
7,09	24,3	P62701	40S ribosomal protein S4, X isoform OS	7	0,52	0,1958	0,871	0,7758
7,83	35,2	P39019	40S ribosomal protein S19 OS	5	1,5417	0,2002	1,1066	0,747
5,05	2,8	Q04637	Eukaryotic translation initiation factor 4 gamma 1 OS	4	0,8091	0,2081	1,0186	0,8358
14,02	30,5	P23396	40S ribosomal protein S3 OS	8	0,8472	0,2119	0,8472	0,1774
45,62	20,9	P46940	Ras GTPase-activating-like protein IQGAP1 OS	28	0,8318	0,2136	0,9638	0,9256
6,31	5,8	P53618	Coatomer subunit beta OS	4	0,8017	0,2165	1	0,9724
8,23	10,8	Q13228	Selenium-binding protein 1 OS	4	0,8395	0,2165	0,9376	0,6705
0,94	10,3	Q71DI3	Histone H3.2 OS	2	1,2134	0,2179	1,1482	0,511
4,69	15,6	P00441	Superoxide dismutase [Cu-Zn] OS	2	1,8365	0,2193	1,7219	0,2291
8,85	23,3	P30443	HLA class I histocompatibility antigen, A-1 alpha chain OS	5	1	0,2205	0,9727	0,6131
12,96	23	Q07960	Rho GTPase-activating protein 1 OS	7	1,5276	0,2212	0,9462	0,9856
2,96	12,6	P02792	Ferritin light chain OS	2	1,3062	0,2218	0,9462	0,7494
6,65	11,4	P14550	Alcohol dehydrogenase [NADP+] OS	3	0,912	0,2231	1,0471	0,4331
6,15	16,5	Q00688	Peptidyl-prolyl cis-trans isomerase FKBP3 OS	3	1,2942	0,2263	1,0864	0,6364

26,62	34	P21589	5'-nucleotidase OS	18	0,929	0,2267	0,9638	0,5234
12,87	18	P36871	Phosphoglucomutase-1 OS	8	0,787	0,2281	1,0765	0,6279
8	40	P30050	60S ribosomal protein L12 OS	6	0,9376	0,2294	0,9817	0,5038
8,57	22,9	P51858	Hepatoma-derived growth factor OS	5	1,5136	0,2342	1,6904	0,2235
7,57	8	P11940	Polyadenylate-binding protein 1 OS	4	0,8241	0,2343	0,879	0,4706
12,53	23,6	P15880	40S ribosomal protein S2 OS	7	0,9376	0,2349	0,9727	0,5394
25,14	33,6	Q5VTE0	Putative elongation factor 1-alpha-like 3 OS	25	0,6855	0,2359	0,6792	0,0962
15,25	27,8	P60842	Eukaryotic initiation factor 4A-I OS	9	0,9036	0,2397	0,9817	0,893
22,96	28,1	P02768	Serum albumin OS	30	1,1066	0,2432	3,3419	0,0342
6,54	5,2	Q15436	Protein transport protein Sec23A OS	3	0,7112	0,2433	0,955	0,8498
24,66	27,2	P06396	Gelsolin OS	19	0,6194	0,2452	0,9204	0,7591
6,07	27,3	P16104	Histone H2A.x OS	6	1,8197	0,2466	1,2023	0,4914
20,21	32,6	P50395	Rab GDP dissociation inhibitor beta OS	11	0,929	0,2529	0,9462	0,3452
8,33	14,4	P11766	Alcohol dehydrogenase class-3 OS	4	0,8395	0,2541	0,9204	0,673
14,82	51	P60660	Myosin light polypeptide 6 OS	12	1,3932	0,2574	1,2942	0,2049
25,03	34,8	P27797	Calreticulin OS	24	1,2823	0,2591	1,2023	0,5234
10,52	17,2	Q15293	Reticulocalbin-1 OS	5	1,5276	0,26	1,7219	0,1243
6,86	19,7	P62269	40S ribosomal protein S18 OS	5	1,2134	0,2613	1,028	0,7971

6,28	3,2	P0C0L5	Complement C4-B OS	5	1,803	0,2644	0,9908	0,97
4,06	10,9	O95336	6-phosphogluconolactonase OS	2	1,1803	0,2678	1,028	0,7972
3,15	3,2	Q14974	Importin subunit beta-1 OS	2	0,879	0,2686	0,9462	0,5822
4,32	10,3	Q14847	LIM and SH3 domain protein 1 OS	3	1,6749	0,2711	1,4454	0,4603
41,5	68,7	P04406	Glyceraldehyde-3-phosphate dehydrogenase OS	46	0,8472	0,2759	1,028	0,9784
9,2	36,7	P62987	Ubiquitin-60S ribosomal protein L40 OS	9	1,3677	0,2768	0,9462	0,903
20,9	35,8	O75874	Isocitrate dehydrogenase [NADP] cytoplasmic OS	12	0,7447	0,278	1,0864	0,6029
17,55	27,7	P78371	T-complex protein 1 subunit beta OS	10	0,7447	0,2789	0,5808	0,0647
23,01	50,3	P04075	Fructose-bisphosphate aldolase A OS	23	0,7727	0,2792	0,8017	0,2621
5,21	17,5	Q9BTV4	Transmembrane protein 43 OS	5	1,0965	0,2795	0,8472	0,1588
76,65	66,7	P08670	Vimentin OS	126	0,492	0,2804	1,0471	0,5945
4,2	5,1	P23246	Splicing factor, proline- and glutamine-rich OS	3	1,0375	0,2822	1,028	0,7539
5,16	25,2	O43399	Tumor protein D54 OS	4	1,1803	0,286	1,1588	0,2596
10,48	19,8	P40925	Malate dehydrogenase, cytoplasmic OS	6	0,5916	0,2877	0,871	0,7537
4,97	9,8	P51884	Lumican OS	4	1,0765	0,2891	1,0471	0,4875
7,4	14,8	P63244	Guanine nucleotide-binding protein subunit beta-2-like 1 OS	4	0,879	0,2904	0,9376	0,6258
4,75	4,5	Q99613	Eukaryotic translation initiation factor 3 subunit C OS	3	0,8551	0,2938	0,863	0,1988
20,97	22,4	Q15582	Transforming growth factor-beta-induced protein ig-h3 OS	14	0,7798	0,2945	0,5754	0,0247

13,71	55,2	P63241	Eukaryotic translation initiation factor 5A-1 OS	9	0,912	0,2956	1	0,7852
6,4	19,4	P62906	60S ribosomal protein L10a OS	4	0,9376	0,301	0,9036	0,4147
14,49	3,5	P16112	Aggrecan core protein OS	10	1,2942	0,3091	0,5649	0,0138
5,46	11,9	P43307	Translocon-associated protein subunit alpha OS	3	1,6144	0,3111	1,0965	0,7615
5,77	24,2	P04216	Thy-1 membrane glycoprotein OS	6	1,5704	0,3123	1,3428	0,6114
23,85	35,4	Q9BUF5	Tubulin beta-6 chain OS	19	0,9462	0,3158	1	0,6288
7,27	7,4	P21980	Protein-glutamine gamma-glutamyltransferase 2 OS	5	0,7311	0,3185	0,7178	0,2233
5,64	12	P62280	40S ribosomal protein S11 OS	4	0,5754	0,3232	0,7178	0,4548
9,44	22,2	Q15365	Poly(rC)-binding protein 1 OS	8	0,7798	0,3296	0,8954	0,6301
20	40,2	Q99536	Synaptic vesicle membrane protein VAT-1 homolog OS	12	0,6668	0,3363	1,0093	0,9324
31,77	76,7	P60174	Triosephosphate isomerase OS	29	1,1376	0,3396	1,2589	0,077
5,82	12,5	P61163	Alpha-centractin OS	3	1,1066	0,3457	1,0471	0,4322
8,39	9,6	Q9Y5X1	Sorting nexin-9 OS	4	0,9908	0,3478	0,9376	0,605
8	22,2	P07910	Heterogeneous nuclear ribonucleoproteins C1/C2 OS	6	1,1912	0,3483	1	0,9234
7,98	7,7	O43776	Asparaginyl-tRNA synthetase, cytoplasmic OS	5	0,8241	0,3513	0,879	0,3545
8,28	24,4	P24534	Elongation factor 1-beta OS	5	1,3062	0,352	1,6444	0,1507
10,43	76,5	P05387	60S acidic ribosomal protein P2 OS	9	1,2474	0,3523	1,3183	0,1738
9,82	42,9	P10599	Thioredoxin OS	8	1,4454	0,3531	1,8197	0,1378

10	23	P16403	Histone H1.2 OS	6	1,3804	0,3542	1,888	0,1427
10,41	16,2	P06753	Tropomyosin alpha-3 chain OS	6	1,2706	0,361	1,1912	0,4717
60,03	37,7	P14625	Endoplasmin OS	37	0,7447	0,3637	1,0965	0,9717
14,18	10,5	P06737	Glycogen phosphorylase, liver form OS	10	0,863	0,3688	0,9817	0,9066
15,41	24,2	Q16851	UTP--glucose-1-phosphate uridylyltransferase OS	11	0,9204	0,3715	0,9817	0,971
21,82	7	P35580	Myosin-10 OS	12	0,871	0,3719	0,929	0,6476
8,61	45,6	P62158	Calmodulin OS	7	2,1478	0,3722	1,9055	0,1345
0,81	16,7	P06703	Protein S100-A6 OS	2	1,1695	0,3745	1,1588	0,4362
4,41	21,6	P61604	10 kDa heat shock protein, mitochondrial OS	2	1,3428	0,3776	1,2589	0,61
6	28,6	Q9Y3U8	60S ribosomal protein L36 OS	3	1,0864	0,3782	1,028	0,7515
3,75	34,8	P62888	60S ribosomal protein L30 OS	4	1,1066	0,3813	0,9727	0,8511
6	12,9	P42765	3-ketoacyl-CoA thiolase, mitochondrial OS	3	0,8091	0,3816	0,8091	0,4022
18,86	14,2	Q14697	Neutral alpha-glucosidase AB OS	9	0,9376	0,3837	0,9727	0,7061
7,77	11,9	P40227	T-complex protein 1 subunit zeta OS	5	0,7047	0,3871	1,1169	0,6416
6,7	8,5	P48643	T-complex protein 1 subunit epsilon OS	4	0,863	0,3885	0,7943	0,3349
9,68	1,5	Q07954	Prolow-density lipoprotein receptor-related protein 1 OS	5	0,6792	0,3954	0,6081	0,1567
6	12,8	Q01105	Protein SET OS	5	1,3183	0,3985	1,2359	0,6857
10,3	32	P84077	ADP-ribosylation factor 1 OS	6	0,9376	0,4006	0,9036	0,1712

3,82	10,3	Q8NC51	Plasminogen activator inhibitor 1 RNA-binding protein OS	3	1,2246	0,4031	1,0965	0,5156
5,3	8,4	Q13510	Acid ceramidase OS	3	0,955	0,4065	1	0,8105
6	15	P02647	Apolipoprotein A-I OS	6	1,8365	0,4066	1,5417	0,7144
13,64	8,6	P27816	Microtubule-associated protein 4 OS	8	1,0375	0,407	1,0471	0,3414
5,52	19,1	P09429	High mobility group protein B1 OS	5	1,2023	0,4104	1,4322	0,2356
4,72	18	P02794	Ferritin heavy chain OS	3	1,1803	0,4181	0,863	0,6203
4,07	13,2	Q9UIJ7	GTP:AMP phosphotransferase, mitochondrial OS	2	1,1803	0,4197	1,1588	0,4763
5,73	27,9	Q13404	Ubiquitin-conjugating enzyme E2 variant 1 OS	3	0,871	0,424	1,028	0,7202
10,8	20,9	Q08431	Lactadherin OS	7	1,3305	0,4242	0,9376	0,9889
16,73	67,8	P22392	Nucleoside diphosphate kinase B OS	12	1,2134	0,4259	1,1695	0,3059
5,92	13,3	P21281	V-type proton ATPase subunit B, brain isoform OS	4	0,8318	0,4297	0,955	0,8724
12	14,4	Q14247	Src substrate cortactin OS	7	1,0666	0,4305	1,0568	0,6266
6	10,2	P45880	Voltage-dependent anion-selective channel protein 2 OS	3	0,8241	0,4306	0,912	0,7622
52,13	40,3	P08238	Heat shock protein HSP 90-beta OS	34	0,8551	0,4317	0,8318	0,5476
58,44	14,6	Q99715	Collagen alpha-1(XII) chain OS	31	0,8017	0,4327	0,4875	0
8,55	5,6	P02461	Collagen alpha-1(III) chain OS	6	0,9204	0,4336	0,879	0,1909
7,68	13,3	P21810	Biglycan OS	5	0,8472	0,4351	0,929	0,7391
3,57	9,6	P09486	SPARC OS	2	0,863	0,4354	1,1066	0,537

4	3,1	O60763	General vesicular transport factor p115 OS	3	0,863	0,4366	0,9036	0,6229
23,16	41,3	P07339	Cathepsin D OS	25	1,1066	0,4378	1,0765	0,758
15,9	17	P50281	Matrix metalloproteinase-14 OS	8	0,912	0,4397	0,9638	0,9838
4,18	2,3	O95782	AP-2 complex subunit alpha-1 OS	2	0,8318	0,4424	0,8395	0,4611
3,02	7,6	P08962	CD63 antigen OS	4	1,406	0,4434	1,0568	0,7404
20,68	22,4	P38646	Stress-70 protein, mitochondrial OS	13	0,7727	0,4435	0,8872	0,9631
5,46	2,8	Q86VP6	Cullin-associated NEDD8-dissociated protein 1 OS	4	1,1912	0,4479	1,0765	0,6526
7,14	6,6	P10253	Lysosomal alpha-glucosidase OS	4	1,028	0,4499	0,9376	0,7197
14,89	22,8	P07195	L-lactate dehydrogenase B chain OS	7	0,929	0,4535	0,9204	0,3657
18,04	64,3	P09211	Glutathione S-transferase P OS	17	0,8166	0,4541	0,9727	0,9173
9,03	49	P04080	Cystatin-B OS	5	1,4191	0,4545	1,6596	0,2812
5,02	6,2	P49368	T-complex protein 1 subunit gamma OS	3	0,929	0,4558	1,0471	0,5896
5,84	7,2	P14314	Glucosidase 2 subunit beta OS	4	1,1482	0,4586	1,1803	0,2742
4,16	2,2	Q08211	ATP-dependent RNA helicase A OS	2	0,8241	0,4636	0,9908	0,9911
4	17,3	P51571	Translocon-associated protein subunit delta OS	3	1,0375	0,4644	0,9727	0,2598
16,4	10,4	P05023	Sodium/potassium-transporting ATPase subunit alpha-1 OS	8	0,8017	0,4647	1,0375	0,8642
5,08	34,5	P59998	Actin-related protein 2/3 complex subunit 4 OS	5	1,1272	0,4663	0,9376	0,7123
3,62	4,2	O60749	Sorting nexin-2 OS	3	1,2023	0,4696	0,9204	0,7727

11,94	16,9	P09493	Tropomyosin alpha-1 chain OS	7	1,3183	0,4718	1,4454	0,4107
32,91	50,5	P07437	Tubulin beta chain OS	39	0,7178	0,4727	0,8551	0,6498
35,96	33,8	P26038	Moesin OS	25	0,9462	0,4745	0,9462	0,3069
3,8	16,4	P62829	60S ribosomal protein L23 OS	2	0,879	0,4792	0,9204	0,6376
6	34,3	P31949	Protein S100-A11 OS	11	1,2246	0,4821	1,2589	0,5449
7,95	13,3	Q9UHG3	Prenylcysteine oxidase 1 OS	5	1,0864	0,4826	1,0375	0,8033
6,36	11,8	P40121	Macrophage-capping protein OS	5	1,2942	0,4829	1,2942	0,4011
9,27	27	Q99880	Histone H2B type 1-L OS	15	1,406	0,4851	1,1482	0,708
5,18	19,4	Q15056	Eukaryotic translation initiation factor 4H OS	3	1,0375	0,4859	1,2023	0,1758
7,64	6,1	P34932	Heat shock 70 kDa protein 4 OS	4	0,9376	0,4871	0,9376	0,4579
13,58	35,8	P60981	Destrin OS	7	0,879	0,4883	0,9376	0,7769
2,88	8,5	O75718	Cartilage-associated protein OS	3	1,1272	0,489	1,0568	0,6912
4	12,8	Q9UKK9	ADP-sugar pyrophosphatase OS	3	0,9376	0,4898	1,0471	0,558
4,35	10,9	Q9UBS4	DnaJ homolog subfamily B member 11 OS	2	0,955	0,4907	1,0965	0,1803
6	26,7	Q14011	Cold-inducible RNA-binding protein OS	3	1,2246	0,4908	1,0864	0,9306
7,13	12,6	P50991	T-complex protein 1 subunit delta OS	5	0,9376	0,4912	1,0666	0,3486
7,75	15,2	P18463	HLA class I histocompatibility antigen, B-37 alpha chain OS	4	1,1695	0,4941	1,0864	0,7139
5,94	14,1	P62140	Serine/threonine-protein phosphatase PP1-beta catalytic subunit OS	4	0,8318	0,4959	0,912	0,8138

4,98	16,4	O15260	Surfeit locus protein 4 OS	5	1,1066	0,4984	1,0666	0,6313
13,96	32,6	P40261	Nicotinamide N-methyltransferase OS	8	0,9036	0,5012	1,1912	0,7562
4,26	3,1	O00469	Procollagen-lysine,2-oxoglutarate 5-dioxygenase 2 OS	2	0,912	0,5012	0,955	0,7843
4,53	4	Q96TA1	Niban-like protein 1 OS	3	0,955	0,5028	1,0186	0,78
4,68	16,2	Q9BVK6	Transmembrane emp24 domain-containing protein 9 OS	4	1,0093	0,5037	0,9817	0,4653
4,03	14,6	P46783	40S ribosomal protein S10 OS	4	1,1588	0,5124	1,0568	0,7626
3,12	3,8	Q92499	ATP-dependent RNA helicase DDX1 OS	2	0,8395	0,5126	0,955	0,8628
20,4	23,9	Q96AY3	Peptidyl-prolyl cis-trans isomerase FKBP10 OS	12	0,929	0,518	0,9908	0,9287
23,94	41,4	P22626	Heterogeneous nuclear ribonucleoproteins A2/B1 OS	19	1,1169	0,5213	1,0375	0,8524
7,68	10	P12956	X-ray repair cross-complementing protein 6 OS	6	0,9376	0,5391	1,0186	0,9189
11,81	14,7	P39656	Dolichyl-diphosphooligosaccharideprotein glycosyltransferase 48 kDa subunit	6	0,9204	0,5397	0,912	0,526
8,6	15,4	Q01518	Adenylyl cyclase-associated protein 1 OS	6	0,9204	0,5402	0,912	0,6468
4,61	9,7	P35998	26S protease regulatory subunit 7 OS	3	0,9036	0,5407	0,9817	0,9627
4,02	19,5	P30046	D-dopachrome decarboxylase OS	2	1,0864	0,546	1,0568	0,6195
4,89	7,3	P04062	Glucosylceramidase OS	3	0,6546	0,5484	0,8954	0,8506
9,27	27	Q8N257	Histone H2B type 3-B OS	15	1,3305	0,5486	1,1376	0,7643
10,86	7,3	P49588	Alanyl-tRNA synthetase, cytoplasmic OS	5	0,929	0,5495	1,0375	0,6479
13,88	18,8	Q14108	Lysosome membrane protein 2 OS	7	1,1066	0,5545	1,0375	0,8768

25,82	34,7	P25705	ATP synthase subunit alpha, mitochondrial OS	20	1,2023	0,5558	0,8472	0,4144
24,09	28,9	P08107	Heat shock 70 kDa protein 1A/1B OS	18	1,028	0,5564	1,028	0,7778
14,08	45,2	O00299	Chloride intracellular channel protein 1 OS	10	0,7112	0,5572	0,9462	0,7566
11,38	15,9	P05455	Lupus La protein OS	6	1,0375	0,558	1,0093	0,9753
13,74	31,4	Q13162	Peroxiredoxin-4 OS	11	1,0965	0,5606	0,871	0,093
3,04	20,4	P68871	Hemoglobin subunit beta OS	6	1,1912	0,5651	0,9817	0,9497
2,24	5	P28838	Cytosol aminopeptidase OS	2	0,8872	0,5699	0,9727	0,8569
15	18,8	P26641	Elongation factor 1-gamma OS	9	0,9462	0,5744	0,929	0,4427
12,01	24,5	P30040	Endoplasmic reticulum resident protein 29 OS	6	1,028	0,5753	1,028	0,6252
6,56	20,7	P62241	40S ribosomal protein S8 OS	5	0,929	0,5761	0,912	0,4754
10	21,4	Q99439	Calponin-2 OS	5	1,0568	0,5857	1,0568	0,5571
3,49	5,1	P20073	Annexin A7 OS	3	0,9462	0,5865	1,0375	0,5036
26,63	38,6	P10809	60 kDa heat shock protein, mitochondrial OS	20	1,1169	0,5887	1,1169	0,7607
17,7	23,2	P13674	Prolyl 4-hydroxylase subunit alpha-1 OS	11	1,0864	0,5894	1,2134	0,5517
10,59	14,8	Q13557	Calcium/calmodulin-dependent protein kinase type II subunit delta OS	7	0,9727	0,5935	0,955	0,9306
4,97	12,3	P10644	cAMP-dependent protein kinase type I-alpha regulatory subunit OS	3	1,0864	0,5961	0,9376	0,5937
2,6	8,6	P63208	S-phase kinase-associated protein 1 OS	2	0,7943	0,5961	1,0666	0,8535

3,27	4,9	P20810	Calpastatin OS	2	1,2589	0,5977	1,1376	0,7286
6	61,4	P62328	Thymosin beta-4 OS	6	1,2823	0,5982	1,3305	0,594
9,65	8,6	Q9Y678	Coatomer subunit gamma OS	5	0,9376	0,5989	0,8954	0,5909
10,02	13,8	Q04446	1,4-alpha-glucan-branching enzyme OS	7	0,9204	0,5993	0,9376	0,7397
3,07	12	P62834	Ras-related protein Rap-1A OS	3	1,0093	0,601	0,8954	0,4461
7,15	8,2	P50990	T-complex protein 1 subunit theta OS	4	0,955	0,603	0,955	0,725
21,93	25,2	P50995	Annexin A11 OS	11	0,6982	0,6043	1,0093	0,4945
6,93	24	P27105	Erythrocyte band 7 integral membrane protein OS	6	0,9204	0,6046	0,9376	0,7339
4,94	25,3	Q03135	Caveolin-1 OS	4	1,1066	0,609	0,955	0,8969
11,89	15,4	P55084	Trifunctional enzyme subunit beta, mitochondrial OS	6	0,9638	0,6095	1	0,871
38,17	25,9	P12110	Collagen alpha-2(VI) chain OS	42	1	0,6103	0,4656	0,0001
4	5,9	P22234	Multifunctional protein ADE2 OS	2	0,863	0,6143	0,9638	0,9921
4	20,4	Q9H299	SH3 domain-binding glutamic acid-rich-like protein 3 OS	5	1,1912	0,6148	1,1169	0,7985
12,76	20,4	P43490	Nicotinamide phosphoribosyltransferase OS	7	0,9817	0,6152	1,0666	0,2484
4	9,2	P09012	U1 small nuclear ribonucleoprotein A OS	2	1,3552	0,617	1,1272	0,8349
7,33	6,8	P17844	Probable ATP-dependent RNA helicase DDX5 OS	4	0,9036	0,6178	0,912	0,6476
22,29	38,4	Q04828	Aldo-keto reductase family 1 member C1 OS	17	0,8241	0,6193	0,8472	0,7736
6	9,7	P55209	Nucleosome assembly protein 1-like 1 OS	4	1,1272	0,6196	1,0864	0,6715

6,92	8,3	P06865	Beta-hexosaminidase subunit alpha OS	4	0,9462	0,621	1,0765	0,4737
16,47	19,7	P06744	Glucose-6-phosphate isomerase OS	13	1,0471	0,6235	1,0186	0,7291
8,13	24	P17931	Galectin-3 OS	7	1,1169	0,6245	1,2023	0,5432
12,61	34,8	P51149	Ras-related protein Rab-7a OS	8	1,0375	0,625	0,912	0,6307
1,41	8,7	Q15907	Ras-related protein Rab-11B OS	2	1,1066	0,6313	0,955	0,9241
47,86	46,7	P07237	Protein disulfide-isomerase OS	44	0,8166	0,6335	1,1803	0,2025
4,26	11,2	P27635	60S ribosomal protein L10 OS	5	0,863	0,6351	1,0568	0,726
20,36	59,1	P18669	Phosphoglycerate mutase 1 OS	17	1,0765	0,6352	1,7865	0,0704
9,61	13	Q8NBS9	Thioredoxin domain-containing protein 5 OS	5	1,0765	0,6354	1,0568	0,6582
25,93	11,9	P01023	Alpha-2-macroglobulin OS	26	0,8872	0,6369	0,955	0,9161
13,78	11,8	P15311	Ezrin OS	8	0,9376	0,6375	0,9817	0,6848
5,95	8,6	P11279	Lysosome-associated membrane glycoprotein 1 OS	4	1,1169	0,6378	1,1803	0,5313
13,92	22,3	Q14103	Heterogeneous nuclear ribonucleoprotein D0 OS	7	0,912	0,6437	1,0666	0,4999
4,78	22,9	Q9Y696	Chloride intracellular channel protein 4 OS	3	0,8872	0,6449	1,1695	0,3659
11,11	41,8	Q99497	Protein DJ-1 OS	7	1,0186	0,6466	1,028	0,5711
3,75	4,5	Q02809	Procollagen-lysine,2-oxoglutarate 5-dioxygenase 1 OS	2	0,8166	0,65	0,8395	0,7366
16,49	35,7	Q06830	Peroxiredoxin-1 OS	12	0,9376	0,652	1,028	0,6989
5,63	17,4	P54727	UV excision repair protein RAD23 homolog B OS	5	1	0,6525	1,1272	0,1949

4	17,4	P14174	Macrophage migration inhibitory factor OS	7	1,2589	0,6539	1,2359	0,717
6	24,4	P62750	60S ribosomal protein L23a OS	4	1,0965	0,6548	1,0186	0,8396
5,82	12,9	P19623	Spermidine synthase OS	4	0,879	0,6556	0,787	0,5353
10,65	8,5	P05556	Integrin beta-1 OS	6	1,0765	0,6611	1,1066	0,6166
2,26	13,5	O75531	Barrier-to-autointegration factor OS	2	1,1482	0,6613	1,2474	0,581
8	30,1	P08134	Rho-related GTP-binding protein RhoC OS	7	0,9727	0,6614	0,879	0,4175
5,08	12,5	P00367	Glutamate dehydrogenase 1, mitochondrial OS	6	0,929	0,6628	0,8954	0,5412
25,45	39,3	P68366	Tubulin alpha-4A chain OS	25	0,8551	0,6637	0,8318	0,5732
5,41	10,4	P49411	Elongation factor Tu, mitochondrial OS	3	0,9036	0,6639	0,7943	0,3648
10,84	30,4	P00568	Adenylate kinase isoenzyme 1 OS	6	1,0375	0,6645	1	0,9998
6,59	22,4	P49755	Transmembrane emp24 domain-containing protein 10 OS	3	0,929	0,665	0,9036	0,6309
5,92	9,3	P15289	Arylsulfatase A OS	3	0,9376	0,6684	0,955	0,8851
7,36	22,7	P61247	40S ribosomal protein S3a OS	7	1,028	0,6713	1,0864	0,5815
13,99	16,6	Q96HC4	PDZ and LIM domain protein 5 OS	9	0,9638	0,6727	1,0186	0,7987
2,52	3,4	Q16891	Mitochondrial inner membrane protein OS	2	0,955	0,6772	1	0,6882
5,51	6,2	P15586	N-acetylglucosamine-6-sulfatase OS	3	1,0666	0,6778	1,0093	0,8892
4	15,2	P62263	40S ribosomal protein S14 OS	3	0,912	0,68	0,9817	0,8883
9,87	10,1	O43390	Heterogeneous nuclear ribonucleoprotein R OS	5	1,0864	0,6807	0,9817	0,964

6	11,9	Q92597	Protein NDRG1 OS	3	0,8954	0,6823	0,9817	0,9636
10	18	P61160	Actin-related protein 2 OS	6	1,0568	0,6857	0,9817	0,8537
9,12	25,6	P16152	Carbonyl reductase [NADPH] 1 OS	6	0,9638	0,6858	1,0568	0,6018
6,33	6,2	O15460	Prolyl 4-hydroxylase subunit alpha-2 OS	3	0,9376	0,6859	0,9727	0,9686
2,95	5,7	P63000	Ras-related C3 botulinum toxin substrate 1 OS	2	1,1588	0,6886	1,028	0,9111
8,46	4,8	P41252	Isoleucyl-tRNA synthetase, cytoplasmic OS	4	1,0186	0,6901	0,9638	0,6492
4,37	3,6	Q9BSJ8	Extended synaptotagmin-1 OS	3	1,0568	0,6902	1,0864	0,6161
4,31	16	P62851	40S ribosomal protein S25 OS	2	1,0965	0,6912	1,0093	0,9491
6,19	21,2	P62249	40S ribosomal protein S16 OS	3	0,9462	0,6956	0,912	0,493
4	6	Q8IWE2	Protein NOXP20 OS	2	1,1482	0,6966	1,406	0,448
2,95	2,3	P46977	Dolichyl-diphosphooligosaccharide--protein glycosyltransferase subunit STT3A OS	2	0,9204	0,7005	0,9036	0,6834
8,17	45,4	P60903	Protein S100-A10 OS	12	1,0186	0,7016	1,0765	0,4036
8,54	17,3	P18124	60S ribosomal protein L7 OS	4	0,929	0,7051	0,863	0,2914
16	54	P30086	Phosphatidylethanolamine-binding protein 1 OS	10	0,9817	0,7061	1,0666	0,2505
4,11	10,2	P30048	Thioredoxin-dependent peroxide reductase, mitochondrial OS	2	1	0,7073	0,9638	0,6741
10,75	6	P01024	Complement C3 OS	9	1,0568	0,7116	2,0324	0,4225
26,68	23,5	P02458	Collagen alpha-1(II) chain OS	32	1,028	0,7131	0,7727	0,3594
0,32	3,2	P02790	Hemopexin OS	2	0,8551	0,7131	1,0375	0,8838

4,05	11,4	P21964	Catechol O-methyltransferase OS	2	1,028	0,7135	0,9817	0,9349
2	12,1	Q01629	Interferon-induced transmembrane protein 2 OS	2	1,1912	0,7153	1,1169	0,9044
4,64	12,7	P61019	Ras-related protein Rab-2A OS	3	1,0568	0,7211	1,0471	0,7835
1,69	7	Q15233	Non-POU domain-containing octamer-binding protein OS	2	1	0,7271	1,0568	0,6902
6	29,1	O15511	Actin-related protein 2/3 complex subunit 5 OS	3	1,1169	0,7278	1,0666	0,6291
7,56	6,2	Q9Y4L1	Hypoxia up-regulated protein 1 OS	4	0,929	0,7369	0,8318	0,0793
9,45	2,8	P49327	Fatty acid synthase OS	5	1,028	0,7385	0,879	0,3086
4,88	5,9	P23381	Tryptophanyl-tRNA synthetase, cytoplasmic OS	2	0,9204	0,7405	0,8318	0,3354
2,18	6,9	P35237	Serpin B6 OS	2	1,0568	0,7423	1,0186	0,8944
15,88	33,9	P00387	NADH-cytochrome b5 reductase 3 OS	10	0,9727	0,7425	0,9376	0,5017
6,87	6,3	P38606	V-type proton ATPase catalytic subunit A OS	3	0,9727	0,7452	0,9908	0,9801
4	25	P62942	Peptidyl-prolyl cis-trans isomerase FKBP1A OS	2	1,0864	0,7455	1,028	0,8596
27,97	37,9	Q16555	Dihydropyrimidinase-related protein 2 OS	18	0,7656	0,7466	0,787	0,6266
7	5,6	P17655	Calpain-2 catalytic subunit OS	3	1	0,7471	1	0,9248
31,74	44,3	Q13885	Tubulin beta-2A chain OS	34	1,0471	0,7475	0,9462	0,8039
2,77	2,8	Q86W92	Liprin-beta-1 OS	2	0,912	0,7528	0,8472	0,5721
3,86	6,9	Q9Y6N5	Sulfide:quinone oxidoreductase, mitochondrial OS	3	0,955	0,7545	1	0,9649
8,92	13,1	O43854	EGF-like repeat and discoidin I-like domain-containing protein 3 OS	5	1,2134	0,7563	1,1482	0,5873

9,64	23,4	Q9BS26	Endoplasmic reticulum resident protein 44 OS	8	0,9817	0,7568	1	0,753
3,73	2,5	P55786	Puromycin-sensitive aminopeptidase OS	2	0,9727	0,7602	0,9638	0,7305
6	15,4	P20618	Proteasome subunit beta type-1 OS	3	0,9638	0,762	0,9638	0,8773
1,61	4,7	O95302	Peptidyl-prolyl cis-trans isomerase FKBP9 OS	2	0,9462	0,7625	0,9638	0,8412
4	33	Q15836	Vesicle-associated membrane protein 3 OS	3	1,0186	0,7655	1,0471	0,6713
4,01	5	P10619	Lysosomal protective protein OS	3	1,1169	0,7692	0,8241	0,6589
7,17	16,4	P17980	26S protease regulatory subunit 6A OS	4	1,0186	0,773	0,8551	0,3144
4	18,8	Q15185	Prostaglandin E synthase 3 OS	2	0,8551	0,7743	1,0666	0,8708
6,55	10,7	Q8N8S7	Protein enabled homolog OS	6	1,0666	0,7747	1,0765	0,8081
11,25	15,9	P49748	Very long-chain specific acyl-CoA dehydrogenase, mitochondrial OS	7	0,929	0,7755	0,5649	0,1255
5,25	15,9	P54920	Alpha-soluble NSF attachment protein OS	5	1,0093	0,7778	1	0,4231
39,31	61,9	P04083	Annexin A1 OS	29	1	0,7786	1	0,3006
4	5,4	P31939	Bifunctional purine biosynthesis protein PURH OS	2	0,871	0,7809	0,9376	0,9028
7,82	10	P29401	Transketolase OS	6	0,955	0,7852	1	0,9688
4	10,8	P62753	40S ribosomal protein S6 OS	3	0,871	0,7869	0,9462	0,873
10,59	33,3	P32119	Peroxiredoxin-2 OS	8	1	0,7869	1,0093	0,7597
15,55	17	P04843	Dolichyl-diphosphooligosaccharide--protein glycosyltransferase subunit 1 OS	9	0,9908	0,7875	0,9638	0,7682

42,64	13,5	Q9Y490	Talin-1 OS	25	1	0,7879	1,028	0,1224
4,61	2,5	Q12906	Interleukin enhancer-binding factor 3 OS	2	1,0186	0,7925	1,0186	0,7621
20,74	7,1	Q6UVK1	Chondroitin sulfate proteoglycan 4 OS	10	0,9908	0,7928	1,0375	0,501
8,32	27,2	P18621	60S ribosomal protein L17 OS	4	0,9817	0,7936	0,9817	0,8973
3,47	11,1	P07711	Cathepsin L1 OS	2	0,9204	0,7937	0,871	0,6395
6,99	25,5	P30085	UMP-CMP kinase OS	4	1,0375	0,7941	1,0666	0,6918
1,25	5,6	P04632	Calpain small subunit 1 OS	3	0,9462	0,7956	1,0965	0,7396
4,52	4,8	P55884	Eukaryotic translation initiation factor 3 subunit B OS	3	0,929	0,798	0,912	0,7372
25,64	30	Q9NZN4	EH domain-containing protein 2 OS	14	1	0,7995	1,028	0,4835
8,28	16,4	P52597	Heterogeneous nuclear ribonucleoprotein F OS	6	1,0765	0,7996	0,9727	0,961
6,37	5,2	Q00839	Heterogeneous nuclear ribonucleoprotein U OS	3	0,9727	0,801	0,9376	0,6344
0,76	7,1	P02741	C-reactive protein OS	3	0,871	0,8038	0,9727	0,8231
18,17	36,1	P62258	14-3-3 protein epsilon OS	11	1,028	0,8042	1,0666	0,5569
6,16	15,6	Q96AG4	Leucine-rich repeat-containing protein 59 OS	5	1,0375	0,8064	1,1588	0,5581
5,58	12	P04844	Dolichyl-diphosphooligosaccharide--protein glycosyltransferase subunit 2 OS	5	0,9462	0,8097	0,9204	0,6452
7,32	24,7	O75396	Vesicle-trafficking protein SEC22b OS	6	1,0375	0,8112	1,0093	0,7545
3,17	10,9	P26373	60S ribosomal protein L13 OS	2	1,0765	0,817	0,9638	0,8341
4	4,7	Q14956	Transmembrane glycoprotein NMB OS	3	1,1376	0,8178	1,0666	0,9004

30,86	44,3	P68371	Tubulin beta-2C chain OS	34	0,929	0,8189	1,0186	0,9306
13,1	17,1	P11413	Glucose-6-phosphate 1-dehydrogenase OS	9	0,9638	0,82	0,9727	0,6496
4,45	11,3	P15559	NAD(P)H dehydrogenase [quinone] 1 OS	3	0,955	0,8201	0,9638	0,6388
4,11	7,3	O75367	Core histone macro-H2A.1 OS	2	1	0,8203	0,9727	0,9841
6,63	5,1	O94832	Myosin-Id OS	4	0,9817	0,8211	0,9817	0,9756
6,32	33,1	P62244	40S ribosomal protein S15a OS	4	1,028	0,8219	0,9727	0,8055
11,72	16,7	O75083	WD repeat-containing protein 1 OS	7	0,9817	0,8222	0,9727	0,9692
6,31	14,5	Q9UK22	F-box only protein 2 OS	3	1,0093	0,832	0,8954	0,2497
8,31	22,6	P52565	Rho GDP-dissociation inhibitor 1 OS	7	1,0471	0,8328	0,9727	0,8672
4	7,1	Q9NTK5	Obg-like ATPase 1 OS	2	1,1169	0,8344	1,1169	0,7986
4	9,6	Q07021	Complement component 1 Q subcomponent-binding protein, mitochondrial	2	1,0666	0,8376	1,1695	0,7216
19,1	21,7	P13667	Protein disulfide-isomerase A4 OS	11	0,9908	0,8391	0,955	0,5221
11,54	30,2	P27348	14-3-3 protein theta OS	9	0,9908	0,8395	1,028	0,8592
7,45	23,2	P62826	GTP-binding nuclear protein Ran OS	4	1,0093	0,8409	0,9638	0,7501
2,02	17,4	P62857	40S ribosomal protein S28 OS	2	1,1695	0,841	1,2246	0,5331
10,76	2,3	O75369	Filamin-B OS	8	0,879	0,8417	0,673	0,4462
3,67	6,5	P41250	Glycyl-tRNA synthetase OS	3	0,929	0,8428	0,8954	0,434
6,03	16,5	P62081	40S ribosomal protein S7 OS	3	1,0375	0,8448	0,955	0,5817

11,69	8,4	O00159	Myosin-Ic OS	7	0,9817	0,8512	0,929	0,6832
16,45	65,7	P07737	Profilin-1 OS	15	0,9638	0,8515	0,9817	0,9827
4,15	6,6	P31948	Stress-induced-phosphoprotein 1 OS	2	0,863	0,8533	1,2246	0,6408
2,57	4,2	P33176	Kinesin-1 heavy chain OS	3	0,9204	0,8534	0,871	0,578
5,18	15,2	O15145	Actin-related protein 2/3 complex subunit 3 OS	3	0,9462	0,8538	1	0,8828
25,88	67,3	P62937	Peptidyl-prolyl cis-trans isomerase A OS	23	0,8395	0,856	1,1695	0,3815
17,03	36,8	P21796	Voltage-dependent anion-selective channel protein 1 OS	10	1,0186	0,8567	0,9727	0,7813
4,06	4,5	Q96AE4	Far upstream element-binding protein 1 OS	3	1,028	0,8575	1,0765	0,6078
7,53	15,8	P55795	Heterogeneous nuclear ribonucleoprotein H2 OS	5	1,0186	0,8578	1	0,9407
12,52	24,1	P07093	Glia-derived nexin OS	9	1,028	0,8581	1,3677	0,1914
24,38	43	P09525	Annexin A4 OS	13	0,863	0,869	0,8395	0,393
4,69	9,3	P62191	26S protease regulatory subunit 4 OS	2	0,9638	0,8696	0,9638	0,8704
8,04	17,2	P46777	60S ribosomal protein L5 OS	5	0,9727	0,8708	1,0471	0,5384
4	19,5	Q9BRA2	Thioredoxin domain-containing protein 17 OS	3	1,028	0,8735	1,0765	0,8262
3,72	9,2	P28482	Mitogen-activated protein kinase 1 OS	3	0,955	0,8748	1,0666	0,8777
11,92	36,9	P30044	Peroxiredoxin-5, mitochondrial OS	10	1,0864	0,8809	1,2589	0,4188
9,76	19,8	Q13642	Four and a half LIM domains protein 1 OS	6	1,0375	0,881	1,2474	0,5325
21,38	69,3	P23528	Cofilin-1 OS	18	1,0568	0,8825	1,2706	0,3638

4	18,8	P26447	Protein S100-A4 OS	3	1,0765	0,8881	1,1803	0,7522
8,1	6,8	Q12884	Seprase OS	4	1,0965	0,8906	1,1588	0,8113
4,16	6,3	Q8IV08	Phospholipase D3 OS	3	1,0186	0,8918	0,9462	0,8582
7,54	4	P07996	Thrombospondin-1 OS	4	1	0,8989	0,4875	0,1265
4	7,6	Q13011	Delta(3,5)-Delta(2,4)-dienoyl-CoA isomerase, mitochondrial OS	2	0,912	0,9002	0,912	0,8782
4	12,8	P46776	60S ribosomal protein L27a OS	3	1,1066	0,9011	0,9908	0,9568
4,45	5,9	Q9Y625	Glypican-6 OS	3	0,9908	0,9012	1,1066	0,6474
12	23,1	P04899	Guanine nucleotide-binding protein G(i) subunit alpha-2 OS	7	0,9908	0,9074	0,955	0,7784
3,46	9,6	P35232	Prohibitin OS	2	0,9817	0,9108	0,912	0,6545
13,6	31,3	P31946	14-3-3 protein beta/alpha OS	13	0,9727	0,9145	1,028	0,7182
6	18,3	P60953	Cell division control protein 42 homolog OS	3	1	0,9162	1,1066	0,6492
4,49	5,5	Q6DD88	Atlastin-3 OS	3	0,9817	0,9167	0,9376	0,612
13,33	27,3	P51991	Heterogeneous nuclear ribonucleoprotein A3 OS	8	0,9036	0,9191	0,9727	0,8815
2,8	15,3	Q02543	60S ribosomal protein L18a OS	2	1,0093	0,9215	1	0,9811
4	11	P60900	Proteasome subunit alpha type-6 OS	3	0,9817	0,9234	1,0186	0,9104
3,8	6,3	P00966	Argininosuccinate synthase OS	2	0,9462	0,9266	0,9817	0,9283
4,87	1,8	Q01082	Spectrin beta chain, brain 1 OS	3	0,9727	0,9269	0,8318	0,3803
10,37	23,6	Q02878	60S ribosomal protein L6 OS	6	0,9817	0,927	0,8954	0,4158

8,94	21,7	P40429	60S ribosomal protein L13a OS	5	1	0,9271	0,9462	0,8094
15,46	13,5	P27824	Calnexin OS	9	0,9817	0,9288	0,9908	0,7564
4,19	25,5	Q04760	Lactoylglutathione lyase OS	3	0,9727	0,9347	0,9727	0,9425
2	2,1	P02748	Complement component C9 OS	2	0,9376	0,9378	0,9817	0,9328
14,35	37,5	P07858	Cathepsin B OS	12	0,9727	0,9414	1,2706	0,5584
6,54	48,5	P25398	40S ribosomal protein S12 OS	6	0,9817	0,9428	1,1066	0,7865
2	8,5	P60033	CD81 antigen OS	4	0,955	0,9436	1,1482	0,7879
1,56	2	O94979	Protein transport protein Sec31A OS	2	0,9817	0,9464	1,028	0,2908
51,11	31,3	P18206	Vinculin OS	32	1,0093	0,9464	1,1272	0,3797
48,3	43,7	P11142	Heat shock cognate 71 kDa protein OS	46	1	0,9485	0,9908	0,863
14,23	20,8	P13489	Ribonuclease inhibitor OS	10	1,0186	0,9523	0,9638	0,5114
4	9,6	Q8IZP2	Putative protein FAM10A4 OS	2	1,028	0,9536	0,9376	0,8936
6,18	12,3	O15144	Actin-related protein 2/3 complex subunit 2 OS	3	0,9727	0,9537	0,9908	0,9808
4	15,7	P13693	Translationally-controlled tumor protein OS	2	1,0186	0,9546	1,1376	0,7284
4,57	7,1	P02765	Alpha-2-HS-glycoprotein OS	3	0,9908	0,9596	2,3988	0,0386
1,48	3,6	P54136	Arginyl-tRNA synthetase, cytoplasmic OS	2	0,9817	0,9611	0,7943	0,3126
6,16	16	Q16181	Septin-7 OS	4	0,912	0,9628	0,929	0,27
2,34	3,4	Q99829	Copine-1 OS	2	0,9462	0,9635	0,9204	0,8332

2,26	5,2	P04004	Vitronectin OS	2	0,9817	0,9637	0,863	0,8054
0,74	10,3	P46781	40S ribosomal protein S9 OS	2	0,9908	0,9657	0,9727	0,7035
4,09	5,3	P49189	4-trimethylaminobutyraldehyde dehydrogenase OS	2	0,929	0,9662	0,9036	0,8274
12,99	42,9	P62820	Ras-related protein Rab-1A OS	10	0,9727	0,9696	0,9817	0,8701
6,17	24,5	O75915	PRA1 family protein 3 OS	5	0,955	0,9697	1,0093	0,7403
3,6	13,3	Q01469	Fatty acid-binding protein, epidermal OS	2	0,912	0,971	0,9908	0,9875
6,19	16,1	O14818	Proteasome subunit alpha type-7 OS	4	1,0093	0,9719	0,9908	0,8364
2,76	12	P36543	V-type proton ATPase subunit E 1 OS	2	1,0471	0,9735	1,0965	0,8205
5,11	7,4	O94905	Erlin-2 OS	3	0,9908	0,9781	0,8395	0,6046
4	5,7	P32969	60S ribosomal protein L9 OS	2	0,9462	0,9796	0,871	0,7991
12,89	31,3	P06748	Nucleophosmin OS	11	0,8017	0,9807	1,7378	0,2327
5,51	28	P21291	Cysteine and glycine-rich protein 1 OS	3	0,9817	0,9816	1,2359	0,4583
6,05	10,5	P04181	Ornithine aminotransferase, mitochondrial OS	3	1,0093	0,9817	0,9462	0,848
8	5,6	Q9NQC3	Reticulon-4 OS	6	0,9908	0,9837	0,9638	0,8991
5,7	4,9	Q9UHB6	LIM domain and actin-binding protein 1 OS	4	0,9908	0,9886	0,9638	0,9157
4,31	4,5	Q9UHL4	Dipeptidyl peptidase 2 OS	2	0,9908	0,99	1,0864	0,7291
2,98	5,5	Q00325	Phosphate carrier protein, mitochondrial OS	2	1,0375	0,9918	0,9727	0,7947
6	23,4	P13987	CD59 glycoprotein OS	4	0,9908	0,9922	1,3552	0,5773

25,11	35,8	P09651	Heterogeneous nuclear ribonucleoprotein A1 OS	15	0,929	0,9931	1,0093	0,8952
23,59	72,8	P30041	Peroxiredoxin-6 OS	15	0,9817	0,9933	0,9908	0,8458
3,75	6,6	Q15181	Inorganic pyrophosphatase OS	2	1,0093	0,9944	0,9638	0,9446
12,82	11,3	P02788	Lactotransferrin OS	12	0,9908	0,9952	1,5417	0,5539
6,26	3,5	Q00341	Vigilin OS	3	1	0,9961	0,9727	0,5973
6,1	25,5	P83731	60S ribosomal protein L24 OS	5	0,9908	0,9968	0,929	0,7074
5,02	12,9	P09496	Clathrin light chain A OS	3	0,9727	0,9987	1,0471	0,7911

Appendix 3: Tables to evaluate the state of mouse.

To evaluate the general state of the mouse, we used a template with criteria of severity that includes those clinical signs that are visibly perceived about its symptomatology with a score of 0 to 4.

Mice will be programmed for slaughter at four months of age according to current regulations, one month before their life expectancy, to decrease the suffering and alterations caused by the mutation in the mice. On the other hand, if, during the follow-up, any of the mice has a score greater than or equal to 10 (Table 2), they will be sacrificed to avoid suffering the animal.

Table 8.2: Table of severity criteria

Observation	**Symptoms**	**punctuation**
Body weight (% peso)	Lose Body weight 0 - 5%	0
	Lose Body weight 5 - 10%	1
	Lose Body weight 11% -15%	2
	Lose Body weight 16% -20%	3
	Lose Body weight al 20%	4
Observation		
Physic Parameters (Appearance)	**Symptoms of Discomfort**	
Skin	Normal	0
	General lack of grooming	1
	Dry skin and/or nasal and/or ocular discharge	2
Hair	Normal	0
	Small changes/piloerection	1
	Coat in poor condition / ocular or nasal secretions	2
Eyes	Normal	0
	Sunken or off	1
Dehydration	Dehydration when pinching the skin. Stretch marks	3
	Dehydration> 48 hours	4

Abnormal postures	Bent Abdomen	1
	Body Stretch	2
Locomotion	Difficulties in locomotion	4
	Weakness or paralysis of the extremities	4
Physiological Parameters	**Síntomas de Malestar**	
Breathe	Normal	0
	Accelerated (Tachypnea)	1
	Slow Breathing (Dyspnea)	2
	Working Breathing (Great Dyspnea)	3
	Respiration Labored and accompanied by nasal discharge and / or cyanosis	4
Tremors	Normal	0
	Transient	1
	Blinking	2
	Continuous	3
Spontaneous Behavior	Normal	0
	Moderate change in behavior and / or away from your cage mates	2
	Reacts violently / vocalization	3
	Repetitive Movements (Stereotypies)	1
Behavior under manipulation	Normal	0
	Small changes	1
	Moderated changes	2
	Aggressive or comatose animal	3
Temperature	Normal	0
	Fever	2
	Hypothermia	1
	Persistent hypothermia	4
Skin	Anemia, as indicated by symptoms such as pale paws	4

	Cyanosis	4
Environmental Parameters	**Symptoms of Discomfort**	
Food and drink	Normal	0
	Increase / Decrease	1

Table 8.3: Scoring table for slaughter according to severity criteria.

Severity score	Action to realise	Severity puntuaction
0	No Action	Leve
1 - 5	Watch more closely	Leve
Up to 5	Increase the frequency of surveillance, consider liquid supplements or monitor the care that should be given to the animal. Account must be taken into account the application of analgesia. Notify to Investigator Principal (IP).	Moderate
6-10	Probable Significant Suffering: Provide some mode of self-relieving, frequent observation, and consideration of a humanitarian endpoint (including euthanasia).	Severe
> 10	Maximum severity limit. Severe suffering. Proceed to euthanasia. It is not recommended to repeat the project. If the project is essential, an exemption must be requested from the Competent Authority.	Severe
Endpoint Criteria	When a symptom appears with a score of 4 points, euthanasia will be performed directly	Euthanasia

Chapter 9: Publication